UNIVERSIDAD DE JAÉN

DEPARTAMENTO DE FÍSICA

TESIS DOCTORAL

SYMULATION OF ELECTROKINETIC AND COLLOIDAL STABILITY PROPERTIES WITH THE PRIMITIVE MODEL OF ELECTROLYTE

PRESENTADA POR:
JOSÉ GUADALUPE IBARRA ARMENTA

DIRIGIDA POR:
DR. D. MANUEL QUESADA PÉREZ
DR. D. ALBERTO MARTÍN MOLINA
DR. D. KLEMEN BOHINC

JAÉN, 1 DE JUNIO DE 2012

ISBN 978-84-8439-686-4

UNIVERSIDAD DE JAÉN

Physics Deparment

Simulation of Electrokinetic and Colloidal Stability Properties with the Primitive Model of Electrolyte

---

José Guadalupe Ibarra Armenta

Ph.D. Thesis

Simulation of Electrokinetic and Colloidal Stability Properties with the Primitive Model of Electrolyte

By

José Guadalupe Ibarra Armenta

Thesis Direction

Doctor
Manuel Quesada Pérez
Universidad de Jaén

Doctor
Alberto Martín Molina
Universidad de Granada

Doctor
Klemen Bohinc
Univerza v Ljubljani

Thesis for the Degree of International Philosophy Doctor in Physics

---

Linares, May 2012

Dedico esta tesis a mis padres en especial a Don Gabriel Ángel Ibarra Leyva que desde chico me inculcó la curiosidad por la ciencia y por las cosas que no conocemos, las que no se pueden explicar y todas las que se pueden hacer al dedicarles un poco de nuestro tiempo.

Abstract

Colloidal suspensions are important in various areas of technology ranging from medical applications in therapy treatments and drug design to the synthesis of biocompatible complex molecules like polymer or polyelectrolyte gels. A profound understanding of the rules behind the electrokinetic and colloidal stability properties of colloids is important for the development of more applications with greater accuracy. At the molecular level, computer simulations within the Primitive Model (PM) of electrolyte appear as a very useful tool. Although this model omits an explicit representation of solvent (water), it provides valuable information about ionic correlations (caused by coulombic interactions and/or ionic size) beyond the classical theories.

In the present thesis, different aspects of colloidal suspensions and polyelectrolyte solutions are studied with the help of Monte Carlo (MC) simulations within the PM of electrolyte. The role of ionic correlations in the Electrical Double Layer (EDL) is tested contrasting computer simulations with a modified classical theory that includes ionic size effects. After the inclusion of dispersion forces in the PM, salt specificity is tested for colloidal suspensions in the presence of mono- and divalent electrolytes. The EDL interactions are studied through net pressure calculations for a pair of equally and oppositely charged plates in the presence of mono- and divalent electrolyte solutions. The inclusion of bonding interactions between monomers in the PM makes possible to model polyelectrolyte networks. The dependence on charge and temperature of thermo-shrinking polyelectrolyte gels is analyzed with the help of a hydrophobic model for the interaction between uncharged monomers of unbounded polymer units. The basic PM can also be modified to model ions with internal charge distribution. A model of spheroidal ions with two elementary charges is proposed. Thus, the quadrupolar interactions arising from the added orientational degrees of freedom and their effects on the EDL are analyzed providing further insight into the role of ionic correlations of coulombic and non-coulombic origins.

The different analyses carried out exhibit a remarkable impact of ionic correlations. Through the consideration of realistic hydrated ionic diameters in the MC simulations, important disagreements appear with the classical EDL theories and even with previous computer simulation studies where the impact of ionic size was underestimated. Moreover, the importance of the salt specificity is proved to depend strongly on the size of the ions. The behavior of polyelectrolyte gels is found to depend on the competition between the length of the

polyelectrolyte chains (together with the hydrophobic interaction they tend to shrink the network) and the charge of the polyelectrolyte chains (that tends to swell the network). In addition, discontinuous phase transitions arise in the case of weakly hydrophobic polyelectrolyte gels.

List of Papers

I. "Testing a modified model of the Poisson Boltzmann theory that includes ion size effects through Monte Carlo simulations"
José Guadalupe Ibarra-Armenta, Alberto Martín-Molina and Manuel Quesada-Pérez
Phys. Chem. Chem. Phys., **2009**, *11*, 309.

II. "Effect of ion dispersion forces on the electric double layer of colloids: A Monte Carlo simulation study"
Alberto Martín-Molina, José G. Ibarra-Armenta and Manuel Quesada-Pérez
J. Phys. Chem. B, **2009**, *113*, 2414.

III. "Influence of monovalent ion size in colloidal forces probed by Monte Carlo simulations"
José Guadalupe Ibarra-Armenta, Alberto Martín-Molina and Manuel Quesada-Pérez
Phys. Chem. Chem Phys., **2011**, *13*, 13349.

IV. "Monte Carlo simulations of the electrical double layer forces in the presence of divalent electrolyte solutions: Effect of the ion size"
Alberto Martín-Molina, José Guadalupe Ibarra-Armenta, Enrique González-Tovar, Roque Hidalgo-Álvarez and Manuel Quesada-Pérez
*Soft Matter, **2011**, 7, 1441.*

V. "Computer Simulations of Thermo-Shrinking Polyelectrolyte Gels"
Manuel Quesada-Pérez, José Guadalupe Ibarra-Armenta, and Alberto Martín-Molina
J. Chem. Phys., **2011**, *135*, 094109.

VI. "Effects of the Internal Structure of Charge of Divalent Ions on the Electrical Double Layer"
José Guadalupe Ibarra-Armenta, Alberto Martín-Molina, Klemen Bohinc and Manuel Quesada-Pérez
Manuscript to send to *J. Phys. Chem. B*

Acknowledgments

I wish to thank first of all to my advisors Manuel Quesada Pérez, Alberto Martín Molina and Klemen Bohinc for their time and efforts during the elaboration of this thesis. In especial to Manuel for years of working close together in Linares and for introducing me into the world of physical chemistry by sharing all the knowledge he could give me in a field where I never worked before. I want also to thank to Alberto for following all my activities from Granada during these years. And finally, I want to thank to Klemen for helping me during my stay in Slovenia.

I am also grateful with my family for their confidence, although we were in different continents they unconditionally supported my decisions and I know that feel proud as me for any of my achievements whether these are significant or not.

I want also to thank to other students from the PhD program from all over Spain for their friendship, to the people from the students hall in Granada, especially to Cesar to whom I meet from my early years in Spain and has become an important support for anything I had to do in Granada. Although we meet by the half of my stay in Spain I will never forget all the funny moments I share with my officemates in Linares especially with the most “broken people” at the researchers hall. Pedro and Juan how many broken coffees it takes to get a PhD? Thanks to Antoñico for showing me the importance of a good hydration during the work hours. I will miss a lot of people from Linares after I leave Spain, I wish we keep on seen us in the future. I will especially miss to “los gañanes” David, JM, Edinson and Luis Eugenio and to my original housemates Javier and Antonio as well.

Finally, I want to thank to the Spanish people in general and particularly to science departments of the Spanish government and European Regional Development Funds (ERDF) for the financial support with the reference BES-2007-15853 and the research projects MAT2006-12918-C05-02 and MAT2009-13155-C04-04.

Introduction

The study of electrokinetic properties of colloids in suspension as well as their stability in the presence of electrolyte and polyelectrolyte solutions has a great relevance in the development of new technologies in several fields. Applications are broad, examples can be easily found in the industrial (paints and aerosols), pharmaceutical (drug design and controlled drug delivery), biological (DNA complexation, Alzheimer treatments) fields. According to their size, colloidal particles and the electrolyte ions are ranged within the mesoscopic scale. At this scale it is a well known fact that material properties are different from those of the massive material.

Mesoscopic objects play the role of the elementary building blocks for macroscopic objects. Statistical mechanics is applied but interactions at the mesoscopic range are affected by the *size* of the components and local fluctuations of properties such as polarizability, local particle concentrations or charge distributions. The size threshold from which a material behavior changes to the mesoscopic range is not well defined. Particles of few micrometers like bacteria, hair, microgels, etc. could define an upper limit. Single molecules and atoms could be the smallest objects considered into the mesoscopic scale. For objects below the mesoscopic scale, their interactions are ruled by quantum mechanics instead of statistical mechanics.

There are different approximations to describe the behavior of colloidal suspensions. In any case, a profound understanding of the rules behind the electrokinetic and colloidal stability properties of colloidal suspensions in the mesoscopic range by any means could significantly increase our ability to exploit the current technological applications.

Electrical Double Layer

The presence of charged colloidal particles in an electrolyte solution modifies the ordering of the ions. The ion-colloid and ion-ion interactions define the nature of the resulting structure. Such interactions can be long range coulombic interactions, dispersion interactions, chemical interactions (hydrogen bonds on the surface), even the ion-ion and ion-colloid collisions are characteristic for different ionic structures. Ions with the same sign of charge than the charged surface of the colloid are coions and ions with the opposite sign are counterions. Due to the sign of their charge and especially for high surface charge densities, counterions are strongly attracted by coulombic interactions to the charged surface as much as it is allowed by their excluded

volume. In addition to this coulombic attraction, chemical reactions can take place on the colloidal charged surface. Thus, the electrolyte composition in the immediate vicinity of the charged surface is dominated by counterions as some of them are practically *immobile* or adsorbed onto the surface. In contrast, the presence of the colloidal charge is imperceptible in the bulk of the solution. There is a continuous transition from the immobile ions settled onto the charged surface to the solution bulk. The region of electrolyte solution where this transition takes place is denominated as the *diffuse layer*. In general, these two regions of the electrolyte define the structure of ions around a colloidal particle denominated as an Electrical Double Layer (EDL), which play a fundamental role in many phenomena of everyday life.

Electrical double layers are present in practically all heterogeneous colloidal suspensions such as blood, paint, ink, cement and ceramic pastes, etc. Each EDL is characteristic of the medium where it forms and the colloidal particles that it contains. They define the attractive or repulsive interactions between colloids and hence the stability of colloidal systems. Aggregation phenomena like flocculation and coagulation are ruled to a great extent by EDL interactions between colloidal particles into the solution. For instance, milk is prevented to become butter because the EDL surrounding the fat clusters interacts in a repulsive manner stabilizing the system.

Several theoretical models have been developed through time in order to describe the EDL of colloidal systems. The first attempt is historically attributed (1879) to Helmholtz. This German physicist considered the EDL mathematically as a capacitor with fixed ions on the charged surface (without a diffuse layer) neutralizing the colloidal charge. These assumptions make sense for some colloidal systems, because a high affinity between the charged surface and ions from electrolyte solution induces ionic adsorption (a layer of immobile ions). However, the Helmholtz model is certainly arbitrary and not general enough for most of the cases. In 1910, Gouy and Chapman (GC) proposed as model for the EDL a diffuse layer of point ions described by a Boltzmann distribution discarding ion size and ionic correlations.[1,2] This model omits the possible existence of a layer of adsorbed ions and hence any traces of ionic size effects. As a consequence, Stern upgraded it by considering an internal layer of adsorbed ions with certain similarity with the one proposed originally by Helmholtz.[3] The difference is that now ions do not necessarily neutralize completely the charged surface and the thickness of the Stern layer (or Helmholtz plane) depends on the *size of ions*, *i.e.*, ions have now excluded volume. Nevertheless, this model still lacks of precision. Grahame enhanced the EDL model by the inclusion of hydration effects on ions.[4] In this fashion he proposed two layers of adsorbed ions, the thickness of the *inner Helmholtz plane* depends on the size of *unhydrated ions* and the *outer Helmholtz plane* on the size of *hydrated ions*.

Nowadays more sophisticated models have been developed; however, the most general features are still based on the assumptions of the early models. The colloid-electrolyte interface is assumed to be plain, charge is considered to be smoothly spread on the colloidal surface and the solvent is represented as a homogeneous medium with constant dielectric permittivity. Although

the GC picture presents important limitations, this model provides simple *analytical* expressions to describe the EDL of colloids. If we suppose for example that the electrical potential $\psi(\vec{r})$ varies linearly with the distance from the charged surface, the charge distribution is straightforwardly obtained. This approximation makes sense for systems whose electrical potential is low enough and is commonly denominated as the linearized Poisson-Boltzmann (PB) equation or Debye-Huckel approximation.[5]

$$\nabla^2\psi(\vec{r}) = \kappa^2\psi(\vec{r}) \tag{1}$$

Where the notion of the Debye-Huckel parameter κ has been introduced

$$\kappa = \left(\frac{1}{\varepsilon kT} \sum_{i=1}^{N} Z_i^2 e^2 n_i \right)^{1/2} \tag{2}$$

Here n_i is the bulk concentration of i-species, e is the elementary charge, Z_i is the ionic valence, ε is the dielectric permittivity, T is the absolute temperature and k_B is the Boltzmann constant. The inverse of κ is denominated as the Debye length, which is closely related to the thickness of the EDL. This approximation makes sense for systems whose electrical potential is low enough respect to the thermal energy $e\psi(\vec{r}) << k_B T$.

In particular, the evaluation of the electrical potential at the DCA of the hydrated ions to the charged surface (or equivalently, the outer Helmholtz plane) defines one of the key parameters in the description of the EDL, the diffuse potential ψ_d. This parameter closely related to the ζ-potential (experimental quantity useful in the description of electrokinetic phenomena).[6] Moreover, some authors claim that ζ-potential and ψ_d are practically indistinguishable for smooth and regular colloidal surfaces free of impurities.[6,7]

DLVO theory

As mentioned above, the GC model neglects the effects of ionic size on the EDL. Moreover, it assumes that the charge of colloids is continuous and uniformly distributed on their surface. In addition, any description of the fluctuations of the charge distributions or ionic concentrations is avoided. Despite the fact that this model does not include the ionic correlations derived from ion size, it provides analytical solutions to the description of the EDL. Usually, the analytical solutions to the EDL descriptions on the basis of the GC model are referred to as the PB theory or PB approach. The PB approach became the basis for the first analytical theory about colloidal stability, the classical Derjaguin-Landau-Verwey-Overbeek (DLVO) theory.[8,9] The DLVO theory has been widely applied through the decades in colloidal stability since its early apparition in 1947 despite the fact that its deficiencies were patent from the beginning. Colloidal stability depends upon the net balance of the repulsive and attractive forces that exist between particles as they approach depending not only on their charge but also on their surrounding EDL. If the particles have a mutual repulsion then the solution will remain stable. However, if the particles have little or no repulsive force, some instability mechanism will eventually take place such as flocculation

or aggregation. Different factors modify the EDL interactions along time like degradation of the components colloidal particles or salts. Some suspensions are stable for long periods of time until their net EDL interactions become attractive and they flocculate or coagulate.

In the framework of the classical DLVO theory, the net force between a pair of colloidal particles is expressed as the sum of an attractive van der Waals term and an effective electrostatic term calculated according to the PB scheme. The electrostatic term is purely repulsive in the PB approach, although it has been demonstrated by other approximations that ionic correlations could change the EDL interactions into a net attractive interaction.[10-17] The forces arising from the van der Waals term are denominated as Hamaker forces since 1937. In order to find the van der Waals interaction between two macroscopic bodies (colloidal particles made up of molecules), the Hamaker theory assumes that the interactions between the component molecules are pairwise additive.[18] The Hamaker theory has three major shortcomings. Firstly, it does not consider the interaction of macromolecules with the neighboring individual ions from electrolyte solution and between the individual ions. Secondly, induced dipoles are known to have a retardation effect but they are considered as instantaneous. Finally, the pairwise additivity of energy is valid only if the colloidal suspension is diluted enough. Nowadays, there are more advanced theories for the calculation of dispersion forces such as the Lifshitz theory.[19,20] However, these theories apply only for coarse grained models like PM and not for continuous models like GC model.

All shortcomings of the GC model and Hamaker approach are expected to be translated to the DLVO theory. Therefore the classical DLVO theory works well only for monovalent ions, low colloidal surface charge densities and not too high electrolyte concentrations. Trying to overcome some of these problems, several modified PB models have been presented through time in order to give an appropriate description of ionic size.[21-32] Nowadays, there exist more modern and successful approaches to describing the EDL of real colloids dealing with ionic size effects. Lattice based models,[33-38] Density Functional Theories (DFT)[14,39] or approaches based on integral equation theories like the hyper netted chain approximation[40-43] offer a chance to test other features of real colloidal systems inaccessible through the classical theories.[44-49] In addition, there is also an everyday increasing development of new computational resources that were not available in the early years of the first EDL studies. In the present thesis MC simulations within a PM of electrolyte, are chosen so that ionic correlations (coulombic and those caused by excluded volume) can be clearly elucidated.

Computer simulations and the *Primitive Model of Electrolyte*

There are numerous computer simulation implementations emulating an EDL available in specialized literature. In the present thesis we have chosen a MC simulation within a PM of electrolyte to carry out the pertinent calculations. The procedure of MC simulations is based on the generation of random numbers. The method tries random displacements of ions and their acceptation (or rejection) depends only on the total energy variation according to the so-called

Metropolis algorithm.[50] After a single displacement is attempted the energy variation of the whole system is calculated. If the total energy augments there is a higher probability that the displacement is rejected and the test particle stays in the same position. On the contrary, if the total energy is reduced the displacements are accepted. The Metropolis algorithm forces the system to enter into thermodynamic equilibrium conditions through the minimization of the total energy of the system after a *thermalization* period. An initial configuration for the simulation needs to be chosen although the equilibrium conditions are independent of it. Once the equilibrium conditions are reached it is possible to compute ionic concentration profiles. From them and the symmetry of the system, valence of ions, etc. it is possible to calculate more information about macroscopic variables such as EDL forces, electrochemical potential μ or electrical potential $\psi(\vec{r})$. This macroscopic information obtained by means of computer simulations is useful to compare with other approaches where it is also calculated (and it is even more valuable in case it is not possible to calculate by other approaches). An important advantage of simulation models is that a profound understanding of the system in its basic level is granted by the fact that all the interactions and correlations of the model are known from its very conception.

In the case of colloidal solutions, there are different symmetries to be considered for colloidal particles, such as spheres, cylinders, planes, etc. In any case, since colloids are (in general) much larger than ions, the surface of the colloidal particle can be usually approximated as planar. For instance, for spherical colloids the mathematical condition is that the colloidal diameter is greater than the Debye length.[42,51,52] For a pair of charged plates, the simulation cell contains ions corresponding to the desired bulk solution and the counterion excess neutralizing the charge located on the charged plates to ensure that the whole simulation cell is electroneutral. The charge distribution on the colloidal surface can be approximated by a discrete distribution or a simpler continuous one, depending on the system conditions this choice can lead to different results.[53,54] For sake of simplicity planar charged plates with continuous charge distributions are employed along the present thesis.

Concerning the representation of the electrolyte solution in which the colloidal particles are immersed, the PM of electrolyte is chosen because it is advantageous to test ionic correlations induced by the size of ions and their coulombic interactions. This model represents ions as charged hard spheres interacting by pairwise coulombic interactions. The solvent (water) is not considered explicitly; but it is modeled as a homogeneous continuum of constant dielectric permittivity and constant temperature. In this model, the discreteness of charge distribution (of the electrolyte solution) is well defined since ions are represented as individual entities. Consequently, the ionic correlations arising from the coulombic interactions among ions are implicitly present. Other so-called *civilized* solvent models represent the solvent explicitly as dipolar hard (or soft) spheres (or with some other geometry more similar to the actual solvent molecule). In such models the dielectric permittivity is not constant; it is calculated from the dipolar interactions and local concentrations of dipolar solvent molecules. Charged particles

induce the formation of a surrounding hydration layer increasing the excluded volume of ions but not necessarily in a uniform way leading to a not well defined structure for the ion and its hydration shell. Thus, the size of the ions is not well defined entity. Computer simulation studies have demonstrated in the past that ion size influences significantly the EDL structure beyond the predictions of classical framework.[12,16,17]

Due to its general features, the PM is an excellent candidate to probe ion size effects and also to test many theoretical approaches. Ionic correlations arise naturally due to the discreteness of the charge in the electrolyte solution. The fluctuations of local concentrations or charge distributions are also accessible. Thus, despite the limitations of the PM to describe real systems, this model provides answers to some burning issues that challenge the long-standing PB theory.

Applicability of the PM of electrolyte

In addition to the coulombic interactions, the PM allows the inclusion of non coulombic interactions. This can actually serve to increase the reliability of the simulation results when compared to those of real colloidal systems. For instance, dispersion forces can be included with the aim to test salt specificity; phenomenon widely confirmed by experimental results. In the past, Lewith and Hofmeister found great differences for the minimum salt concentration required to precipitate a given protein from solution (critical coagulation concentration).[55,56] This experimental work concluded with the proposition of the so-called Hofmeister series, which classifies in ascendant or descendant way the ability of ions to modify the water structure at their vicinity.[56] A large amount of typical examples like protein solubility, critical micelle concentration, bubble coalescence or surface tension of electrolytes was consciously studied by Collins and Washabaugh[57] and more recently by Ninham and Yamisky.[58] In the classical models of EDL, ions are only characterized by their valence. Then, the following question arises, why ions with the same valence behave in such a different manner? We could try to ascribe these effects to a specific interaction with the colloidal surface with the inclusion of additional parameters from specific (chemical) adsorption. However, by invoking a specificity that is *a priori* unknown we renounce to any predictive power.[59,60] Alternatively, the inclusion of dispersion ion-ion and ion-surface interactions (Van der Waals forces) has been used in the past to solve this problem in the framework of the classical DLVO theory and also on the PM of electrolyte.[60-67] In this manner, specific effects arise naturally since dispersion interactions depend on ionic polarizability, which is different for ions with the same valence. Salt specificity is always present in colloidal science but still lacks of a widely accepted explanation.

It is also not difficult to study more complex structures for the electrolyte solutions in the PM such as charged ions with internal structure or polyelectrolyte networks. For instance, in addition to the charged hard spheres, we could also consider rod-like ions, Langevin dipoles, spheroidal particles with quadrupolar charge distribution, etc. There are theoretical models that consider different structures for the charge distribution of ions which has been demonstrated to be significantly relevant for some systems.[68-72] For instance, linking of DNA to lipid layers could be

more easily explained by considering rod-like ions instead of the simple charged hard spheres.[73] Another useful possibility is the inclusion of bonding interactions between ions to conform ionic chains, *i.e.*, polyelectrolyte chains. Cross-linking interactions between polyelectrolyte chains can also be added. In this manner, polyelectrolyte networks can be easily modeled on the basis of the PM.[74-76] In general, polyelectrolyte networks like microgels and *nanogels* have attracted a lot of attention in recent years due to their broad field of applications. They have a large swelling capacity and ability to tune their swelling behavior to different stimuli like temperature, ionic strength, $p\mathrm{H}$, solvent nature and external stress. These polyelectrolyte networks are found in hygiene products like diapers, but there are also novel and more precise technological applications like controlled drug delivery, optoelectronic switches and artificial muscles.[77-82] In order to control the swelling capacity of polyelectrolyte network a good understanding of their molecular properties is needed. There is still not a general model to study the properties of such complex system as polyelectrolyte networks due to the long range interactions between charged groups in the polyelectrolyte chains and into the solution.[83]

Summarizing, the PM appears as an excellent candidate to model complex solutions of electrolyte, polyelectrolyte and other charged entities with internal structure. The main goal of this work is to find the physical mechanisms behind the behavior of colloidal suspensions whose components are small enough to be into the mesoscopic scale. Correlations of such small objects arising from the size of ions and coulombic interactions are inherent to the herein adopted simulation scheme to carry out calculations. Different interactions can be added to the PM, opening even more possibilities to study several features of such complex systems.

The rest of thesis is organized as follows. First, the main goals of the individual papers are discussed. Then, the general background that supports the elaboration of this thesis is introduced referring the current state of the art in colloidal science. After that, the most relevant results are briefly discussed in terms of the physical mechanisms ruling the behavior of the studied systems. Finally, the concluding remarks are presented and some perspectives for future work are given.

Goals

In this section the goals of the thesis are listed by individual papers. Along these papers different studies are proposed dealing with electrokinetic properties, effect of dispersion forces, salt specificity, colloidal stability, ionic size effects, internal structure of ions and temperature dependence in the shrinking behavior of thermo-responsive polyelectrolyte gels. In any case, we should keep in mind that our main goal is the understanding of colloidal systems and the correct interpretation of the physical mechanisms behind their behavior.

Paper I

The goal is to test some of the assumptions of the modified PB theories when the ionic size is included. In particular we test an analytical charge-potential relation that includes ion size effects through a Langmuir type correction. The electrophoretic properties of a colloidal particle are determined by the EDL structure around the colloidal particle. Originally, the classical GC model for the EDL on which the PB theory is based does not consider any trace of ionic size. The Langmuir type corrections consider monotonic ionic concentration profiles that cannot exceed a fixed value determined by the close packing fraction on the vicinity of the charged surface. In consequence, counterion concentrations on the charged surface are limited below the PB values. These assumptions are worthwhile to test. It is a well known fact that if the surface charge density is large enough, computer simulations (and other approaches that include ionic size) predict ionic concentration profiles that are not necessarily monotonic. These non-monotonic profiles reveal the formation of layers of ions in the vicinity of the charged surface whose origin is strongly related to the size of ions and ionic correlations. Computer simulations in the PM have also revealed that ionic size could lead to counterion concentration calculations on the charged surface larger than those predicted by the PB theory.

Paper II

The effect of dispersion interactions on the diffuse potential ψ_d for mono- and divalent electrolyte solutions is analyzed. ψ_d (closely related to the ζ -potential) is a highly relevant electrokinetic property in colloidal systems. Charged surface-ion and ion-ion dispersion forces depend on ionic polarizability, which is calculated through the Lifshitz theory. Thus, independent counterion-counterion, counterion-coion, coion-coion, counterion-charged surface and coion-

charged surface dispersion parameters can be included in the simulation scheme. Because of the dependence of these parameters on the ionic polarizability of individual materials, it is expected that different results are obtained for different salts in the solution, *i.e*., salt specificity will arise naturally in computer simulations. The effect of ion size on dispersion forces is also tested; hydration and dehydration effects are probed by varying the size of ions as they approach the charged surface. The goal is to provide an alternative to the theoretical approaches for the explanation of salt specificity effects based on the ionic polarizability and hydration effects.

Paper III

Some deficiencies of the DLVO theory come from the negligence of ionic size, which is known to be relevant in colloidal science because of the associated ionic correlations and the excluded volume region defined by the Distance of Closest Approach (DCA) (or the outer Helmholtz plane). The classical framework is known to work well only for monovalent ions, but fails for too large surface charge densities and also has problems if the salt concentrations are large enough. The goal is therefore to test the ionic size effects on the colloidal stability. To this end, predictions from classical DLVO theory and from computer simulations in the PM will be compared. The EDL forces are calculated from the contact densities only, this method is an alternative to the most classical mid-plane method employed within the PM. All calculations carried out correspond to electrolyte solutions of monovalent ions for which the DLVO is expected to work well; thus, the valence of ions is discarded as the origin of the discrepancies with computer simulation results. In any case, the statement that DLVO works well for monovalent ions is based on tests where an ionic diameter around 0.4 nm was employed. Further insight into the role of ionic size in colloidal stability is consequently required.

Paper IV

Attractive forces between equally charged surfaces can appear in the presence of divalent ions. The goal is to analyze systematically the role of ionic size on the colloidal stability via the calculation of EDL forces between a pair of charged surfaces (plates) in the presence of divalent electrolyte solutions. Like and oppositely charged plates with different surface charge densities, and two extreme ionic strengths are considered. The range of surface charge density chosen is from 1 to 20 μC/cm^2, *i.e*., into the biological regime. The excess charge (counterions) dominates the electrolyte composition at short separations between the charged plates because most of the salt is expelled from the electrolyte solution. For this reason, very low and very high salt concentrations are employed to verify if any difference is observed on EDL interactions. The ion size is probed by comparing two sets of results: those obtained for the classical ionic diameter found in literature (around 0.4 nm) and those results for larger ionic diameters corresponding to the hydrated ions. Data about the appropriate diameter for hydrated ions comes from experiments. However, it has also been applied in previous studies with the PM demonstrating that it could affect to a great extent the electrokinetic properties of a colloidal system.

Paper V

The thermo-response of polyelectrolyte networks with diamond like topology is analyzed. The goal is to find the physical mechanisms behind the shrinking behavior of some nanogels and their temperature dependence. A broad range of situations is systematically studied. The PM includes bonding interactions between polymer beads in order to build the polyelectrolyte chains conforming the polyelectrolyte network. It also includes a non-coulombic interaction, *i.e.*, an effective solvent-mediated potential for the hydrophobic interaction between non-bonded polymer beads. The model for the hydrophobic interactions predicts that the strength of the attractive hydrophobic forces increases with temperature. This potential is analytically solvable and is derived from a one-dimensional lattice model. Although it could overestimate the interactions at high temperature, this is a first approach to explaining the behavior of polyelectrolyte gels that shrink upon increasing temperature. Discontinuous volume changes are expected to be hindered by the strength of these hydrophobic interactions. MC simulations in the *NVT* and *NPT* ensembles were implemented within the PM for these analyses.

Paper VI

The effects on the EDL of an internal structure for ions are studied in *Paper VI*. The goal is to explore the effect of different parameters such as surface charge density or ionic diameter for the particular case of spheroidal ions and to understand the underlying physical mechanisms. The original PM consists of charged hard spheres whose charge is all concentrated in its center. This PM is modified in order to consider internal structure for the charge distribution. These spheroidal divalent ions have two elementary charges on opposite locations over the surface of the spheroid. Positively and negatively charged ions are considered. The added salt of spheroidal ions is controlled by establishing a thermodynamic equilibrium conditions with a grand canonical ensemble. The additional orientational degrees of freedom are expected to yield ionic profiles different than those obtained from the basic PM.

Background

In this section, previous works related with the thesis are reviewed. The state of the art is analyzed remarking all those asseverations that motivate the present thesis. For sake of order and clarity they are presented in groups to make them more readable: Computer simulations, electrokinetic phenomena, colloidal stability and other applications of the PM. The computer simulations employed in this thesis are reviewed in terms of their original conception and implementations within the PM. The studied electrokinetic phenomena are strictly those connected to the diffuse potential ψ_d. Colloidal stability is restricted to the EDL interaction, *i.e.*, van der Waals interactions between particles are not calculated. Other implementations of the PM deal with more complex types of ions than the classical charged hard spheres.

Computer simulations

The simulation scheme implemented in the present thesis consists of MC simulations within a PM of electrolyte. MC simulation is a statistical method employing random numbers to approximate complex mathematical expressions whose analytical evaluation is not possible or hard to achieve. This computer technique appeared around 1944 during the Second World War. It was used as a research tool to build the first atomic bomb in human history in Los Alamos National Laboratory in USA.[84] Due to the requirement of random numbers the method has been improved and diversified upon evolution of computer resources along the decades. Concerning colloidal suspensions, it was not until the 1970's when Valleau *et al*. presented the first MC simulations within a Restricted PM (RPM) of electrolyte, *i.e.*, ionic species are restricted to have the same size.[85,86] These simulations were carried out in the *NVT* ensemble, which has a constant number of particles, volume and temperature.

Valleau *et al.* demonstrated the feasibility of the *NVT* ensemble to carry out MC simulations within the PM for a pair of planar charged surfaces. However, a constant number of particles may constitute an important problem in some cases. Inside the simulation box there are ions and counterions corresponding to the desired salt concentration, whose ionic distributions in the bulk of the solution (far from the charged surfaces) should tend to the desired salt concentration. But there is also a counterion excess neutralizing the charged surfaces and augmenting the bulk salt concentrations above the desired values. Thus, the simulation box must be large enough to vanish the presence of excess counterions, ensuring that the desired bulk salt concentration is

simulated. For instance, ψ_d can be calculated from the ionic distributions of all intervening species. These data are accessible with a *NVT* ensemble but, for colloidal stability analyses this ensemble might not be the most appropriate one. In order to analyze the stability of a pair of colloidal particles, the mean force between them at all separations is required. Actually, the most interesting range of separations is below the distance where the EDL of charged surfaces overlaps*, i.e.*, the bulk of the solution disappears from the simulation box.

To carry out simulations within a *μVT* ensemble with constant electrochemical potential, volume and temperature appears as the solution to this problem. For this ensemble, the simulation box is interchanging electroneutral groups of ions in thermodynamic equilibrium with an external reservoir where the desired salt concentration is fixed. In this manner, the desired salt concentration is imposed to the simulation box via an external reservoir and the size of the simulation box can vary freely without altering the bulk salt concentration. In 1974 Adams presented the first Grand Canonical MC (GCMC) simulations for uncharged particles via the thermodynamic equilibrium of the simulation box with a *μVT* ensemble of uncharged hard spheres.[87-88] The GCMC simulation model was later extended for charged hard spheres by Valleau *et al*. allowing for the first time a precise control of the electrolyte solution in a MC simulation with planar charged surfaces.[89,90] In the original work of Valleau *et al*. a mean activity coefficient is provided as input to obtain a salt concentration that *is a priori* unknown. Therefore, we need to develop an inverse iterative method to obtain the activity coefficient corresponding to the desired salt concentration. We propose a method where the activity coefficient is periodically recalculated based on the output mean value of the desired salt concentration and its deviation from the desired one. Recently, other iterative methods have been proposed by other authors allowing us to test successfully the reliability of our method.[91-93]

Since the long range of coulombic interactions, a correction to the energy calculations is required. In the original work of Valleau *et al*. for the GCMC simulation, they use the so-called *minimum image* approximation. In this approximation, all ions are replicated in space but each ion interacts only with the closest replica of each one (that can be also the original one). This approximation might be insufficient if the simulation box is too small to enclose the range of coulombic interactions. Torrie and Valleau improved the minimum image approximation by the addition of charged sheets with a squared hole in the region where the minimum image of ions is located.[90] Other options are available for long range corrections such as Ewald summations, Lekner corrections, etc. Ewald summations truly consider the periodicity of the replicated system, replacing the interaction energies in real space with an equivalent summation in Fourier space. The advantages of the Ewald summations are the fast convergence of the summation in the Fourier space compared to its real space equivalent and that the minimum image approximation is not needed. However, these conversions between the real and Fourier space are time consuming and the periodicity may introduce unphysical correlations to the calculations.[90]

Lekner corrections are an adaptation of the traditional Ewald summations for systems with periodicity in two dimensions.[94,95] Lekner corrections are also very precise and do not require the minimum image correction, but they are very time consuming. In the present thesis Lekner corrections are used in the first and second papers. Minimum image approximation together with long range corrections similar to those of Torrie and Valleau are employed in the third, fourth and sixth papers. Direct Ewald summations are employed in the fifth paper. Similar long range corrections to those provided by Torrie and Valleau, were proposed by Boda in 1998.[96] However, they are more precise and require considerably less computational resources than Ewald summations and Lekner corrections.

We should always keep in mind that the main limitation of the PM from its conception: the solvent is not *explicitly* considered. The only influence of the solvent on the EDL is introduced on the model through a constant dielectric permittivity and temperature. However, explicit solvent models have been recently contrasted to the PM and the same qualitative effects of surface charge density, ionic valence and dielectric permittivity were found.[97] Alternatively, the PM can be improved without a molecular description by the consideration of a variable permittivity. This can lead to the apparition of image charges between the charged surfaces, but their influence is expected to be screened by the presence of ions in the solution.[47] In any case, one of our main concerns is to study the ionic size and its ionic correlations. If we compare the PM with classical theories where a dielectric continuum is also assumed, ionic size effects could be more easily differentiated.

Mechanisms behind the EDL conformation: Electrokinetic phenomena

In general terms, the conformation of the EDL defines the electrokinetic properties of a colloidal system. The movement of a charged colloidal particle in the presence of an external electrical field (electrophoresis) is not obvious when multivalent electrolytes are in the solution. Under this situation, the counterion concentration in the vicinity of a charged colloid can be so large that the colloidal charge is overcompensated (*overcharging*).[98] In this case, a reversal in the electrophoretic mobility can occur, *i.e.*, a negative colloidal particle can move towards the anode (with the same charge) or conversely a positive colloidal particle can move towards the cathode. Two possible explanations for this phenomenon are proposed, on the one hand, specific adsorption (of chemical origin) and ionic correlations (of physical origin) on the other. The most general explanation should include both type of effects (of chemical and physical origin) and not simply one of them.[48] However, there is recent experimental evidence that overcharging can occur even in absence of specific adsorption.[99] This remarks the importance of looking for other effects of physical origin (ionic correlations) and their influence on the EDL conformation.

The ionic specificity can also play a very important role in some colloidal systems. Hofmeister series register experimental evidence of these phenomena in electrolyte solutions with colloidal particles[55,56,100-102] and polymer networks.[103-105] Specific adsorption could also serve as a valid explanation for the occurrence of salt specificity, at least to some extent. For this purpose,

additional parameters must be included in the description of the EDL. However, the values for these additional parameters are *a priori* unknown. As a consequence, we renounce to any predictive power through the inclusion of specific adsorption parameters.[59,60] An alternative EDL description independent of specific adsorption can be accomplished by the inclusion of dispersion forces. These forces depend on the ionic polarizability, which is different for ions of the same valence. In this manner it is guaranteed that different salts have specific effects on the EDL conformation, *i.e.*, specific effects are expected to arise naturally if dispersion forces are considered. Inclusion of dispersion forces has proved to be helpful in previous studies of salt specificity in the framework of the classical DLVO theory[60,62,65,66] and also on computer simulations.[61,63,64,67] However, in these previous studies dealing with dispersion forces, the dependence of these interactions with the ionic size has not been assessed.

In the classical framework ions are considered as point charges (GC model) embedded in a dielectric continuum. In some cases, this leads to unrealistic predictions in the EDL description and inconsistencies with other approaches where ionic size is taken into account. To overcome this problem, it is imperative to modify the PB scheme to include ionic size effects. Stern was the first one to prove that the GC model leads to unrealistic counterion concentrations in the vicinity of the charged interface between the colloidal particle and the electrolyte solution. For this reason, he included the so-called Stern layer.[3] However, the first direct modification of the PB equation inspired by ionic size effects is ascribed to Bikerman. He proposed the addition of an excess term to the ideal electrochemical potential.[21] Since then, more alternatives have been developed based on corrections to the electrochemical potential[9-12,18,19] or lattice models.[33-38] The role of ionic size in ionic layering at high salt concentrations, colloidal overcharging and competition between different ionic species in electrolyte mixtures has been recently studied.[29,30,43] Also the deviations from the PB predictions of the charge-potential relationship have been looked into.[13-15] López-García *et al*. have analyzed a modified PB model that takes into account the finite size of ions into account through a Langmuir type correction.[106] They put forward an approximate analytical expression for the charge-potential relationship. The surface charge density and the ψ_d are the key parameters in the description of the EDL. Even in experimental grounds, since ψ_d is claimed to be closely related with the experimental ζ-potential.[6,7]

López-García *et al*. claim that significant discrepancies with the classical predictions can appear even for hydrated ionic diameters, *i.e.*, ionic diameters from 0.75 to 1 nm.[5] These authors have also extended their results to treat the nonequilibrium problem of the electrophoretic mobility of a rigid spherical particle.[107] They use a model developed in the 1990's by Adamczyk *et al*.[108-110] based on theories of the 1950's.[111,112] Ionic concentrations and the electrical potential are obtained as functions of the maximum attainable concentration of ions of the *i*-species due to close packing $c_i^{\max}$. Ionic profiles predicted by this scheme are monotonic, which is in disagreement with other approaches and computer simulations.[17,29] Due to the fact that ionic

concentrations are limited by the $c_i^{\max}$ values, they are forced to remain below the PB predictions as well. However, under certain circumstances ionic concentrations on the charged surface predicted by integral equation theories have been found to be larger than those predicted by the PB theory.[17,43,113] Thus, the dependence of this useful expression on ionic size deserves further insight.

The definitions of the outer and inner Helmholtz planes were included by Grahame in the framework of the classical GC model. They define the DCA for hydrated and dehydrated ions. This means that the effect of hydration of ions is included, although it is only considered exactly on the charged surface and not in the diffuse layer or the bulk of the solution. However, if similar assumptions are taken on computer simulations, a direct comparison can be accomplished for the elucidation of hydration effects on the EDL. It is not a complicated task since different ionic sizes for each ionic species are already considered in the PM. The reduction on the size of ions due to dehydration could augment the strength of charged surface-ion and ion-ion dispersion forces. This could indeed enhance the ionic adsorption on the DCA in terms of specific interactions of physical origin.

Colloidal Stability

At this stage, we have analyzed some of the factors intervening on the conformation of the EDL, which in fact is in close connection to the colloidal stability. The EDL interactions have a great practical relevance in natural and industrial phenomena. Nowadays, it is possible to measure them directly with the help of the surface force apparatus or the atomic force microscope. A significant amount of data are available for electrolyte solutions within polystyrene spheres, silica, acetate surfactant bilayers,[59,114-118] and mica surfaces with various geometries that date back to the 1980's from the experiments of Pashley *et al*.[119-123]

In solutions with multivalent ions, ionic correlations are expected to be more significant. For the case of monovalent salts, few works have explicitly compared DLVO predictions on colloidal stability with calculations from other approaches. However, it is widely accepted that DLVO theory works well for monovalent ions. Guldbrand *et al*. published one of the pioneering works on computer simulations in 1984. In this work, the validity of the DLVO theory for monovalent electrolytes was probed for moderate surface charge densities.[51] Tang *et al*. contrasted DFT and DLVO calculations corroborating a good agreement between them if surface charge density and salt concentrations are low enough.[39] However, DLVO theory fails to describe some of the most fascinating phenomena reported experimentally, the attraction between equally charged colloidal particles and conversely the repulsion between oppositely charged ones (especially in the presence of multivalent counterions).[115-118,123-125] This kind of phenomena is usually explained in terms of ion-ion correlations, which are neglected by the PB scheme but easily accessible through computer simulations.[44,47,126,127]

The existence of attractive EDL interactions in the presence of multivalent counterions between like-charged plates[51,52] and colloidal particles of other geometries such as cylinders and spheres have been proved using either MC or molecular dynamics simulations.[128-131] Other related aspects, such as the discreteness of the surface charge density have been addressed recently.[53,62,63,131-139] In any case, an ionic diameter around 0.4 nm (referred in this thesis as the classical ionic diameter) was assumed for hydrated ions in most of the calculations, which is rather small when compared to those suggested by experimental works, especially for multivalent ions.[5] The electrokinetic behavior of some latexes in the presence of calcium, magnesium and lanthanum can be properly described only if ionic diameters larger than the classical one are assumed. In any case, we can conclude that ionic size plays a major role in colloidal suspensions with divalent and trivalent counterions.[113,140]

Few authors have calculated EDL interactions with ionic diameters larger than the classical one.[115,138,139] Only Ravindran and Wu analyzed specifically ionic size effects on the EDL interactions.[131] In particular, Ravindran and Wu used MC simulations within the RPM of electrolyte and reported a proportional increase of the attraction between like-charged spheres with increasing ionic size. This is indeed a valuable finding but it was obtained for spheres with a particular surface charge density and for a fixed symmetric electrolyte concentration. The largest ionic diameter they considered was of 0.6 nm but according to the previously cited literature, one could even consider larger ions.[5] In our opinion, the effect of ionic size should be studied for a broader collection of situations.

Other Applications of the *Primitive Model of Electrolyte*

Polyelectrolyte gels are cross-linked structures of polymer chains, linked via chemical interactions containing ionizable functional groups. They stand as a burning issue in physical chemistry due to the number and novelty of applications.[141-143] When polymer chains are immersed in polar solvents (like water) the ionizable groups can dissociate, yielding charges on polymer chains and releasing counterions into the solution as well.[144] The electrostatic interactions between these polyelectrolytes (whether they are natural or synthetic) and the dissociated counterions are quite essential for several processes such as fabrication of multilayer films, packaging of DNA into chromosomes, gene therapy, protein separation, etc.[145-148] Polyelectrolytes can form complexes with proteins enhancing precipitation, and they are essential in the development of lithium batteries and proton exchange membranes for fuel cell technology.[149,150] Among the available biomaterials, polyelectrolyte gels stand as an excellent candidate to the design of efficient drug delivery carriers.[151] These materials are able to take up large amounts of water (or physiological fluids) while maintaining their internal structure at relatively low surface tension enhancing their biocompatibility.[152,153] Some polyelectrolyte gels combine a high loading capacity for bioactive compounds and the ability to release this therapeutic payload in a controlled fashion.[154] These features accounts for their applicability in tissue engineering, drug delivery and diagnosis.[155] Although research has been mainly centered on macroscopic polyelectrolyte gels, there is now a

growing interest on polyelectrolyte gels constricted to micro- and nanoscopic dimensions, so-called micro- and nanogels, respectively.[156,157] Their properties are very similar to those of their macroscopic counterparts. Nonetheless, they have the capability of entering in physiological areas not accessible to the macroscopic gels allowing the realization of intracellular drug delivery mechanisms.[158] At any extent, the correct understanding about the factors controlling the properties of polyelectrolyte gels is needed in order to enhance their widespread and useful applicability.

In the past decade, computer simulations and theoretical models have proved to be helpful in elucidating the static and dynamic properties of polyelectrolyte gels, their swelling behavior, multilayer assembly, as well as their adsorption onto surfaces and interfaces.[83] The first simulations of neutral polymer networks (uncharged gels) are attributed to Escobedo and de Pablo.[74] However, polyelectrolyte gels were not simulated until 1996. In most of the publications up to date a PM with a diamond-like topology has been chosen to model the polymer network.[75,76,159-170] Due to the large swelling capacity of polyelectrolyte gels a large amount of solvent particles is needed if solvent is modeled explicitly. For this reason, most authors prefer a coarse grained model for calculations without explicit solvent (PM).[83] Concerning the size of polymer networks, nanogels have been simulated explicitly by some authors. Claudio *et al*. calculated the fraction of counterions inside the network as a function of the nanogel size.[169] Olvera de la Cruz suggests that nanogel size is crucial due to the charge excess generated in the gel interface.[171] Jha *et al*. analyzed the effects of the cross-linking degree, solvent quality, and charge fraction of polymer backbone; they also reported discontinuous volume phase transitions.[170]

Several aspects of polyelectrolyte gels have been simulated in the past. However, the issue of thermo-responsive polyelectrolyte gels has been scarcely treated so far. Escobedo and de Pablo reported the swelling curves of *uncharged* polymer networks as a function of the temperature for sub- and supercritical solvent conditions.[74] However, simulation of thermo-sensitive polyelectrolyte gels stands as a challenging task. The thermo-response of these systems is known to be driven by polymer-polymer hydrophobic forces and hydrogen bonds, both of molecular origin.[172,173] Moreover, hydrophobic forces are solvent mediated, this constitutes a major limitation for a model where the solvent is not explicitly represented.

An effective polymer-polymer interaction potential is required and the temperature dependence of this potential must be *a priori* known. Kolomeisky *et al*. derived a suitable potential from a one-dimensional lattice model, which may be simple indeed, but is advantageous for the modeling of thermo-responsive polyelectrolyte gels.[174] It incorporates a basic mechanism for hydrophobic forces by means of analytical equations that provide the dependence of these interactions with the temperature. Barkema and Widom proved through simulations that main features of the proposed potential are also valid for two and three dimensions.[175] Moreover, Koga *et al*. proved that the model can justify solubility data of methane within accurate results, which supports its applicability in 3D real systems.[176]

There are recent experimental data for Poly(N-isopropylacrylamide) (PNIPAM) gels (with a relatively large amount of charged monomers) and others synthesized from vinylcaprolactam that shrink upon heating.[81,177-183] There are also recent sophisticated approaches for temperature-sensitive polymer gels but they are only valid for weakly charged polyelectrolytes networks.[172,173] Therefore, the test for the proposed hydrophobic model when compared to the available experimental data could provide new insight on the temperature dependence of polymer gels and the effects of charge for highly charged polymers.

Concerning the possibility of defining an internal structure for ions, we should keep in mind the basic conception of the PM. This model considers ions as individual charged entities with spherical shape where the charge is concentrated at their geometric centers. However for some electrolyte solutions, the internal structure of ions at their molecular level plays a very important role. For instance, dispersion interactions appeared as alternative to specific adsorption for the description of salt specificity.[58,61,62,65-67] Thus computer simulations were able to reproduce salt specificity without invoking additional parameter for specific adsorption, which might indeed eliminate any predictive capacity in the EDL description.[59,60] We should remind that these ion-ion, ion-colloid and colloid-colloid dispersion forces arise from permanent and induced dipoles correlations. These dipolar correlations obviously depend on the internal structure of ions.

Modifications to the PM can be achieved by defining an internal structure for the charge distribution. Internal structures have been studied previously, proposing density functional theories and carrying out MC simulations for rod-like ions, Langevin dipoles and dendrimers.[68-72,184] It was found that the added orientational degrees of freedom may induce a bridging mechanism between a pair of charged plates with the same sign of charge causing a correlated net attraction.[73] Dendrimers were found to induce long range attractive forces between a pair of equally charged plates and this correlated attraction was experimentally confirmed by direct measurements with an atomic force microscope.[184]

To stay in close connection with experiments, it is better to define structures with elementary charges. Thus, the simplest modification to the PM should include two charges. It would be also the best option to understand as much as possible the underlying physical mechanisms. Electrolyte solutions of spheroidal divalent ions are chosen with this purpose. These spheroidal ions are inspired on a real system of monoclonal antibodies that were found to induce coalescence on giant unilamellar phospholipid vesicles at short separations.[69,185,186] After modification of the basic PM it would be possible to work with spheroidal ions in simulations. Thus, the ionic correlations derived from the internal structure of ions (intracorrelations) and the ones related to the interaction between different ions (intercorrelations) could be sampled.

Results

The preceding sections reveal issues that keep on challenging colloidal science nowadays. Computer simulations appear as an excellent choice to test these unsolved issues, which are the main motivation for the various analyses carried out during the realization of the present thesis. The pertinent MC simulations have been implemented in order to give further insight on general topics in colloidal science beyond the classical framework based on the PB approximation. Due to the fact that a PM has been chosen to represent the solvent, the role of ionic size has been clearly elucidated and it has been found to be of tremendous importance at different levels.
Now we proceed to discuss the most important results obtained from the different analyses. These are presented in three different groups of interest for sake of clarity. The concluding remarks and perspectives are left for next section. In any case, it should be stressed that results and discussions are highly summarized in this section. Consequently, readers interested in further details are rather referred to the corresponding papers.

Electrokinetic phenomena

The MC simulations of this subsection have been carried out within a RPM in a *NVT* ensemble and using the Lekner-Sperb corrections to the long range coulombic interactions. The Lekner-Sperb corrections are a variant of the Lekner corrections proposed by Sperb to solve an occasional divergence problem.[95] In addition, a truncation criterion for the summation proposed by Moreira and Netz has been applied.[134] The charge-potential relationship that includes ionic size effects provided by the model of López-García et al.[106] has been analyzed and its theoretical predictions have been contrasted with the results from the MC simulations. Calculations for 1:1 and 2:1 salts have been carried out with three representative ionic diameters 2, 1 and 0.75 nm. The greatest value of 2 nm is rather large but is presented with illustrative purposes. The referred theory assumes that counterion concentrations remain limited below the close packing fraction, which implies that they remain limited below the PB limit as well. This assumption clearly contradicts previous analyses where the conclusion was that counterion concentrations are not limited by the PB prediction.[11,43,113] In *Paper I* a saturation regime could be identified from which the ionic concentrations could remain below the PB picture and even below the close packing fraction value. However, below this saturation regime the ionic size and ionic correlations can increase counterion concentrations beyond both limits.

In consideration of the excluded volume, the space between the charged surface and a counterion close to it cannot be occupied by other counterions; consequently the attraction towards the charged surface is strengthened. It should be stressed, however, that if certain excluded volume threshold is surpassed a saturation regime is reached. In that case, the excluded volume is so large that the counterion concentration close to the charged surface is reduced (as expected) respect to the PB framework (where excluded volume is not considered). If the saturation regime is reached, the MC simulations provide a better agreement with the PB predictions. The saturation regime is more easily reproduced for monovalent counterions due to the fact that two monovalent counterions occupy the double of volume than a divalent one. Moreover, the coulombic attraction to the charged surface is twice stronger for divalent ions than that for monovalent ions. In other words, divalent counterions are more efficient to neutralize the charged surface than monovalent ones. The modified PB theory that includes ionic size effects works well only for monovalent ions. In addition, layering effects were found by MC simulations that cannot be predicted by the theory. The assumption of monotonic profiles and the limit for the counterion concentrations should be reconsidered, especially for high surface charge densities.

To elucidate the effect of dispersion forces, in *Paper II* this interaction is included in the MC simulations to calculate the diffuse potential ψ_d which is assumed to be the ζ -potential. Calculations for monovalent and divalent cations are carried out looking for traces of salt specificity. Dispersion parameters already calculated through the Lifshitz theory by other authors are considered.[61,62] ζ -potentials obtained from simulations for monovalent (LiCl and CsCl) and divalent asymmetric ($MgCl_2$ and $BaCl_2$) salts as a function of the bulk salt concentration (the classical PB picture is calculated as well). An ionic diameter of 0.7 nm was deliberately taken for all ions of 1:1 salts and 0.8 nm for all ions of the asymmetric 2:1 salts. The selected salts are representative of the lowest and the highest dispersion parameters (from the references) among the mono- (Li^+, Cs^+) and divalent (Mg^{2+}, Ba^{2+}) cations, respectively. However, almost identical results are obtained for the mono- and divalent cations separately. Similar tendencies are reported from experimental data of *Paper II*. In contrast, a previous study carried out by Tavares *et al.* concluded that the mean force between macroions could be quite sensitive to dispersion parameters.[61] In any case, we should remark that their calculations were carried out assuming a classical ionic diameter of 0.4 nm for all ionic species. The apparent discrepancies can be more easily understood by calculating the ζ -potential for 1:1 and 2:1 salts as a function of the ionic diameter (see Fig. 4 of *Paper II*). These calculations demonstrate that a higher ionic size hinders the effects of dispersion forces. It is not a surprising result, since this dispersion forces are short ranged and even at contact distance they introduce energies to the calculations that can hardly surpass the thermal agitation energy (when realistic ionic diameters are considered).

Calculations for a series of monovalent anions Cl^-, I^- and SCN^- with and without dispersion parameters are also included in *Paper II*. The corresponding ionic diameters were estimated as

0.65 nm for Cl^- and I^-. For SCN^-, an ionic diameter of 0.5 nm was chosen based on the total excluded volume according to its atomic structure. As expected, the differences between the ζ-potential data obtained from simulations for NaCl and for NaI, are negligible. Nevertheless, a large difference is reported between data from the simulations of NaSCN respect to that of NaCl, NaI and even to data without dispersion parameters. Calculations without dispersion parameters were carried out to test if the reduced ionic diameter of SCN^- could be responsible for the differences. However, the reported differences are not reproduced if dispersion forces are absent. This reveals that specific ion effects are extremely sensitive to ionic size. Moreover, the classical model of EDL proposed by Grahame[4] suggests that the consideration of hydration effects of ions could enhance the classical PB approach. Following this idea, a dehydration model is proposed in the frame of the PM, assuming that all ions are dehydrated below the DCA at for hydrated ions (Outer Helmholtz plane). This is certainly a rather simple dehydration model but the intention is to sample the dependence of salt specificity on ionic size. When the theoretical predictions from the Grahame model are calculated, they qualitatively fit the simulation results at low salt concentrations. But they are limited by an asymptotical trend that cannot surpass to negative values of ζ-potential. However, we should keep in mind that we are adjusting rather than predicting with the classical frame. The ζ-potential obtained from simulations presents a reversal for lower salt concentrations; this is in fact an outstanding result in line with previous experimental data for a cationic latex in the presence of SCN^-.[100]

The obtained results for dispersion forces states an alternative to the inclusion of extra parameters of specific adsorption and the corresponding loose of predictive power.[59,60] The ionic size is found to hinder dispersion forces (and coulombic interactions). In any case, specific ionic diameters (hydrated and dehydrated) altogether with specific polarizabilities enables the elaboration of a model where salt specificity is naturally predicted. High dispersion parameters combined with small ionic diameters (and/or dehydration effects) could explain the reversal of electrophoretic mobility for colloidal systems in the presence of a NaSCN salt, in agreement with some experiments with cationic latexes.

Colloidal Stability

The classical DLVO theory is usually given in terms of a mean potential energy U. However, it can be equivalently presented in terms of a force F. Once one of them is known, the other can be straightforwardly calculated since they are mathematically related

$$U(r) = \int_r^\infty F(r)dr \tag{3}$$

In the present thesis colloidal stability is analyzed for a pair of infinitely charged plates, *i.e.*, the symmetry of the system is planar. Thus, colloidal stability calculations are presented in terms of forces per unit area (pressures). We analyzed in so much detail as possible the several features that appeared on net pressure calculations for equally and oppositely charged plates in the

presence of mono- and divalent electrolyte solutions. Calculations are carried out for hydrated ionic diameters (0.7 nm for monovalent and 0.85 nm for divalent ions) and the classical one (0.4 nm for all ionic species).

In order to carry out the colloidal stability analyses, GCMC simulations are performed within a PM of electrolyte. In simulations, the *net pressure* is calculated as the difference between the contact densities (ionic densities at DCA) in the confined region (between the charged plates) and the contact density at the interface between the charged plate and the bulk electrolyte solution (outer region). Simulation results are obtained via the so-called charged surface method. In this method the net pressure calculations do not depend on collisional or electrostatic terms. This reduces the number of terms contributing to the net pressure from three to one (the one that depends on contact densities). No information about the other two terms is obtained. The reliability of this method was contrasted to that of the mid-plane method, which is preferred by most of the authors, under the assumption that it is more accurate.[187-192] However, our calculations point out in the direction that both methods work with a reasonably good accuracy. However, the results evaluated in the fashion of the charged surface method provide an alternative to the previous studies where the mid-plane method was preferred.

The variation of charge density, salt concentration (or equivalently ionic strength) and ionic valence are known to be relevant in colloidal stability. Previous studies where a classical ionic diameter was chosen supported the idea that DLVO theory is accurate enough for monovalent ions. However, our study provides evidence that ionic correlations (not considered in the classical framework) originated by exclude volume and coulombic interactions can dramatically change the net pressure calculations. For instance, a correlated attraction of ions toward the core of the electrolyte leads to short ranged attractive net pressures for monovalent ions while the DLVO theory predicts a null interaction at all separations (mechanism that is also operative for oppositely charged plates in the presence of asymmetric divalent electrolytes). If hydrated ionic diameters are chosen, a shift towards higher values and non-monotonic trends for the net pressure are evidenced, which are inaccessible by means of the DLVO theory. These trends are driven by the repulsion between excess counterions at short separations.

Since the electrochemical potential increases as the available space decreases, the ions of the added salt are (eventually) expelled from the confined region. Thus, for charged plates there is a separation threshold from which counterions are mainly found in the electrolyte solution of the confined region. As surface charge density increases, net pressures from simulations for ions of 0.7 nm of diameter are shifted toward larger separations and a non-monotonic behavior appears for separations below two ionic diameters. The net pressure calculations in simulations and in the classical DLVO theory are affected in a similar manner by the coulombic repulsion among excess counterions. However, effects of the excluded volume have a great influence on the simulations. For larger ionic diameters, an important contribution from excluded volume is registered in the confined region increasing the estimations of contact densities and hence the net pressure calculations.

For equally charged plates in the presence of divalent ions, net pressure calculations turned from attractive into repulsive values by changing from classical to hydrated ionic diameters. This is indeed an outstanding result; especially taking into account that values of the hydrated ionic diameters used in the simulations are based on experimental measurements instead of the classical ionic diameter employed by many authors. Ionic size is also responsible for the appearance of non-monotonic trends below two ionic diameters for mono- and divalent electrolyte solutions (also in disagreement with the classical DLVO theory). This non-monotonic trend was also reported previously by Kjellander *et al*., for classical ionic diameters but for a much higher surface charge density (26.7 μC/cm^2).[42] They ascribed this trend to the variation of the collisional term of the pressure, which is absent in the present calculations. Therefore, an alternative explanation based on contact densities is provided. As mentioned before, at short separations (but above two ionic diameters) between the charged plates, ions from the added salt are expelled from the confined region. If the surface charge density is high enough, two layers of highly packed counterions (one on each charged plate) are promoted as well as the movement of ions on the directions parallel to the charged surfaces. If the separation between the charged plates is reduced below two ionic diameters, the ions from opposite layers interact due to their excluded volume. This EDL interaction of highly packed counterions promotes thermal fluctuations in the directions perpendicular to the charged plate reducing the contact density and hence the net pressure. In spite of the thermal fluctuations, for very short distances, counterions can contribute to contact density estimations on both charged plates and therefore the net pressure increases again.

Net pressure profiles are calculated for five different ionic diameters in *Paper III*. For ionic diameters above 0.7 nm the non-monotonic trend previously reported, is observed again. Moreover, its effects increase in magnitude with the ionic size. This is not a surprising result since this non-monotonic trend is caused by excluded volume of excess counterions to a great extent. However, for ions of 1 nm of diameter, the trend is again monotonic. The reason behind this surprising result is that as ionic size is increased the proposed mechanism becomes inoperative. The ions are so large that below two ionic diameters, no free space remains on the opposite plate to promote the thermal fluctuations of counterions in the perpendicular direction to the charged plates. The packing fraction for ions for ions of 1 nm of diameter reaches a value of 32.5%, comparable to the 52% from a simple cubic arrangement.

For equally charged plates, ionic size is found to be extremely relevant in the confined region for highly concentrated electrolyte solutions (since the system is ruled to a great extent by excess counterions). Quite different results are obtained for oppositely charged plates (in the case of divalent ions) where coulombic correlations rule to a great extent the calculations and surprisingly ionic diameter seems to be irrelevant. In this case, salt concentration (or ionic strength) seems to have some effect on the net pressure calculations

Other Applications of the *Primitive Model of Electrolyte*

Modifications to the PM can provide statistics of different systems and the possibility of studying correlations beyond the basic PM. The first modification carried out in this thesis is for the studies of polyelectrolyte gels. The inclusion of bonding interactions between ions allow us to build polymer chains and with the help of crosslinkers it is possible to build polymer network structures. The second modification deals with the definition of an internal structure for the charge of ions.

Concerning simulations of polyelectrolyte gels in *Paper VI*, a PM with charged soft spheres was chosen, *i.e.*, the short range repulsion between any pair of particles is described by a truncated Lennard-Jones potential. The same ionic diameter of 0.7 nm was assumed for monomers, cross-linkers and ions in the solution. The polyelectrolyte chains consist of monomers connected by harmonic bonds.[75,76,166,167] The polyelectrolyte network is done by connecting each chain end to the tetrafunctional cross-linker. For sake of simplicity a diamond-like network with polyelectrolyte chains of equal length is employed. The chosen ensemble to carry out simulations of polyelectrolyte gels was the *NVT* ensemble. The long range coulombic interactions are corrected by Ewald summations, following the procedures and recommendations of Linse.[136] In order to reproduce equilibrium conditions for a polyelectrolyte gel the osmotic pressure Π should be zero. It is not straightforward to find such value with MC simulations implemented in an ensemble where the pressure varies freely (*NVT*). Other authors has preferred the *NPT* ensemble to perform simulations admitting that the simulation result might depend on the input volume fraction φ.[76,178] In any case, *NPT* simulations were also implemented. This dependence of the simulation results with the initial volume fraction was confirmed. Furthermore, it varied with the length of the polymers. These simulations were also useful to corroborate the results obtained via the *NVT* ensemble.

A rather simple hydrophobic interaction potential dependent on temperature and derived by Kolomeisky *et al*. from a one-dimensional lattice model is included as well to simulate the solvent mediated hydrophobic forces between non-bonded polyelectrolyte beads.[174] It should be stressed however, that charged chemical groups are generally hydrophilic rather than hydrophobic. Because of this reason, the hydrophobic interaction is omitted if any of the two interacting polyelectrolyte beads is charged, *i.e*., hydrophobic forces are assumed for uncharged and non-bonded polyelectrolyte beads only. Different functional forms for the hydrophobic potential are defined by two sets of parameters, denominated in terms of a Weakly Hydrophobic (WH) and a Strongly Hydrophobic (SH) interaction. The WH interaction parameters are of the same order of magnitude than those fitting solubility data of methane within accurate results.[176] The set of parameters for the SH potential are around twice larger than their WH counterparts. Two representative lengths for the polyelectrolyte chains are studied; a Short Chain (SC) and a Long Chain (LC) of 24 and 48 beads per chain, respectively.

The proposed hydrophobic potential was found to be responsible for the shrinking of the nanogel, whereas the swelling procedure was mainly ascribed to effect of free counterions in solution. Discontinuous phase transitions and critical temperatures for the transition from

swollen to shrunken states are found to depend on the competition between these two opposite effects. WH- systems show discontinuous phase transitions, in line with previously reported experimental data. In contrast, SH- gels do not exhibit hallmarks of phase transitions. The absence of discontinuous phase transitions is in disagreement with the theoretical predictions based on the Flory-Rehner formalism[193,194] where this feature is predicted even for weakly charged gels.[177,195-201] In any case, there is also experimental data where discontinuous phase transitions are not reported.[180,181]

The proposed model for the hydrophobic interactions is determinant in the obtained results. Only Escobedo and de Pablo studied previously by means of simulations the thermo-response of neutral gels in sub- and supercritical conditions for the solvent. However, solvent was explicitly modeled and a solvent mediated interaction potential for the hydrophobic forces was not included.[74] We could also expect that polyelectrolyte chains expand with thermal agitation above a critical value which has been confirmed by previous simulation studies.[76,202] Schneider and Linse proved that the gel expands if the ratio between the thermal energy and the depth of the well potential modeling the hydrophobic interaction surpass a critical value.[76] But in our model the strength of the hydrophobic interaction increases with temperature. Thus, hydrophobic effects can prevail over thermal agitation. The hydrophobic model dramatically increases the strength of hydrophobic force with temperature above a critical value. This could indeed lead to overestimations of the hydrophobic interactions. As a consequence, the shrunken state could be forced by the hydrophobic interactions whereas it is expected that polyelectrolyte chains unfold upon increasing temperature due to thermal agitation.

Concerning the studies of the internal structure of ions, ionic profiles for a pair of charged plates immersed in an electrolyte solution of divalent spheroidal ions with internal structure are analyzed. These spheroidal particles include two individual elementary charges on opposite locations at the surface of the spheroid. GCMC simulations are implemented to control the number of coions and counterions, *i.e.*, the salt concentration. The obtained results are contrasted to the DFT predictions for the same system.

For a set of parameters into the physiological regime, DFT and MC simulations agree fairly well even in the case where the hard spheres interaction is included in the MC simulations. In general, the ionic profiles are strongly influenced by the operation of a bridging mechanism, orienting the spheroidal ions preferably in a perpendicular direction respect to the charged plates. Depending on the separation between the charged plates, ionic profiles show one or two peaks on the concentration profiles of the individual elementary charges. For a special case of zero charge density, the classical PB theory is not able to predict neither a salt concentration nor an ionic profile in the confined region between the charged plates. However, the DFT predicts a non-zero salt concentration despite the fact that the electrochemical potential of the electrolyte solution is underestimated.

The internal structure of charge is modified in order to sample with GCMC simulations the transition from the basic PM to the modified PM. In this analysis, the distance of individual

charges is varied gradually from the center to the surface of the spheroid. In case that both individual charges are located at the center of the spheroid, ionic profiles are in agreement with those from the PM with regular divalent ions. The proof was carried in terms of a direct comparison with GCMC simulations within a basic PM.

In general, direct comparisons between the computer simulations and the DFT yield an excellent qualitative agreement. Orientational ordering parameters strongly affect the EDL beyond the basic PM and the classical framework. These parameters introduce new intra- and intercorrelations in the calculations easily sampled by the GCMC simulations. However, the DFT neglects some intercorrelations related to the excluded volume of spheroidal ions. This can lead significant quantitative differences between both approximations in some particular situations.

Conclusions

MC simulations have been implemented in order to give further insight on general issues in colloidal science beyond the classical framework based on the PB approximation and some other previous simulation works. The variation of charge density, salt concentration and ionic valence are known to be relevant parameters even in the classical framework. However, the size of components is known to be quite relevant in the mesoscopic scale. Our study provides evidence that ionic correlations not considered in the classical framework originated by the excluded volume and coulombic interactions can dramatically change the system behavior. Since the PM was chosen to model the solvent, the role of ionic size has been clearly elucidated and it has been found to be of tremendous importance at different levels.

The correct understanding of the underlying physical mechanisms at the molecular level can change our general conception of the colloidal systems and can be useful when proposing theoretical approximations to describing the EDL. It is important to develop more precise models in order to achieve analytical equations in close connection to the reality of the EDL.

Below conclusions and perspectives of particular issues are presented.

Electrokinetic phenomena

The charge-potential relationship from the modified PB theory that includes ionic size is found to work appreciably well for 1:1 salts, particularly for high surface charge densities and/or large ionic diameters. In contrast, the theory dramatically fails for 2:1 salts. The predictions of the dimensionless diffuse potential above the classic PB prediction are not corroborated by data from simulations, which are mostly under the PB curve. In consideration of the ionic correlations and excluded volume effects, a saturation regime was clearly identified from which the limitation of the theoretical model for the counterion concentrations in the vicinity of the charged surface contrasted dramatically with simulations results.

Our study of the effect of ionic dispersion forces on the behavior of the ζ-potential reveals that the ionic van der Waals interactions could contribute to salt specificity, but ionic size plays a fundamental role. According to the MC simulation data reported here, the hydrated ion size prevents intense ion-ion and colloid-ion dispersion forces in the case of mono- and divalent cations and some anions as well. Ionic dispersion forces would be responsible (to a great extent) for the salt specificity on ions with smaller diameters and larger ion-ion and colloid-ion dispersion parameters (such as SCN^-). These findings are in agreement with experimental electrophoretic

mobility data previously reported in the literature. A dehydration model that reduces the diameter of ions below the DCA is proposed. This incomplete hydration of ions close to the interface might enhance the specificity due to dispersion forces and serves as an alternative to specific adsorption when describing salt specificity.

Colloidal Stability

For monovalent ions, a broad collection of simulations was carried out and compared directly with the predictions of the classical DLVO theory. The net pressure is always repulsive for charged plates in both theoretical predictions and simulation results. A good agreement is found for ionic diameters of 0.4 nm (ionic diameter widely used in previous simulation works). For larger ionic diameters (from 0.7 nm), certain disagreements between theory and simulations are reported. If we admit that 0.4 nm is a rather small and unrealistic ionic diameter for many monovalent hydrated ions, the forces predicted by DLVO theory should be carefully reconsidered. Non-monotonic pressure profiles are reported by simulations for separations smaller than two ionic diameters if the surface charge density and/or ionic size are large enough. These discrepancies with the classical framework might be explained by thermal fluctuation of excess counterions in the confined region at small separations. The case of uncharged plates exhibits negative net pressures in the presence of monovalent electrolytes, whereas the classical theory predicts a null EDL interaction. This behavior can be explained in terms of correlated attractions among ions in the confined region (between the charged plates). This feature cannot be reproduced by the classical description of the EDL because it only considers continuous charge distributions.

For divalent ions we carried out calculations for both likely and oppositely charged plates, different surface charge densities and two very different ionic strengths. The effect of ion size is essential in the case of likely charged plates, because it is responsible for turning attraction into repulsion for highly charged systems. But, ion size seems irrelevant for oppositely charged plates. In relation to the effect of salt concentration, like-charged plates are not very sensitive to this parameter in the case of moderate and highly charged plates. On the contrary, we find the expected behavior for oppositely charged plates: electrostatic forces decay more rapidly when salt is added. Concerning the asymmetry between likely and oppositely charged plates, one should keep in mind that there is an excess of counterions for like-charged objects neutralizing their net charge. However, this excess is not required in the case of oppositely charged plates. Our simulations reveal that these divalent excess counterions rule to a great extent the behavior of like-charged plates.

The PM could be enhanced in order to compare with stability data of real colloids. The polarizability of materials should be included in the calculations (ion-ion and ion-colloid dispersion forces as well as macroion-macroion Hamaker forces). In this manner, even the role of salt specificity could be addressed by this model.

Other Applications of the *Primitive Model of Electrolyte*

Thermo-shrinking polyelectrolyte gels have been simulated within the framework of the PM. Hydrophobic forces have been considered through an effective solvent-mediated polymer-polymer interaction whose strength increases with temperature. This feature, which constitutes a novelty, plays an essential role in the mechanism underlying the thermo-shrinking behavior. However, our work also reveals that such potential derived from a one dimensional lattice model could overestimate the value of this interaction at high temperature. Two representative hydrophobic systems have been studied. For strongly hydrophobic systems, this interaction grows rapidly above certain temperature. Meanwhile for weakly hydrophobic systems, hydrophobic forces are weak and increase very gently upon heating. In both cases, polyelectrolyte gels shrink with temperature. However, weakly hydrophobic systems exhibit discontinuous volume changes, in agreement with many theories for thermo-sensitive gels and some experimental results. On the contrary, strongly hydrophobic gels do not show hallmarks of phase transitions, even for highly charged polyelectrolyte chains. Although this finding disagrees with theoretical predictions, it is in agreement with some experimental results. In the case of large polyelectrolyte chains, coexistence of swollen and shrunken states was also found for strongly hydrophobic gels, but this phenomenon is restricted to very short temperature intervals that would be hardly observable in practice.

There are still many issues to be addressed for polyelectrolyte gels such as the effect of added salt and ionic valence. To study the role of ionic size in polyelectrolyte gels could also provide valuable information for the behavior of these systems.

Concerning the electrolyte solutions of spheroidal ions, these have been analyzed with the help of computer simulations and a DFT. Both approaches appear as excellent tools for sampling the ionic correlations. Intra- and intercorrelations are found to affect the EDL. Ionic profiles are studied for two representative ionic diameters. In general, an excellent qualitative agreement between both approaches is depicted for conditions in the physiological regime. However, some intercorrelations arising from the excluded volume are neglected by the DFT leading to some inconsistencies. For instance, the DFT underestimates the electrochemical potential for the symmetric case of uncharged plates. When both individual elementary charges are at the center of the spheroid, the GCMC simulations within the modified PM were found to be in agreement with the basic PM.

The orientational ordering of spheroidal ions and the derived inter- and intracorrelations define ionic profiles beyond the classical PB theory. Further insight into the internal structures and the derived correlations should provide more knowledge and understanding of real systems with complex charge distributions.

References

1. Gouy, G. *J. Phys. (Paris)* **1910,** *9,* 457.
2. Chapman, D. L. *Philos. Mag.* **1913,** *25,* 475.
3. Stern, O. *Z. Electrochem.* **1924,** *30,* 508.
4. Grahame, D. C. *Chem. Rev.* **1947,** *41,* 441.
5. Israelachvili, J. N. *Intermolecular and Surface Forces;* Academic Press: London, 1985.
6. Hunter, R. J. *Z Potential in Colloid Science. Principles and Applications;* Academic Press: London, 1981.
7. Lyklema, J. In *Solid/Liquid Dispersions;* Academic Press: London, 1987; p Chapter 3.
8. Derjaguin, B. V.; Landau, L. *Acta Phys. Chim. (URSS)* **1941,** *14,* 633.
9. Verwey, E. J. W.; Overbeck, J. T. G. *Theory of the Stability of Lyophobic Colloids;* Elsevier: Amsterdam, 1948.
10. Craig, V. S. J.; Ninham, B. W.; Pashley, R. M. *J. Phys. Chem.* **1993,** *97,* 10192.
11. Messina, R.; González-Tovar, E.; Lozada-Cassou, M.; Holm, C. *Europhys. Lett.* **2002,** *60,* 383.
12. Boda, D.; Fawcett, W. R.; Henderson, D.; Sokolowski, S. *J. Chem. Phys.* **2002,** *116,* 7170.
13. Boda, D.; Henderson, D.; Plaschko, P.; Fawcett, W. R. *Mol. Simul.* **2004,** *30,* 137.
14. Bhuiyan, L. B.; Outhwaite, C. W. *Phys. Chem. Chem. Phys.* **2004,** *6,* 3467.
15. González-Tovar, E.; Jiménez-Ángeles, F.; Messina, R.; Lozada-Cassou, M. *J. Chem. Phys.* **2004,** *120,* 9782.
16. Valiskó, M.; Henderson, D.; Boda, D. *J. Phys. Chem. B* **2004,** *108,* 16548.
17. Quesada-Pérez, M.; Martín-Molina, A.; Hidalgo-Álvarez, R. *J. Chem. Phys.* **2004,** *121,* 8618.
18. Hamaker, H. C. *Physics* **1937,** *4,* 1058.
19. Lifshitz, E. M. *Sov. Phys. Usp.* **1956,** *2,* 73.
20. Dzyaloshinski, I. E.; Lifshitz, E. M.; Pitaevski, L. P. *Adv. Phys.* **1961,** *10,* 165.
21. Bikerman, J. J. *Philos. Mag.* **1942,** *33,* 384.
22. Sparnay, M. J. *Trav. Chim. Pays-Bas* **1954,** *51,* 635.
23. Carnahan, N. F.; Starling, K. E. *J. Chem. Phys.* **1969,** *51,* 635.
24. Boublik, T. *J. Chem. Phys.* **1970,** *53,* 471.
25. Mansoori, G. A.; Carnahan, N. F.; Starling, K. E.; Leland, T. W. *J. Chem. Phys.* **1971,** *54,* 1523.

26. Bhuiyan, L. B.; Outhwaite, C. W.; Levine, S. *Mol. Phys.* **1981,** *42,* 1271.
27. Levine, S.; Outhwaite, C. W.; Bhuiyan, L. B. *J. Electroanal. Chem.* **1981,** *123,* 105.
28. Lamperski, S.; Outhwaite, C. W. *Langmuir* **2002,** *18,* 3423.
29. Lamperski, S.; Bhuiyan, L. B. *J. Electroanal. Chem.* **2003,** *540,* 79.
30. Biesheuvel, P. M.; Lyklema, J. *J. Phys.: Condens. Matter* **2005,** *17,* 6337.
31. Biesheuvel, P. M.; Leermakers, F. A. M.; Cohen Stuart, M. A. *Phys. Rev. E* **2006,** *73,* 011802.
32. Biesheuvel, P. M.; van Soestbergen, M. *J. Colloid Interface Sci.* **2007,** *316,* 490.
33. Mcdonald, J. R. *J. Electroanalytical Chem.* **1987,** *223,* 1.
34. Kralj-Iglic, V.; Iglic, A. *J. Phys. II (France)* **1996,** *6,* 477.
35. Lue, L.; Zoeller, N.; Blankschtein, D. *Langmuir* **1999,** *15,* 3726.
36. Bohinc, K.; Kralj-Iglic, V.; Iglic, A. *Electrochim. Acta* **2001,** *46,* 3033.
37. Borukhov, I.; Andelman, D.; Orland, H. *Phys. Rev. Lett.* **1997,** *79,* 435.
38. González-Amezcua, O.; Hernádez-Contreras, M. *J. Chem. Phys.* **2004,** *121,* 10742.
39. Tang, Z.; Scriven, L. E.; Davis, H. T. *J. Chem. Phys.* **1992,** *97,* 9258.
40. Carnie, S. L.; Chan, D. Y. C.; Mitchell, D. J.; Ninham, B. W. *J. Chem. Phys.* **1981,** *74,* 1472.
41. Lozada-Casou, M.; Saavedra-Barrera, R.; Henderson, D. *J. Chem. Phys.* **1982,** *77,* 5150.
42. Kjellander, R.; Åkesson, T.; Jönsson, B.; Marcelja, S. *J. Chem. Phys.* **1992,** *97,* 1424.
43. Quesada-Pérez, M.; González-Tovar, E.; Martín-Molina, A.; Lozada-Cassou, M.; Hidalgo-Álvarez, R. *Chem. Phys. Chem.* **2003,** *4,* 234.
44. Belloni, L. *J. Phys.: Condens. Matter* **2000,** *12,* R549.
45. Hansen, J. P.; Löwen, H. *Annu. Rev. Phys. Chem.* **2000,** *51,* 209.
46. Quesada-Pérez, M.; Callejas-Fernández, J.; Hidalgo-Álvarez, R. *Adv. Colloid Interface Sci.* **2002,** *95,* 295.
47. Hatlo, M. M.; Lue, L. *Soft Matter* **2008,** *4,* 1582.
48. Lyklema, J. *Adv. Colloid Interface Sci.* **2009,** *147-148,* 205.
49. Dahirel, V.; Jardat, M. *Curr. Op. Colloid Interface Sci.* **2010,** *15,* 2.
50. Frenkel, D.; Smit, B. *Understanding Molecular Simulation from Algorithms to Applications;* Academic Press: London, 1992.
51. Guldbrand, L.; Jönsson, B.; Wennerström, H.; Linse, P. *J. Chem. Phys.* **1984,** *80,* 2221.
52. Valleau, J. P.; Ikov, R.; Torrie, G. M. *J. Chem. Phys.* **1991,** *95,* 520.
53. Khan, M. O.; Petris, S.; Chan, D. Y. C. *J. Chem. Phys.* **2005,** *122,* 104705.
54. Madurga, S.; Martín-Molina, A.; Vilaseca, E.; Mas, F.; Quesada-Peréz, M. *J. Chem. Phys.* **2007,** *126,* 234703.
55. Lewith, S. *Arch. Exp. Pathol. Pharmakol.* **1888,** *24,* 1.
56. Hofmeister, F. *Arch. Exp. Pathol. Pharmakol.* **1888,** *24,* 247.
57. Collins, K. D.; Washabaugh, M. W. *Q. Rev. Biophys.* **1985,** *18,* 323.
58. Ninham, B. W.; Yaminsky, V. *Langmuir* **1997,** *13,* 2097.

59. Schubin, V. E.; Kekicheff, P. *J. Colloid Interface Sci.* **1993,** *155,* 108.
60. Boström, M.; Williams, D. R. M.; Ninham, B. W. *Phys. Rev. Lett.* **2001,** *87,* 168103.
61. Tavares, F. W.; Bratko, D.; Blanch, H. W.; Prausnitz, J. M. *J. Phys. Chem. B* **2004,** *108,* 9228.
62. Boström, M.; Tavares, F. W.; Ninham, B. W.; Prausnitz, J. M. *J. Phys. Chem. B* **2006,** *110,* 24757.
63. Lima, E. R. A.; Horinek, D.; Netz, R. R.; Biscaia, E. C.; Tavares, F. W.; Kunz, W.; Boström, M. *J. Phys. Chem. B* **2008,** *112,* 1580.
64. Quesada-Perez, M.; Hidalgo-Álvarez, R.; Martín-Molina, A. *Colloid Polym. Sci.* **2010,** *288,* 151.
65. Parsons, D. F.; Ninham, B. W. *Langmuir* **2010,** *26,* 1816.
66. Parsons, D. F.; Boström, M.; Maceina, T. J.; Salis, A.; Ninham, B. W. *Langmuir* **2010,** *26,* 3323.
67. Boström, M.; Tavares, F. W.; Bratko, D.; Ninham, B. W. *J. Phys. Chem.* **2005,** *109,* 24489.
68. Maset, S.; Bohinc, K. *J. Phys. A: Math. Theor.* **2007,** *40,* 11815.
69. Urbanija, J.; Bohinc, K.; Bellen, A.; Maset, S.; Iglič, A.; Kralj-Iglič, V.; Kumar, P. B. S. *J. Chem. Phys.* **2008,** *129,* 105101.
70. Maset, S.; Reščič, J.; May, S.; Pavlič, J. I.; Bohinc, K. *J. Phys. A: Math. Theor.* **2009,** *42,* 105401.
71. Megistu, D. H.; Bohinc, K.; May, S. *EPL* **2009,** *88,* 14003.
72. Grime, J. M. A.; Khan, M. O.; Bohinc, K. *Langmuir* **2010,** *26,* 6343.
73. Megistu, D. H.; Bohinc, K.; May, S. *J. Phys. Chem. B* **2009,** *113,* 12277.
74. Escobedo, F. A.; de Pablo, J. J. *Phys. Rep.* **1999,** *318,* 85.
75. Schneider, S.; Linse, P. *J. Chem. B* **2003,** *107,* 8030.
76. Schneider, S.; Linse, P. *Macromolecules* **2004,** *37,* 3850.
77. Sawai, T.; Yamazaki, S.; Ikariyama, Y.; Aizawa, M. *J. Electroanal. Chem.* **1992,** *322,* 1.
78. Kajiwara, K.; Rossmurphy, S. B. *Nature (London)* **1992,** *355,* 208.
79. Murray, M. J.; Snowden, M. J. *Adv. Colloid Interface Sci.* **1995,** *54,* 73.
80. Peppas, N. A. *Curr. Opin. Colloid Interface Sci.* **1997,** *2,* 531.
81. Pelton, R. *Adv. Colloid Interface Sci.* **2000,** *85,* 1.
82. Ramos, J.; Imaz, A.; Callejas-Fernández, J.; Barbosa-Barros, L.; Estelrich, J.; Quesada-Pérez, M.; Forcada, J. *Soft Matter* **2011,** *7,* 5067.
83. Dobrynin, A. V. *Curr. Opin. Colloid Interface Sci.* **2008,** *13,* 376.
84. Fermi, E.; Pasta, J. G.; Ulam, S. M. *Studies of Non-Linear Problems;* LASL Report: Los Alamos, 1955; LA-1940.
85. Card, D. N.; Valleau, J. P. *J. Chem. Phys.* **1970,** *52,* 6232.
86. Rasaiah, J. C.; Card, D. N.; Valleau, J. P. *J. Chem. Phys.* **1972,** *56,* 248.
87. Adams, D. J. *Mol. Phys.* **1974,** *28,* 1241.
88. Adams, D. J. *Mol. Phys.* **1975,** *29,* 307.
89. Valleau, J. P.; Cohen, L. K. *J. Chem. Phys.* **1980,** *72,* 5935.

90. Torrie, G. M.; Valleau, J. P. *J. Chem. Phys.* **1980,** *73,* 5807.
91. Lamperski, S. *Mol. Sim.* **2007,** *33,* 1193.
92. Lamperski, S.; Outhwaite, C. W. *J. Colloid Interface Sci.* **2008,** *328,* 458.
93. Malasics, A.; Gillespie, D.; Boda, D. *J. Chem. Phys.* **2008,** *128,* 124102.
94. Lekner, J. *Physica A* **1991,** *176,* 485.
95. Sperb, R. *Mol. Sim.* **1998,** *20,* 179.
96. Boda, D.; Chan, K. Y.; Henderson, D. *J. Chem. Phys.* **1998,** *109,* 7362.
97. Pegado, L.; Jönsson, B.; Wennerström, H. *J. Chem. Phys.* **2008,** *129,* 184503.
98. Martín-Molina, A.; Quesada-Pérez, M.; Galisteo-González, F.; Hidalgo-Álvarez, R. *J. Chem. Phys.* **2003,** *118,* 4183.
99. Wernersson, E.; Kjellander, R.; Lyklema, J. *J. Phys. Chem. C* **2010,** *114,* 1849.
100. López-León, T.; Jódar-Reyes, A. B.; Bastos-González, D.; Ortega-Vinuesa, J. L. *J. Phys. Chem.* **2003,** *107,* 5696.
101. López-León, T.; Jódar-Reyes, A. B.; Ortega-Vinuesa, J. L.; Bastos-González, D. *J. Colloid Interface Sci.* **2005,** *284,* 139.
102. López-León, T.; Gea-Jódar, P. M.; Bastos-González, D.; Ortega-Vinuesa, J. L. *Langmuir* **2005,** *284,* 139.
103. López-León, T.; Elaïssari, A.; Ortega-Vinuesa, J. L.; Bastos-González, D. *Chem. Phys. Chem.* **2007,** *8,* 148.
104. López-León, T.; Fernández-Nieves, A. *Phys. Rev. E* **2007,** *75,* 011801.
105. López-León, T.; Bastos-González, D.; Ortega-Vinuesa, J. L.; Elaïssari, A. *Chem. Phys. Chem.* **2010,** *11,* 188.
106. López-García, J. J.; Aranda-Rascón, M. J.; Horno, J. *Colloid Interface Sci.* **2007,** *316,* 196.
107. López-García, J. J.; Aranda-Rascón, M. J.; Horno, J. *J. Colloid Interface Sci.* **2008,** *323,* 146.
108. Adamczyk, Z.; Belouschek, P.; Lorenz, D. *Ber. Bunsenges. Phys.* **1990,** *94,* 1483.
109. Adamczyk, Z.; Belouschek, P.; Lorenz, D. *Bull. Pol. Ac. Chem.* **1991,** *39,* 424.
110. Adamczyk, Z.; Belouschek, P.; Lorenz, D. *Adv. Colloid Interface Sci.* **1996,** *63,* 41.
111. Brodowsky, H.; Strehlow, H. *Z. Electrochem.* **1950,** *63,* 262.
112. Wicke, E.; Eigen, M. *Z. Electrochem.* **1952,** *56,* 551.
113. Quesada-Pérez, M.; González-Tovar, E.; Martín-Molina, A.; Lozada-Cassou, M.; Hidalgo-Álvarez, R. *Colloid Surf. A* **2005,** *267,* 24.
114. Pashley, R. M.; McGuiggan, P. M.; Ninham, B. W.; Brady, J.; Evans, D. F. *J. Phys. Chem.* **1986,** *90,* 1637.
115. Kekicheff, P.; Marcelja, S.; Senden, T. J.; Shubin, V. E. *J. Chem. Phys.* **1993,** *99,* 6098.
116. Considine, R. F.; Hayes, R. A.; Horn, R. G. *Langmuir* **1999,** *15,* 1657.
117. Besteman, K.; Zevenbergen, M. A. G.; Heering, H. A.; Lemay, S. G. *Phys. Rev. Lett.* **2004,** *93,* 170802.
118. Besteman, K.; Zevenbergen, M. A. G.; Lemay, S. G. *Phys. Rev. E* **2005,** *72,* 061501.

119. Pashley, R. M.; Israelachvili, J. N. *J. Colloid Interface Sci.* **1983,** *97,* 446.
120. Pashley, R. M.; Israelachvili, J. N. *J. Colloid Interface Sci.* **1984,** *101,* 511.
121. Pashley, R. M.; Quirk, J. P. *Colloids and Surfaces* **1984,** *9,* 1.
122. McGuiggan, P. M.; Pashley, R. M. *J. Phys. Chem.* **1988,** *92,* 1235.
123. Kjellander, R.; Marcelja, S.; Pashley, R. M.; Quirk, J. P. *J. Chem. Phys.* **1990,** *92,* 4399.
124. Pashley, R. M. *J. Colloid Interface Sci.* **1981,** *83,* 531.
125. Fielden, M. L.; Hayes, R. A.; Ralston, J. *Phys. Chem. Chem. Phys.* **2000,** *2,* 2623.
126. Vlachy, V. *Annu. Rev. Phys. Chem.* **1999,** *50,* 145.
127. Attard, P. *Curr. Opin. Colloid Interface Sci.* **2001,** *6,* 366.
128. Allahyarov, E.; Damico, I.; Lowen, H. *Phys. Rev. Lett.* **1998,** *81,* 1334.
129. Wu, J. Z.; Bratko, D.; Blanch, H. W.; Prausnitz, J. M. *J. Chem. Phys.* **1999,** *111,* 7084.
130. Wu, J. Z.; Bratko, D.; Blanch, H. W.; Prausnitz, J. M. *J. Chem. Phys.* **2000,** *113,* 3360.
131. Ravindran, S.; Wu, J. Z. *J. Phys.: Condens. Matter* **2005,** *8,* 377.
132. Meyer, S.; Delville, A. *Langmuir* **2001,** *17,* 7433.
133. Marrink, S. J.; Marcelja, S. *Langmuir* **2001,** *17,* 7929.
134. Moreira, A. G.; Netz, R. R. *Eur. Phys. J. E* **2002,** *8,* 33.
135. Angelescu, D. G.; Linse, P. *Langmuir* **2003,** *19,* 9661.
136. Linse, P. *Adv. Polym. Sci.* **2005,** *185,* 111.
137. Jönsson, B.; Nonat, A.; Labbez, C.; Cabane, B.; Wennerström, H. *Langmuir* **2005,** *21,* 9211.
138. Taboada-Serrano, P.; Yiacoumi, S.; Tsouris, C. *J. Chem. Phys.* **2006,** *125,* 054716.
139. Trulsson, M.; Jönsson, B.; Åkesson, T.; Forsman, J. *Langmuir* **2007,** *23,* 11562.
140. Martín-Molina, A.; Maroto-Centeno, J. A.; Hidalgo-Álvarez, R.; Quesada-Pérez, M. *Colloid. Surf. A* **2007,** *319,* 103.
141. Holm, C.; Joanny, J. F.; Kremer, K.; Netz, R. R.; Reineker, P.; Seidel, C.; Vilgis, T. A.; Winkler, R. G. *Adv. Polym. Sci.* **2004,** *166,* 67.
142. Dobrynin, A. V. *Prog. Polym. Sci.* **2005,** *30,* 1049.
143. Khokhlov, A. R.; Khalatur, P. G. *Curr. Opin. Colloid Interface Sci.* **2005,** *10,* 22.
144. Dobrynin, A. V.; Colby, R. H.; Rubinstein, M. *J. Polym. Sci. B* **2004,** *42,* 3513.
145. Thunemann, A. F.; Muller, M.; Dautzenberg, H.; Joanny, J. F.; Lowne, H. *Adv. Polym. Sci.* **2004,** *166,* 113.
146. Cooper, C. L.; Dubin, P. L.; Kayitmazer, A. B.; Turksen, S. *Curr. Opin. Colloid Interface Sci.* **2005,** *10,* 52.
147. Ulrich, S.; Seijo, M.; Stoll, S. *Curr. Opin.Colloid Interface Sci.* **2006,** *11,* 268.
148. Teif, V. B.; Bohinc, K. *Prog. Biophys. Mol. Biol.* **2011,** *105,* 208.
149. Lutkenhaus, J. L.; Hammond, P. T. *Soft Matter* **2007,** *3,* 804.
150. Korin, E.; Siton, O.; Bettelheim, A. *Rev. Chem. Eng.* **2007,** *23,* 35.
151. Remaut, K.; Sanders, N. N.; De Geest, B. G.; Braeckmans, K.; Demeester, J.; De Esmedt, S. C.

Mat. Sci. Eng. R **2007,** *58,* 117.

152. Peppas, N. A.; Bures, P.; Leobandung, W.; Ichikawa, H. *Eur. J. Pharm. Biopharm.* **2000,** *50,* 27.
153. Gupta, P.; Vermani, K.; Garg, S. *Drug Discovery Today* **2002,** *7,* 569.
154. Raemdonck, K.; Demeester, J.; De Smedt, S. *Soft Matter* **2009,** *5,* 707.
155. Peppas, N. A.; Hilt, J. Z.; Khademhosseini, A.; Langer, R. *Adv. Matter.* **2006,** *18,* 1345.
156. Nayak, S.; Lyon, L. A. *Angew. Chem. Int. Ed.* **2005,** *44,* 7686.
157. Oh, J. K.; Drumright, R.; Siegwart, D. J.; Matyjaszewski, K. *Prog. Polym. Sci.* **2008,** *33,* 448.
158. Malmsten, M. *Soft Matter* **2006,** *2,* 760.
159. Aalberts, D. P. *J. Chem. Phys.* **1996,** *104,* 4309.
160. Yan, Q.; de Pablo, J. J. *Phys. Rev. Lett.* **2003,** *91,* 018301.
161. Lu, Z.-Y.; Hentschke, R. *Phys. Rev. E* **2003,** *67,* 061807.
162. Edgecombe, S.; Schneider, S.; Linse, P. *Macromolecules* **2004,** *37,* 10089.
163. Mann, B. A.; Everaers, R.; Holm, C.; Kremer, K. *Europhys. Lett.* **2004,** *67,* 786.
164. Mann, B. A.; Holm, C.; Kremer, K. *J. Chem. Phys.* **2005,** *122,* 154903.
165. Yin, D. -W.; Yan, Q.; de Pablo, J. J. *J. Chem. Phys.* **2005,** *123,* 174909.
166. Edgecombe, S.; Linse, P. *Langmuir* **2006,** *22,* 3836.
167. Edgecombe, S.; Linse, P. *Macromolecules* **2007,** *40,* 3868.
168. Yin, D. -W.; Olvera de la Cruz, M.; de Pablo, J. J. *J. Chem. Phys.* **2009,** *131,* 194907.
169. Claudio, G. C.; Kremer, K.; Holm, C. *J. Chem. Phys.* **2009,** *131,* 094903.
170. Jha, P. K.; Zwanikken, J. W.; Detcheverry, F. A.; de Pablo, J. J.; Olvera de la Cruz, M. *Soft Matter* **2011,** *7,* 5965.
171. Olvera de la Cruz, M. *Soft Matter* **2008,** *4,* 1735.
172. Shibayama, M.; Tanaka, T. Phase Transitions and Related Phenomena. In *Responsive Gels: Volume Transitions I;* Dusek, K., Ed.; Springer-Verlag: Berlin, 1993.
173. Kokofuta, E. Phase Transitions in Polyelectrolyte Gels. In *Physical Chemistry of Polyelectrolytes;* Radeva, T., Ed.; Marcel Dekker: New York, 2001.
174. Kolomeisky, A. B.; Widom, B. *Faraday Discuss.* **1999,** *112,* 81.
175. Barkema, G. T.; Widom, B. *J. Chem. Phys.* **2000,** *113,* 2349.
176. Koga, K.; Bhimalapuram, P.; Widom, B. *Mol. Phys.* **2000,** *100,* 3795.
177. Hirotsu, S.; Hirokawa, Y.; Tanaka, T. *J. Chem. Phys.* **1987,** *87,* 1392.
178. Shibayama, M.; Shirotani, Y.; Hirose, H.; Nomura, S. *Macromolecules* **1997,** *30,* 7307.
179. László, K.; Kosik, K.; Geissler, E. *Macromolecules* **2004,** *37,* 10067.
180. Capriles-González, D.; Sierra-Martín, B.; Fernández-Nieves, A.; Fernández-Barbero, A. *J. Phys. Chem. B* **2008,** *112,* 12195.
181. Mamytbekov, G.; Bouchal, K.; Ilavsky, M. *Eur. Polym. J.* **1999,** *35,* 1925.
182. Imaz, A.; Forcada, J. *J. Polym. Sci., Part A: Polym. Chem.* **2008,** *46,* 2510.

183. Imaz, A.; Forcada, J. *J. Polym. Sci., Part A:Polym. Chem.* **2008,** *46,* 2766.
184. Popa, I.; Trulsson, M.; Papastavrou, G.; Borkovec, M.; Jönsson, B. *Langmuir* **2009,** *25,* 12435.
185. Igarashi, M.; Matsuura, E.; Igarashi, Y.; Nagae, H.; Ichikawa, K.; Triplett, D. A.; Koike, T. *blood* **1996,** *87,* 3262.
186. Urbanija, J.; Tomšič, N.; Lokar, M.; Ambrožič, A.; Čučnik, S.; Rozman, B.; Kandušer, M.; Iglič, A.; Kralj-Iglič, V. *Chem. Phys. Lip.* **2007,** *150,* 49.
187. Henderson, D.; Blum, L. *J. Chem. Phys.* **1978,** *69,* 5441.
188. Henderson, D.; Blum, L.; Lebowitz, L. *J. Electroanal. Chem.* **1979,** *102,* 315.
189. Kjellander, R.; Bunsenges, B. *Phys. Chem.* **1996,** *100,* 894.
190. Holovko, M. F.; Badiali, J. P.; di Caprio, D. *J. Chem. Phys.* **2005,** *123,* 234705.
191. Holovko, M. F.; Badiali, J. P. *Condensed Matter Physics* **2005,** *8,* 281.
192. Holovko, M. F.; Badiali, J. P.; di Caprio, D. *J. Chem. Phys.* **2007,** *127,* 014106.
193. Flory, P. J.; Rehner, J. J. *J. Chem. Phys.* **1943,** *11,* 512.
194. Flory, P. J.; Rehner, J. J. *J. Chem. Phys.* **1943,** *11,* 521.
195. Otake, K.; Inomata, H.; Konno, K.; Saito, S. *J. Chem Phys* **1989,** *91,* 1345.
196. Marchetti, M.; Prager, S.; Cussler, E. L. *Macromolecules* **1990,** *23,* 1760.
197. Hino, T.; Prausnitz, J. M. *Polymer* **1998,** *39,* 3279.
198. Hohng, Y. P.; Bae, Y. C. *J. Polym. Sci., Part B: Polym. Phys.* **2002,** *40,* 2333.
199. Li, H.; Wang, X.; Yan, G.; Lam, K. Y.; Cheng, S.; Zou, T.; Zhuo, R. *Chem. Phys.* **2005,** *309,* 201.
200. Huang, Y.; Jin, X.; Liu, H.; Hu, Y. *Fluid Phase Equilib.* **2008,** *263,* 96.
201. Jung, S. C.; Oh, S. Y.; Bae, Y. C. *Polymer* **2009,** *50,* 3370.
202. Khalatur, P. G.; Khokhlov, A. R.; Mologin, D. A.; Reineker, P. *J. Chem. Phys.* **2003,** *113,* 1232.

Paper I

Testing a modified model of the Poisson Boltzmann theory that includes ion size effects through Monte Carlo simulations

José Guadalupe Ibarra-Armenta[1], Alberto Martín-Molina[2] and Manuel Quesada-Pérez[1]•

Phys. Chem. Chem. Phys., **2009**, *11*, 309.

(1) Departamento de Física, Escuela Politécnica Superior de Linares, Universidad de Jaén, 23700, Linares, Jaén, Spain.

(2) Grupo de Física de Fluidos y Biocoloides, Departamento de Física Aplicada, Facultad de Ciencias, Universidad de Granada, 18071 Granada, Spain.

* Corresponding author

Abstract.
In this work we test the validity of a recent modified Poisson-Boltzmann (MPB) theory that includes ion size effects through a Langmuir-type correction. In particular, we will focus on an analytic charge-potential relationship accounting for such effects. Previous electric double layer (EDL) surveys have demonstrated that the inclusion of ions size in classical EDL theories, based on the Poisson-Boltzmann (PB) equation, can yield considerable improvements. In this sense, the theory we analyze assumes that, as a result of the excluded volume, the ion concentration close to the charged surface cannot exceed a fixed value determined by the close packing fraction. This leads to predictions of counterion concentrations (in this region) smaller than the corresponding PB values. In our opinion, it is worthwhile to test the validity of this novel theory. To this end, computer simulations appear as a useful tool for this kind of task. Our results prove that the above-mentioned analytical expression works fairly well for 1:1 electrolytes and large ions, and its predictions can be considerably improved with certain corrections in the estimation of some key parameters. However, it fails for multivalent electrolytes.

1. Introduction.
For many decades, the PB equation has been the cornerstone of the classical EDL theory. It has been extensively applied in colloid science, chemical physics as well as other research fields (e.g., semiconductor physics). Its conceptual and mathematical simplicity is responsible for the success of this classical approach. However, certain limitations of this mean field theory were obvious from the beginning. For instance, Stern was the first who noticed that the PB equation predicts unrealistic concentrations of counterions in the vicinity of the charged interface as a result of neglecting the ion dimensions. He tried to overcome this deficiency introducing the notion of the so-called Stern layer.[1] However, the direct inclusion of ion size effects in the PB equation dates back to Bikerman, who added an excess term to the ideal chemical potential with this purpose.[2] Since then, different corrections to the chemical potential have been proposed.[3-9] Other authors have developed alternative approaches, such as lattice-based models,[10-13] different modified PB equations[14-17] or integral equation theories.[18-20]
Nowadays ion size effects are still a burning issue in colloid science. For instance, some researchers have recently studied their role in the ion layering at high salt concentrations,[17] counterintuitive electrostatic phenomena (e.g. charge inversion[20]) and the competition of different ions in solutions with electrolyte mixtures. [9] The deviations from the PB predictions of the charge-potential relationship have also been looked into in recent times.[21-23] In particular, López-García *et al*. have analyzed a MPB equation that takes the finite ion size into account through a Langmuir-type correction.[24] What is more, they have put forward an approximate analytical expression (including volume effects) for the charge-potential relationship. This could indeed be a valuable result since the surface charge density and the electric potential at the Outer Helmholtz Plane (OHP), usually known as diffuse potential, are key parameters in the description of the EDL. In any case, these authors claim that significant discrepancies with the

classical predictions can appear even for typical sizes of hydrated ions (ranging mostly from 0.75 to 1 nm).[25] In addition, López-García *et al*. have also extended their results to a nonequilibrium problem, calculating the effect of ion size on the electrophoretic mobility of a rigid spherical particle.[26]

In any case, one should keep in mind that the approach and the analytical expression proposed by López-García *et al*. were developed under certain assumptions. For instance, as a consequence of the excluded volume, the ion concentration in the vicinity of the charged surface cannot exceed a given value (determined by close packing). For that reason the Maxwell-Boltzmann distribution is modified introducing a Langmuir-type correction (as mentioned above). This is certainly an approximation whose validity could deserve further studies. In fact, it leads to predictions in disagreement with other approaches and simulations results. More specifically, monotonic ionic profiles with a saturation value next to the charged surface are reported from such approximation whereas other recent approaches predict non-monotonic profiles at high salt concentrations.[17] This feature has also been corroborated by computer simulations.[17,27] In addition, other theoretical and simulation results suggest that ion size effects go beyond expected (and intuitive) excluded volume effects. For instance, under certain conditions, the ion concentration in the proximity of the surface predicted by integral equation theories (accounting for ion size) is larger than that predicted by the PB scheme.[20,27,28] Consequently, the reliability of the approach devised by the above-mentioned authors should be carefully examined. Computer simulations have become a useful tool for tasks like this in the last decades.

The aim of this work is therefore to test the validity of the analytical charge-potential relationship proposed by López-García *et al.* by means of Monte Carlo (MC) simulations. We will restrict ourselves to the case of a planar EDL. In our opinion, this is a good reference system because the solution of the PB equation is exact whereas for spherical particles only approximate solutions exist. Consequently, the discrepancies between simulation/MPB results and the classical PB theory can be unequivocally attributed to the inclusion of ion size effects. In addition, the solution for a planar EDL is widely known and even applied to spherical particles if the salt concentration is high enough. This is just when the ion volume effects are expected to be significant. The rest of the paper is organized as follows. First, some features of the so called charge-potential relationship are outlined and also some technical details about the MC simulations carried out in this work. Then, the computer simulation results are presented and compared to the theoretical predictions. Finally, some conclusions are highlighted.

2. Theory and simulations.

In order to describe the spatial distribution of ionic species and the electrostatic potential distribution in the vicinity of a spherical macroion immersed in an infinite electrolyte solution, López-García *et al.* use a MPB approach that includes the volume excluded by the ions. To this end, the authors use a model developed in the 1990´s by Adamczyk *et al*.[29-31] which is in turn based on certain theories of the 1950's.[32,33] The ionic concentrations and the electric potential

profiles are obtained as functions of the parameter $c^{\max}$, which stands for the maximum attainable concentration of the corresponding ions due to the volume occupied by each one of them (close packing). Considering the Langmuir-type correction for the excluded volume introduced by Adamczyk and Warszysnky,[31] the local ion concentration can be expressed as

$$c_i(\xi) = \frac{c_i^{\infty} \exp[-Z_i y(\xi)]}{1 + \sum_{i=1}^{m} \frac{c_i^{\infty}}{c_i^{\max}} \{\exp[-Z_i y(\xi)] - 1\}} \tag{1}$$

Here Z_i and c_i^{∞} are the valence and the bulk concentration of the ionic species *i*, respectively, $c_i^{\max}$ is the maximum attainable concentration of the given ion type, and y and ξ are the dimensionless electric potential and the dimensionless spatial variable, respectively. The dimensionless electric potential is defined as:

$$y = \frac{e\phi(r)}{k_{\beta}T} \tag{2}$$

where e is the elementary charge, $\phi(r)$ is the electric potential, T is the absolute temperature and k_B is the Boltzmann constant. The dimensionless spatial variable is $\xi = \kappa(r - a)$, where a is the radius of the spherical macroion and κ the reciprocal Debye length,

$$\kappa = \sqrt{\frac{e^2 N_A \sum_{i=1}^{m} Z_i^2 c_i^{\infty}}{k_B T \varepsilon_0 \varepsilon_r}} \tag{3}$$

Here, ε_0 is the permittivity of the free space, ε_r is the relative permittivity of the solvent and N_A is the Avogadro number. In this case, water at room temperature is assumed.

Substituting these dimensionless variables and local ion concentration in the PB equation for a charged spherical particle we obtain

$$\frac{d^2 y(\xi)}{d\xi^2} + \frac{2}{\xi + \kappa a} \frac{dy(\xi)}{d\xi} = - \frac{\sum_{i=1}^{m} Z_i c_i^{\infty} \exp[-Z_i y(\xi)]}{\sum_{i=1}^{m} Z_i^2 c_i^{\infty} \left\{1 + \sum_{i=1}^{m} \frac{c_i^{\infty}}{c_i^{\max}} \{\exp[-Z_i y(\xi)] - 1\}\right\}} \tag{4}$$

This is the MPB equation that describes the spatial variation of the electric potential for the EDL of a spherical charged particle, considering the finite size of ions.

To solve eqn (4) López-García *et al.* performed numerical calculations using the network simulation method, and obtained the electrostatic potential and the ion concentration profiles as a function of the distance from the surface of the macroion. These authors also propose approximate expressions (matching the numerical solution) for the charge-potential relationship. In particular, for large values of κa (planar EDL), such relationship turns out to be:

$$\frac{e\sigma_0}{kT\varepsilon_0\varepsilon_r\kappa}=\left(\frac{2c^{\max}}{\sum_{i=1}^{m}Z_i^2c_i^{\infty}}\ln\left\{1+\sum_{i=1}^{m}\frac{c_i^{\infty}}{c^{\max}}\left[\exp(-Z_ie\psi_d/k_BT)-1\right]\right\}\right)^{1/2} \quad (5)$$

where σ_0 is the surface charge density of the charged wall and ψ_d is the diffuse potential. This is the equation that relates the dimensionless diffuse potential and the dimensionless surface charge density and takes ion size into account (for further details we refer the reader to the original paper[24]).

The MC simulations carried out in this work are based on a primitive model (PM) of electrolyte, in which ions are considered as charged hard spheres and the solvent is modelled as a continuum with a uniform dielectric permittivity. We applied the Metropolis algorithm to a canonical ensemble for a collection of N ions confined in a rectangular prism (simulation cell) at constant temperature. The simulation cell has the dimensions $W\times W\times L$, where a charged plane wall is located at $z=0$ and at $z=L$ another impenetrable but uncharged plane wall is placed. Periodic boundary conditions were used in the lateral directions (x and y). The simulation cell contains the ionic electrolyte mixture corresponding to the bulk solution within a counterion excess neutralizing the surface charge of the charged wall to ensure the whole simulation cell is always neutral. The interaction energy between the mobile ions is given by

$$u(r_{ij})=\frac{Z_iZ_je^2}{4\pi\varepsilon_0\varepsilon_r r_{ij}} \qquad r_{ij}>d$$
$$u(r_{ij})=\infty \qquad r_{ij}<d \quad (6)$$

where d is the hydrated ion diameter (for all the ionic species), and $r_{ij}=\left|\vec{r}_{ij}\right|$ the distance between the ions i and j. Eqn (6) accounts for the hard sphere nature of ions in the PM. The interaction energy of ion i with the charged wall is

$$u(z_i)=-\frac{\sigma_0Z_iez_i}{2\varepsilon_0\varepsilon_r} \quad (7)$$

z_i is the z-coordinate of particle i. Due to the long range of the electrostatic interactions, the energy must be evaluated carefully. In these simulations, we have applied a procedure originally devised by Lekner and improved by Sperb later,[34,35] to which we will refer as the Lekner-Sperb method (LSM). Lekner adapted the conventional Ewald summation for systems with two-dimensional periodicity as follows. A charge at $\vec{r}'$ and its periodic replicas in x and y generate an interaction potential energy, per elementary charge, at $\vec{r}$. This potential energy is given by

$$v(\gamma,\eta,\zeta)=\frac{e^2}{4\pi\varepsilon_0\varepsilon_rW}\sum_{l,m=-\infty}^{\infty}\frac{1}{\sqrt{(\gamma+l)^2+(\eta+m)^2+\zeta^2}}. \quad (8)$$

where the following rescaled coordinates have been used

$$\gamma = |x - x'|/W\ ,\ \eta = |y - y'|/W\ ,\ \zeta = |z - z'|/W\ . \tag{9}$$

According to Lekner, this interaction potential energy can also be expressed as

$$v(\gamma,\eta,\zeta) = \frac{e^2}{4\pi\varepsilon_0\varepsilon_r W}\{C - \ln[\cosh(2\pi\zeta) - \cos(2\pi\eta)] + s(\gamma,\eta,\zeta)\}, \tag{10}$$

where *C* is a constant depending on the reference state, and *s* is the fast converging series

$$s(\gamma,\eta,\zeta) = 4\sum_{l=1}^{+\infty}\cos(2\pi l/\gamma)\times\left\{\sum_{m=-\infty}^{+\infty}K_0\left(2\pi l\sqrt{(\eta+m)^2+\zeta^2}\right)\right\} \tag{11}$$

At large arguments of s this sum can be truncated due to the rapidly vanishing behaviour of the Bessel function, K_0. Nonetheless, for low values of $\sqrt{(\eta+m)^2+\zeta^2}$ the function diverges, and a large number of terms could be required before its truncation. Sperb proposed a solution to this problem,[35] that we have applied together with the truncation criteria developed by Moreira and Netz.[36] Previous studies suggest that the LSM results are practically identical to those obtained with the so-called external potential method (which is not based on Ewald summations).[27] However, LSM simulations are more reliable at low salt concentrations and offers manageable expressions and well established truncation criteria. For these reasons, this method for evaluating energy was preferred.

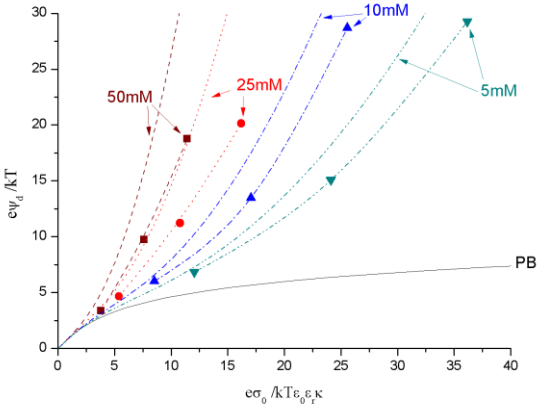

Fig. 1. Diffuse potential as function of surface charge obtained from simulations (symbols) and theoretical predictions (lines) for 2 nm ions at various salt concentrations: 50 mM (squares and dashed lines), 25 mM (circles and dot lines), 10 mM (up triangles and dash-dot lines), 5 mM (down triangles and dash dot dot lines). The lines accompanying the symbols obtained from simulations are just a guide for the eye. PB theory prediction is presented too (solid line). $c^{\max}$ is calculated for a SC arrangement.

Each simulation took between 60000 and 180000 steps per particle and the simulation systems were always thermalized before collecting data for averaging. The number of particles was

maintained around 100 and for some representative systems it was doubled to check that the cell size was large enough and no important statistical deviations were induced. The acceptance ratio was kept between 0.3 and 0.5. The values of W, L and N vary according to the ion concentrations employed.

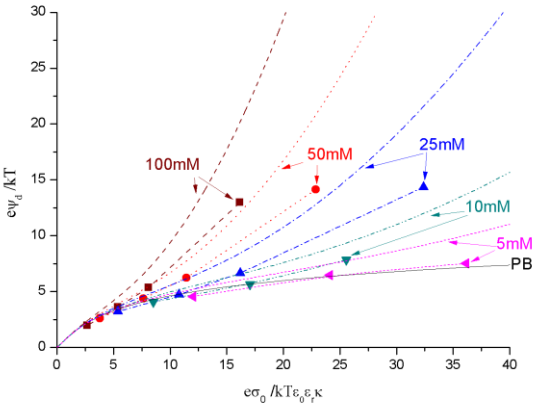

Fig. 2. Diffuse potential as function of surface charge obtained from simulations (symbols) and theoretical predictions (lines) for 1 nm ions at various salt concentrations: 100 mM (squares and dashed lines), 50 mM (circles and dot lines), 25 mM (up triangles and dash dot lines), 10 mM (down triangles and dash dot dot lines), 5 mM (left triangles and short dashed lines). The lines accompanying the symbols obtained from simulations are just a guide for the eye. PB theory prediction is presented too (solid line). $c^{\max}$ is calculated for a SC arrangement.

The diffuse potential can be calculated from the simulated local ion concentrations as

$$\psi_d \equiv \psi(d/2) = \frac{e}{\varepsilon_0 \varepsilon_r} \int_{d/2}^{\infty} (d/2 - z) \sum_{i=1}^{m} Z_i \rho_i(z) dz \qquad (12)$$

where $\rho_i(z)$ is the local ion density, of the different ionic species (obtained from simulations), at a distance z from the charged surface. Technically, the integral in eqn (12) must be evaluated over a finite interval. For this reason, the upper limit is replaced by a cut-off distance, L_c. This cut-off distance can be chosen to lie anyplace into the solution bulk, where the electroneutrality condition ($\sum_{i=1}^{m} Z_i \rho_i(z) dz = 0$) must be satisfied. Nonetheless, it should be noticed that the computed fluctuations of $\sum_{i=1}^{m} Z_i \rho_i(z) dz$ could be highly amplified due to the factor $d/2 - z$ appearing in eqn (12). To avoid this possible divergence on the ψ_d calculation, L_c must not be too large. In our simulations we employed values of L_c around 0.5 L.

3. Results and discussion.

Monovalent ions.

First, the case of monovalent 1:1 ions with the representative diameters 2, 1 and 0.75 nm will be analyzed. In Fig. 1 we show the dimensionless diffuse potential as function of the dimensionless surface charge density for ions of 2 nm, with $c^{\max} = 0.2$ M (according to LópezGarcía *et al*.) and various salt concentrations (50, 25, 10 and 5 mM). In particular, the curves obtained from eqn (5), our computer simulation results and the PB prediction are plotted. A qualitative agreement between theory and simulation can be observed: each pair of curves (MPB and MC) corresponding to different salt concentrations exhibit a similar trend. However, there are certain quantitative deviations between them. Concerning general aspects, we should stress two features of the theory that are perfectly reproduced by the MC results. First, in a dimensionless charge-potential plot, there is a unique PB curve since the PB charge-potential relationship expressed in this manner does not depend on the salt concentration. However, the expression developed by López-García *et al.* predicts different curves for each salt concentration (through the $c_i^{\infty} / c^{\max}$ ratio in eqn (5)), which is completely corroborated by our simulations. Second, the dimensionless diffuse potentials obtained from eqn (5) are larger than the PB values and the differences between them increase with the salt concentration and the dimensionless surface charge density. These features are entirely confirmed by the MC data. In any case, the large dimensionless diffuse potential values obtained at high surface charge densities deserve an additional comment. Given that counterions are strongly attracted to the charged surface, the space close to the macroion is expected to be replete of them. However, it should be kept in mind that the ionic diameter of 2 nm employed is rather large (and even unusual for certain monovalent ions, such as alkaline cations). Consequently, the space near the charged macroion is easily occupied by only a few counterions and turns into a practically inaccessible area to the other ions due to the hard core repulsion between them. Thus, counterions are unable to neutralize properly the surface charge of the macroion and extremely high values of the diffuse potential can be reported.

In Fig. 2 we present the dimensionless diffuse potential as function of the dimensionless surface charge density, now for 1 nm ions with $c^{\max} = 1.5$ M at different salt concentrations (100, 50, 25, 10 and 5 mM). A good qualitative agreement between theory and simulations is observed again. As in the case of larger ions (Fig. 1), the dimensionless diffuse potentials remain above the PB curve. However, the values of this property are not so large. In fact, for low salt concentrations and/or surface charge densities the MC potentials do not differ significantly from the PB results (in contrast with the large deviations reported for 2 nm). This feature is reasonable since the charged macroion surface charge is more easily neutralized by smaller ions.

In Fig. 3 the dimensionless diffuse potential as function of the dimensionless surface charge density is shown for 0.75 nm ions, with $c^{\max} = 4$ M, at the same salt concentrations that in the case of 1 nm ions. As in the two cases analyzed before, predictions from eqn (5) and simulation results show similar trends and, to some extent, a good qualitative agreement is found once

again. As expected, the theory accounting for ion size predicts results above the PB curve. However, under certain conditions (e.g., 5 mM), the simulated diffuse potentials are slightly smaller than their corresponding PB predictions.

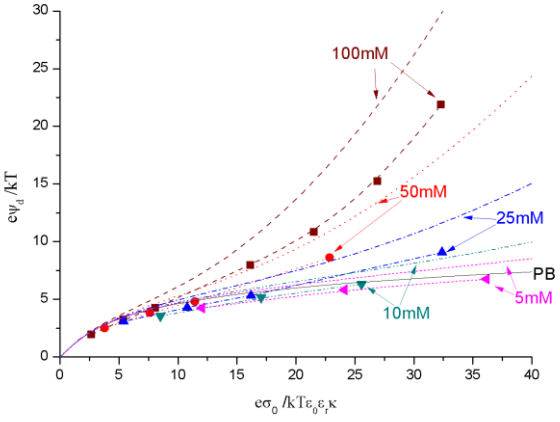

Fig. 3. Diffuse potential as function of surface charge obtained from simulations and theoretical predictions for 0.75 nm ions at various salt concentrations, $c^{\max}$ is calculated for a SC arrangement. Lines and symbols represent the same as in Fig. 2.

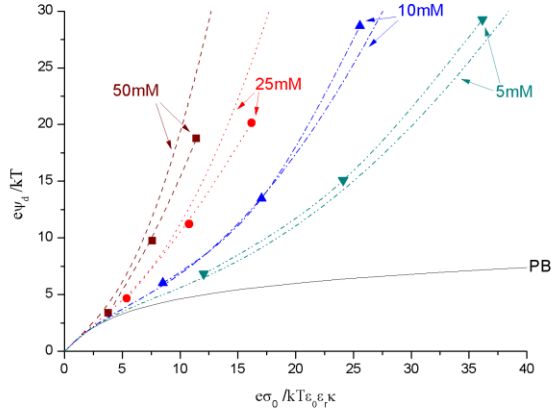

Fig. 4. Diffuse potential as function of surface charge obtained from simulations and theoretical predictions for 2 nm ions at various salt concentrations, $c^{\max}$ is calculated for a HCP arrangement. Lines and symbols represent the same as in Fig. 1.

From the analysis of the three figures presented for monovalent ions, we can conclude that eqn (5) works reasonably well for large ions and/or high salt concentrations (at least, qualitatively

speaking). For the smallest size studied here (0.75 nm), some discrepancies are reported. For instance, unlike the simulations, the theory never predicts dimensionless diffuse potentials under the PB values.

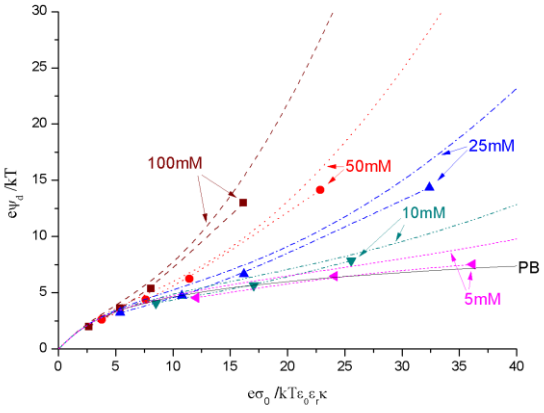

Fig. 5. Diffuse potential as function of surface charge obtained from simulations and theoretical predictions for 1 nm ions at various salt concentrations, $c^{\max}$ is calculated for a HCP arrangement. Lines and symbols represent the same as in Fig. 2.

Improving the results for monovalent ions.

As stated before, the ion size is included in the MPB theory through $c^{\max}$ (and assuming that $c^{\max}$ is the same for all ionic species, as the PM). The values of $c^{\max}$ corresponding to the effective ion diameters 2, 1 and 0.75 nm are 0.2, 1.5 and 4 M (in round numbers). These values (which were also used by López-García *et al.*[24]) can be calculated from

$$c^{\max} = \frac{1}{N_A d^3} \tag{13}$$

which involves the assumption of a simple cubic (SC) crystal (whose packing fraction is 52%). However, other lattices can also be assumed. For instance, we can consider the hexagonal close packed (HCP) structure, whose packing fraction is 74.05%. In such a case, the following approximate values for $c^{\max}$ are obtained: 0.28, 2.13 and 5.69 M (corresponding again to the effective ion diameters 2, 1 and 0.75 nm, respectively). In the light of this observation, the previous theoretical predictions were recalculated with the corresponding correction in $c^{\max}$ and compared again to the simulation data already presented.

In Fig. 4 we show the same simulation data as in Fig. 1 for 2 nm ions but now the theoretical curves are obtained from eqn (5) with $c^{\max}$ = 0.28 M (calculated for a HCP structure). As can be seen comparing with Fig. 1, the agreement between predictions and simulation data is much

better. Thus the new assumption about the arrangement of ions can improve the results obtained from eqn (5) considerably.

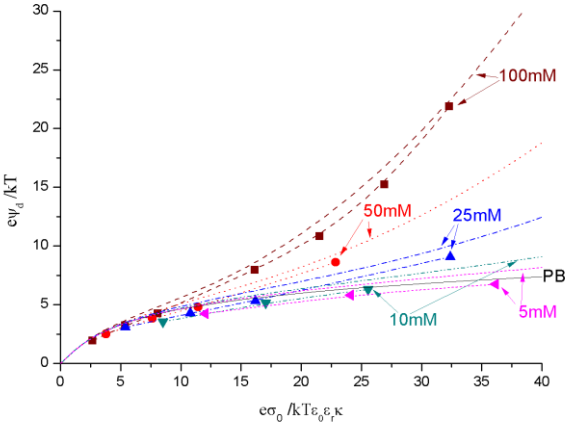

Fig. 6. Diffuse potential as function of surface charge obtained from simulations and theoretical predictions for 0.75 nm ions at various salt concentrations, $c^{\max}$ is calculated for a HCP arrangement. Lines and symbols represent the same as in Fig. 2.

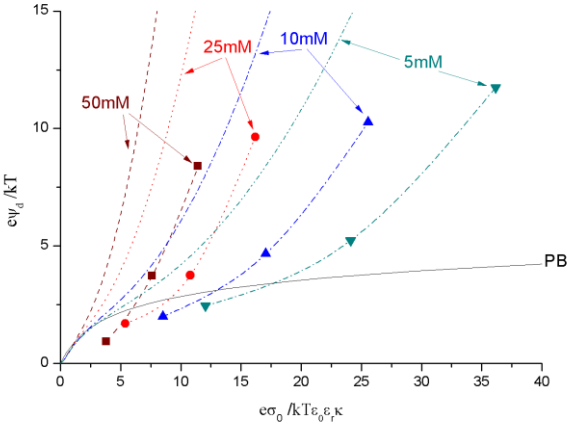

Fig. 7. Diffuse potential as function of surface charge obtained from simulations and theoretical predictions for 2 nm divalent ions at various salt concentrations, $c^{\max}$ is calculated for a HCP arrangement. Lines and symbols represent the same as in Fig. 1.

Similarly, in Fig. 5 we present the simulation data for 1 nm ions again. The theoretical predictions have been calculated with the $c^{\max}$ for a HCP structure (2.13 M). As in the previous case, the agreement between theory and simulations improves.

In Fig. 6 we finally display simulation results and theoretical predictions for 0.75 nm ions considering the ions form a HCP structure (c^{max} = 5.69 M). Once more, the agreement between theory and simulations is enhanced. We can therefore conclude that the most reliable results are those obtained for the HCP structure. Consequently, we will only use the c^{max} values corresponding to a HCP structure hereafter.

Before ending the discussion of monovalent electrolytes, there is an aspect of eqn (5) that deserves an additional comment. As mentioned before, the dimensionless charge-potential relationships predicted from eqn (5) show very similar features: such curves are above the PB one and always bend upwards with increasing the surface charge density and/or the salt concentration. Our simulations confirm to a great extent such features. However, one should keep in mind that we are dealing with large ions. If smaller sizes are examined, the behaviour of the ψ_d -σ_0 function becomes much richer. There are charge-potential relationships under and above the classical prediction, bending upwards and downwards. For instance, Bhuiyan *et al.* studied the charge-potential relationship by comparing a MPB equation with density functional theories (DFT) as well as MC simulations.[22] In all cases shown therein, the diffuse potential bends downwards with increasing surface charge density. In relation to this, we would like to remark that these authors used an effective ion diameter of 0.3 nm in their calculations. Boda *et al.* analyzed the charge-potential for different ion diameters (0.2, 0.3 and 0.425 nm) by means of MC and DFT.[21] Their results were similar to those obtained by Bhuiyan *et al.* On the other hand, González-Tovar *et al.* used the so-called hyper-netted-chain/mean-spherical approximation (HNC/MSA) and predicted both charge-potential relationships bending upwards and downwards.[23] In this case, effective ion diameters between 0.425 nm and 0.9 nm were employed, reporting different behaviours in charge-potential curves depending on the ion size. In particular, they found functions that bend downwards for the smaller ion diameters, an inflexion curve for a diameter of 0.6 nm, and functions that bend upwards for larger ions. Finally, Quesada-Pérez *et al.* tested HNC/MSA through MC simulations and obtained the same inflexion in the potential curves for monovalent ions between 0.425 nm and 0.72 nm.[27]

Divalent counterions.

Now the case of the asymmetric salt 2:1 will be analyzed. A previously published paper suggests that the electrokinetic behaviour of model colloids does not depend strongly on the coion valence.[37] Consequently, the case of divalent coions will not be studied here. In Fig. 7 we present the dimensionless diffuse potential as function of the dimensionless surface charge density for 2 nm ions at different salt concentrations (50, 25, 10 and 5 mM). Unlike the case of 2 nm monovalent ions, the discrepancies between predictions and simulations are now outstanding. The predictions for the dimensionless diffuse potential show lower values and the qualitative differences between theory and simulations are now greater. In particular, the MC results for small surface charge densities are under the PB curve.

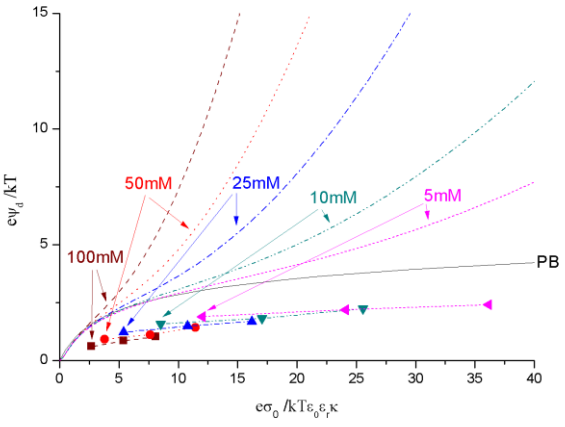

Fig. 8. Diffuse potential as function of surface charge obtained from simulations and theoretical predictions for 1 nm divalent ions at various salt concentrations, $c^{\max}$ is calculated for a HCP arrangement. Lines and symbols represent the same as in Fig. 2.

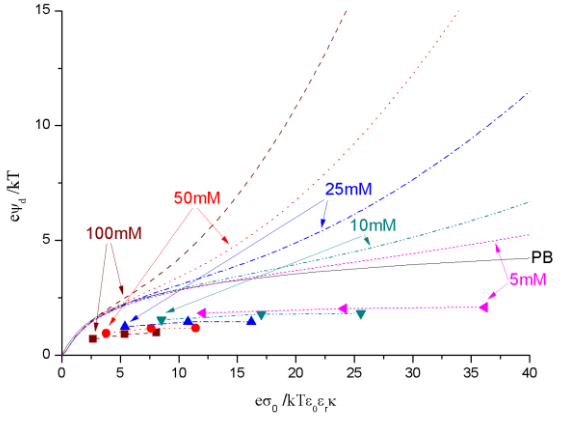

Fig. 9. Diffuse potential as function of surface charge obtained from simulations and theoretical predictions for 0.75 nm divalent ions at various salt concentrations, $c^{\max}$ is calculated for a HCP arrangement. Lines and symbols represent the same as in Fig. 2.

In Fig. 8 we show predictions from eqn (5) and simulation data for a 2:1 salt made up of 1 nm ions at different concentrations (100, 50, 25, 10 and 5 mM). Compared to the case of 1 nm monovalent ions, the agreement between theory and simulations seems to have disappeared completely and MC data are all under the PB prediction, which should not occur according to eqn (5).

To end the analysis of divalent counterions, the results from simulations and predictions from eqn (5) for 0.75 nm divalent ions are displayed in Fig. 9 with the same salt concentrations as in Fig. 8. The theoretical dimensionless diffuse potentials are smaller than those obtained for monovalent 0.75 nm ions (Fig. 6) and for divalent 2 and 1 nm counterions (Figures 7 and 8). However, simulation data remain under the PB curve (as expected). In general, for divalent counterions, the disagreement between theory and simulations is remarkable. As matters stand, we would like to point out a feasible cause for the failure of the theory for divalent counterions.

A final consideration.

In our opinion, ion size correlations can yield two types of very different (and even opposite) effects. The former occurs at extremely high electrolyte concentrations of large ions. Under such conditions, the excluded volume effect could be responsible for the saturation of the ionic profiles near the charge surface. This involves that the predictions of the counterion concentrations (in the vicinity of the surface) must be smaller than the corresponding PB values. We will refer to this situation, which is just one of the main assumptions of the theory analyzed here, as the *saturation regime*.

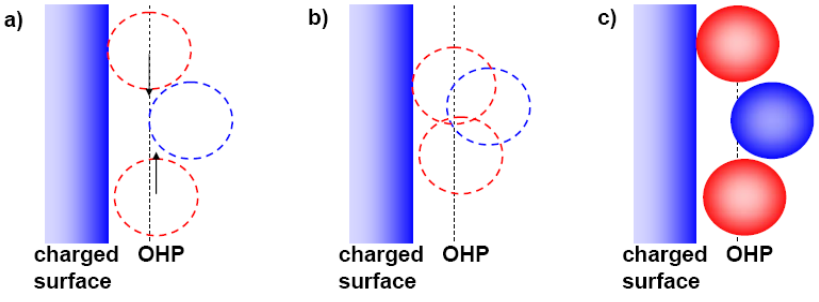

Fig. 10. a) Some counterions close to the OHP. Let us consider one of them as reference (for example, the one in the middle). b) In a PB picture, the other counterions can temporally interpose between the reference ion and the charged surface. c) In considering the ion size, the space between the charged surface and the reference counterion cannot be occupied by others.

The other effect takes place if the saturation regime is not operative. More sophisticated approaches and simulations have proved that, in this other regime, the ion size correlations can lead to counterion concentrations larger than the PB values in the neighbourhood of the charged colloid, in contrast with saturation regime.[20] The underlying physical mechanism of this somewhat paradoxical behaviour can be briefly elucidated as follows.[28] Let us consider (as reference) a counterion in the proximity of the OHP (see Fig. 10). In a PB picture, other counterions can temporally interpose between the above-mentioned counterion and the colloid. Thus these other counterions screen the attraction experienced by the first one towards the charged surface. In considering the ionic size, however, the space between the charged surface

and the first counterion cannot be occupied by others (due to their exclusion volumes). Consequently, the effective attraction between the counterion close to the OHP and the colloidal surface will be stronger than in the PB case (since the screening of other counterions between them will be avoided). The counterion concentration near the particle surface will therefore be larger than that predicted by a PB approach. Messina *et al*. have also analyzed the role of the excluded volume, but in terms of entropy.[38]

In any case, our simulations (and previous studies) reveal that the success or failure of the theory analyzed here depends on whether the saturation regime appears or not. On the one hand, large monovalent counterions can reach the saturation regime easily. Thus, the counterion concentrations would be smaller than the PB predictions and the modified model of the PB theory would therefore work properly. On the other hand, the saturation regime would be unlikely for divalent (in general multivalent) counterions since: i) strong electrostatic repulsions would prevent from high packing fractions; ii) the number of counterions needed to neutralize the surface would be considerably smaller. As the situation would be far from the saturation regime, the number of ions in the vicinity of the charged colloid might be larger than the PB prediction, in contradiction with the modified model of the PB theory.

4. Conclusions.

With the aim to test a modified PB theory that includes ion size effects through a Langmuir-type correction, we have performed MC simulations within a PM of electrolyte to generate numerically the dimensionless diffuse potential as a function of the dimensionless surface charge density, for 1:1 and 2:1 electrolytes. For 1:1 salts, the theory is found to work appreciably well, particularly for high surface charge densities and/or large ionic sizes. Simulations confirm the existence of diffuse potentials considerably larger than the PB ones. In addition, this technique corroborates that the dimensionless charge-potential relationship does depend on the salt concentration (in contrast with the PB case). In any case, the predictions of the theory can be considerably improved assuming that counterions form a HCP structure instead a simple cubic one. On the other hand, for 2:1 salts, the theory dramatically fails. The predictions of dimensionless diffuse potentials above the classic PB relationship are not corroborated by the MC charge-potential functions, which are mostly under such curve.

Acknowledgements The authors are grateful to “Ministerio de Educación y Ciencia, Plan Nacional de Investigación, Desarrollo e Innovación Tecnológica (I+D+i)”, Project MAT2006-12918-C05-02, “Consejería de Innovación, Ciencia y Empresa de la Junta de Andalucía”, Projects P06-FQM-01869, P07-FQM-02496 and P07-FQM-02517, as well as the European Regional Development Fund (ERDF) for financial support. A.M.-M. also thanks the “Programa Ramón y Cajal, 2005, Ministerio de Educación y Ciencia - Fondo Social Europeo (RYC-2005-000829)”.

References

1. O. Stern, Z. Elektrochem. 30 (1924) 508.
2. J.J. Bikerman, Philos. Mag. 33 (1942) 384.
3. M.J. Sparnaay, Trav. Chim. Pays-Bas 77 (1954) 872.
4. N.F. Carnahan, K.E. Starling, J. Chem. Phys. 51 (1969) 635.
5. T. Boublik, J. Chem. Phys. 53 (1970) 471.
6. G.A. Mansoori, N.F. Carnahan, K.E. Starling, T.W. Leland, J. Chem. Phys. 54 (1971) 1523.
7. P.M. Biesheuvel, J. Lyklema, J. Phys. Condens. Matter 17 (2005) 6337.
8. P.M. Biesheuvel, F.A.M. Leermakers, M.A. Cohen Stuart, Phys. Rev. E 73 (2006) 011802.
9. P.M. Biesheuvel, M. van Soestbergen, J. Colloid Interface Sci. 316 (2007) 490.
10. I. Borukhov, D. Andelman, H. Orland, Phys. Rev. Lett. 79 (1997) 435.
11. V. Kralj-Iglic, A. Iglic, J. Phys. II France 6 (1996) 477.
12. K. Bohinc, V. Kralj-Iglic, A. Iglic, Electrochim. Acta 46 (2001) 3033.
13. O. González-Amezcua, M. Hernández-Contreras, J. Chem. Phys. 121 (2004) 10742.
14. L. B. Bhuiyan, C. W. Outhwaite, S. Levine, Mol. Phys. 42 (1981) 105.
15. S. Levine, C. W. Outhwaite, L. B. Bhuiyan, J. Electroanal. Chem. 123 (1981) 105.
16. S. Lamperski, C.W. Outhwaite, Langmuir 18 (2002) 3423.
17. S. Lamperski, L. B. Bhuiyan, J. Electroanal. Chem. 540 (2003) 79.
18. S.L. Carnie, D.Y.C. Chan, D.J. Mitchell, B.W. Ninham, J. Chem. Phys. 74 (1981) 1472.
19. M. Lozada-Cassou, R. Saavedra-Barrera, D. Henderson, J. Chem. Phys. 77 (1982) 5150.
20. M. Quesada-Pérez, E. González-Tovar, A. Martín-Molina, M. Lozada-Cassou, R. Hidalgo-Álvarez, ChemPhysChem 4 (2003) 234.
21. D. Boda, D Henderson, P. Plaschko, W. R. Fawcett, Molecular simulation 30 (2004) 137.
22. L. B. Bhuiyan, C. W. Outhwaite, Phys. Chem. Chem. Phys. 6 (2004) 3467.
23. E. González-Tovar, F. Jiménez-Ángeles, R. Messina, M. Lozada-Cassou, J. Chem. Phys. 120 (2004) 9782.
24. J. J. López-García, M. J. Aranda-Rascón, J. Horno, J. Colloid Interface Sci. 316 (2007) 196.
25. Israelachvili, J. N. Intermolecular and Surface Forces; Academic Press: London, 1992.
26. J. J. López-García, M. J. Aranda-Rascón, J. Horno, J. Colloid Interface Sci. 323 (2008) 146.
27 M. Quesada-Pérez, A. Martín-Molina, R. Hidalgo-Álvarez J. Chem. Phys. 121 (2004) 8618.
28. M. Quesada-Pérez, E. González-Tovar, A. Martín-Molina, M. Lozada-Cassou, R. Hidalgo-Álvarez, Colloids and Surf. A 267 (2005) 24.
29. Z. Adamczyk, P. Belouschek, D. Lorenz, Ber. Bunsenges. Phys 94 (1990) 1483.
30. Z. Adamczyk, P. Belouschek, D. Lorenz, Bull. Pol. Ac. Chem. 39 (1991) 424.
31. Z. Adamczyk, P. Warszysnky, Adv. Colloid Interface Sci. 63 (1996) 41.
32. H. Brodowsky, H. Strehlow, Z. Electrochem. 63 (1950) 262.
33. E. Wicke, M. Eigen, Z. Electrochem 56 (1952) 551.
34. J. Lekner, Physica A 176 (1991) 485.
35. R. Sperb, Mol. Simul. 20 (1998) 179.

36. A. G. Moreira, R. R. Netz, Eur. Phys. J. E 8 (2002) 33.
37. A. Martín-Molina, M. Quesada-Pérez, F. Galisteo-González, R. Hidalgo-Álvarez, Colloids and Surf. A 222 (2003) 155.
38. R. Messina, E. González-Tovar, M. Lozada-Cassou, C. Holm, Europhys. Lett. 60 (2002) 383.

Paper II

Effect of ion dispersion forces on the electric double layer of colloids: A Monte Carlo simulation study

Alberto Martín-Molina[(1)], José G. Ibarra-Armenta[(2)] and Manuel Quesada-Pérez[(2)] •

J. Phys. Chem. B, 2009, *113*, 2414.

(1) Grupo de Física de Fluidos y Biocoloides, Departamento de Física Aplicada, Facultad de Ciencias, Universidad de Granada, 18071 Granada, Spain.

(2) Departamento de Física, Escuela Politécnica Superior de Linares, Universidad de Jaén, 23700, Linares, Jaén, Spain.

* Corresponding author.

Abstract.
In this work, the effect of ionic dispersion forces on the electric double layer of colloids is evaluated through Monte Carlo simulations. Particularly, the influence of these forces on the ζ-potential (as a representative electrokinetic property) is assessed. Ion polarizability is included in the primitive model with the help of the Lifshitz theory. In this way, ion specificity is not considered by means of phenomenological (and unknown *a priori*) parameters. Our results reveal that the ionic van der Waals forces are responsible (to some extent) for the specificity of the zeta potential. In any case, the specific ion effects due to ion polarizability are strongly influenced by ion size. Furthermore, a preliminary study on the effect of ionic dehydration shows how this phenomenon improves the qualitative agreement between experimental data and simulations achieved in considering ionic dispersion forces.

1. Introduction.
The distribution of ions in the proximity of a charged surface is a fundamental issue in colloid science. Gouy and Chapman were the first who developed a sophisticated theory for the electric double layer (EDL).[1,2] According to this classical picture, ions are considered as point charges embedded in a continuum of constant dielectric permittivity. The Gouy-Chapman (GC) model became a cornerstone of the classical theory of colloidal stability (DLVO theory), and has been widely applied for many decades. However, its shortcomings were patent from the beginning and even nowadays the behaviour of real colloids goes on challenging this classical approach.
Specific ion effects are a clear and well-known example of its weak points. Such effects are ubiquitous in colloid science and still lack a widely accepted explanation. Many typical examples (such as protein solubility, critical micelle concentration, surface tension of electrolytes, forces between charged surfaces or bubble coalescence) were advisably reviewed by Collins and Washabaugh[3] and, more recently, by Ninham *et al.*[4] Since the standard models of EDL describe ions only by their valence, the following question arises: Why do ions with identical valence behave in very different ways?
One could be tempted to ascribe these salt-sensitive effects to *specific* but *unspecified* ion-surface interaction, which would be incorporated in the theory by means of extra effective parameters. However, in invoking a specificity that is not a priori known and varies from case to case, one is renouncing any capability of prediction. Furthermore, the use of such effective parameters will not contribute to the right physical understanding of reality if the underlying model is not adequate.
In order to overcome this discouraging situation, some authors have proposed to include ion-ion and ion-surface dispersion forces (*i.e.*, the van der Waals interaction) in the classical EDL theory.[5-11] In this way, ion specificity arises naturally since such forces depend on the ionic polarizability, which differs for ions with the same valence. Ninham and co-workers have done this through the Lifshitz theory. They have also proved the relevance of these ionic interactions on forces between

charged surfaces,[6] binding of peptides to membranes,[7] distributions of ions around micelles,[9] osmotic coefficients and surface tensions.[12]

Regarding electrokinetic properties, the effect of different electrolytes has been experimentally studied long time ago. Recently, the electrophoretic mobility of polystyrene latexes has been measured in the presence of various salts.[13] According to this work, anionic latexes seem to be insensitive to the nature of different monovalent ions. The situation is more complex for cationic latexes. These do not exhibit significant differences for NaCl or NH_4NO_3. For NaSCN, however, a noticeable behaviour, which includes a mobility reversal at high salt concentrations, is observed. This somehow puzzling behaviour will be revisited later with the help of simulation techniques.

Computer simulations have been a valuable tool for studying colloidal phenomena since the early 80s.[14-15] More recently, simulations have also explored and/or revisited certain aspects of the EDL models. For example, the effect of the ion size,[16-19] the discreteness of the surface charge,[20-23] or the mixtures of different electrolytes.[24-31] Other works have focused on the electrostatic forces between two charged surfaces immersed in an electrolyte solution[32-39] and, more specifically, Monte Carlo (MC) simulations have begun to examine the effect of ion-ion and ion-surface dispersion forces on surface-surface interactions, confirming that the mean force is very sensitive to ionic van der Waals interactions.[40-41] Moreover, Tavares *et al*. even report attractive forces at intermediate distances for polarizable monovalent salts.

According to these premises, the aim of this work is to evaluate the effect of ionic dispersion forces on the electric double layer of colloids by means of computer simulations. More specifically, we will assess the effect of such forces on the ζ-potential, since this property is essential to understand the electrokinetic behaviour of colloids. For such purpose, ion-ion and ion-colloid dispersion forces have been included in the so-called primitive model, which assumes that the solvent is a dielectric continuum whereas ions are modelled as charged hard spheres. Following the work carried out by Tavares *et al.*[40], the effect of the ion polarizability was considered through the Lifshitz theory. In this way, specificity does not need to be postulated *ad hoc*. We will also pay attention to the ion size since, in previous papers, it turned out to be a key parameter to justify and understand the electrokinetic properties of certain colloids[19,23,28,29] as well as the colloid-colloid forces.[38] As far as we know, the effect of ionic dispersion forces on the ζ-potential has not been addressed by means of computer simulations yet. Although Huang *et al*. have examined anomalous electrokinetic effects (due to ion specificity) in nanochannels, their approach is quite different.[42,43] Their simulations are atomistic and interactions are modelled through Lennard-Jonnes potentials (since they are focused on the interfacial structure of water). In addition, the conditions for a considerable effect of ionic dipersion forces on electrokinetic properties will be identified in this work. In particular we will show how such interactions can have a significant impact in the case of small but highly polarizable ions, being even responsible for a sign reversal within 1:1 electrolytes. The rest of the paper is organized as follows. First, some details about the model and the simulations are outlined. Then, the results are presented and discussed. Finally, some conclusions are highlighted.

2. Model and simulations.

Our simulations have been carried out in the framework of the primitive model. In particular we have simulated a planar EDL compound of a charged wall immersed in a dielectric continuum (water at 298 K) whereas ions are hard spheres. The interaction energy between ions i and j is given by:

$$u(r_{ij}) = \frac{Z_i Z_j e^2}{4\pi\varepsilon_0\varepsilon_r r_{ij}} - \frac{B_{ij}}{r_{ij}^6} \qquad r_{ij} \geq a_i + a_j$$

$$u(r_{ij}) = \infty \qquad r_{ij} < a_i + a_j \tag{1}$$

where a_i and Z_i are the hydrated ion radius and the valence, respectively, of species i, e is the elementary charge, ε_0 is the permittivity of vacuum, $\varepsilon_r = 78.5$ is the relative permittivity, $\vec{r}_{ij}$ is the relative position vector and $r_{ij} = \left|\vec{r}_{ij}\right|$ is the distance between ions i and j, and B_{ij} is the parameter characterizing the dispersion interaction between species i and j. These dispersion forces were obtained following the Lifshitz theory. In our simulations, we have used the dispersion parameters calculated by Tavares *et al.*[40] and Boström *et al.*[44] Further details about the calculation of such parameters can be found therein.

Table 1. Values of *W*, *L*, *N* and the Debye length (κ^{-1}) for two representative systems ($\sigma_0 =$ -0.115 C/m^2 at 5 mM and 200 mM of LiCl).

Electrolyte concentration(mM)	*W* (nm)	*L* (nm)	*N* (particles)	κ^{-1} (nm)
5	11.2	35.0	114	4.24
200	7.0	7.0	109	0.68

Table 2. Dispersion parameters and hydrated cation radius for electrolytes with Cl^-.

Electrolyte	$B_{cation\text{-}cation}/k_BT$ (nm^6)	$B_{Cl^-\text{-}Cl^-}/k_BT$ (nm^6)	$B_{cation\text{-}Cl^-}/k_BT$ (nm^6)	$B_{macroion\text{-}cation}/k_BT$ (nm^3)	$B_{macroion\text{-}Cl^-}/k_BT$ (nm^3)	a_{cation} (nm)
LiCl	$0.983\cdot10^{-6}$	$8.03\cdot10^{-4}$	$1.40\cdot10^{-5}$	$2.57\cdot10^{-4}$	$8.69\cdot10^{-3}$	0.35
CsCl	$8.76\cdot10^{-4}$	$8.03\cdot10^{-4}$	$7.45\cdot10^{-4}$	$1.08\cdot10^{-2}$	$8.69\cdot10^{-3}$	0.35
$MgCl_2$	$4.79\cdot10^{-6}$	$8.03\cdot10^{-4}$	$3.40\cdot10^{-5}$	$6.07\cdot10^{-4}$	$8.69\cdot10^{-3}$	0.40
$BaCl_2$	$5.81\cdot10^{-4}$	$8.03\cdot10^{-4}$	$5.53\cdot10^{-4}$	$8.17\cdot10^{-3}$	$8.69\cdot10^{-3}$	0.40

The plane wall is assumed to be smooth and uniformly charged. The interaction energy of ion i with the charged wall, which is located at $z = 0$, is given by:

$$u(z_i) = -\frac{\sigma_0 Z_i e z_i}{2\varepsilon_0 \varepsilon_r} - \frac{B_{mi}}{z_i^3} \qquad z_i \geq a_i$$
$$u(z_i) = \infty \qquad z_i < a_i \tag{2}$$

where z_i is the z-coordinate of particle i, σ_0 is the surface charge density of the charged wall, and B_{mi} is the dispersion parameter corresponding to the interaction between the ionic species i and the macroion charged surface (calculated from the Lifshitz theory). Again, we take as reference the values provided by other researchers. [40,44]

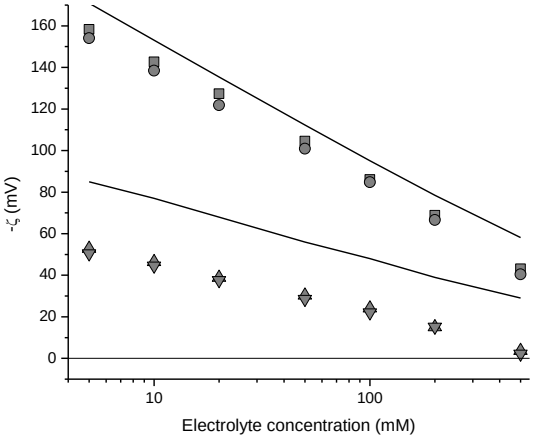

Figure 1. Zeta potential (obtained from simulations) as a function of the salt concentration for a surface charge density of -0.115 Cm^{-2} and the following electrolytes: LiCl (squares) CsCl (circles), $MgCl_2$ (up triangles) and $BaCl_2$ (down triangles). Solid lines denote the predictions obtained from eq. 4 assuming that $\sigma_d = -\sigma_0$ for monovalent and divalent cations (upper and lower, respectively). The hydrated cation radii and dispersion parameters are shown in Table 2.

Simulations have been carried out by using the Metropolis algorithm applied to a canonical ensemble for a collection of N ions confined in a rectangular prism (or cell) of dimensions $W \times W \times L$. As mentioned above, the impenetrable charged wall is located at $z = 0$ whereas at $z = L$ another impenetrable wall without charge is placed. Accordingly, periodic boundary conditions were used in the lateral directions (x and y). The cell contains the ionic mixture corresponding to the bulk electrolyte solution together with an excess of counterions neutralizing the surface charge. Moreover, the systems were always thermalized before collecting data for averaging and the acceptance ratio was kept between 0.3 and 0.5. Due to the long range of the electrostatic interactions, the energy must be evaluated very carefully. In these simulations, we

have applied the so-called Lekner-Sperb method (see Reference 19 for further details). The values of W, L and N vary from one simulation to another in order to keep to the previous premises. In any case, they are quite similar to those employed in previous works where the Lekner-Sperb methods was also applied.[19,29] Just to give an idea, the values of W, L and N for two representative systems ($\sigma_0 = -0.15$ C/m^2 at 5 mM and 200 mM of LiCl) are shown in Table 1. The length of the cell (L) must be large enough to include a considerable portion of the solution bulk in the simulation box, which involves that L must be significantly larger than the Debye screening length. As can be seen in Table 1, in our simulations L is about one order of magnitude larger than the Debye length (κ^{-1}). We check that the ratio L/κ^{-1} is large enough to avoid unreliable results. On the other hand, the particle numbers might seem rather small at first sight. However, it should be mentioned that the right performance of the Lekner-Sperb method (within these particle numbers) was proved in previous simulation works[19,29] comparing with other methods for calculating energies. In addition, to check that the cell size was large enough, the simulation cell dimensions (and hence the number of particles) were doubled for some systems.

From the local ion concentrations given by the simulations we can compute the diffuse potential (ψ_d), defined as the electric potential at the plane of closest approach of the hydrated ions to the charged surface, also known Outer Helmholtz plane (OHP). This EDL property is quite useful in comparing with experiments, since it is closely related to the ζ-potential, which is an essential quantity to characterize and analyze electrokinetic phenomena. In fact, many authors suggest that ζ and ψ_d are practically identical.[46-47] Assuming that both the outer Helmholtz plane and the shear plane are located at the position of closest approach of the highly-charged ions, the ζ-potential can be calculated from:

$$\zeta \approx \psi_d \equiv \psi(a_1) = \frac{e}{\varepsilon_r \varepsilon_0} \int_{a_1}^{\infty} (a_1 - z) \sum_i Z_i \rho_i(z) dz \qquad (3)$$

where a_1 is the hydrated ion radius of counterions and $\rho_i(z)$ is the local density of i-ions at a distance z from the charged surface. In practice, the integral appearing in eq. 3 can only be evaluated over a finite interval, whose upper limit is L_c. From this cut-off distance, the condition of local electroneutrality (in the bulk of the solution) is supposed to guarantee that $\sum_i Z_i \rho_i(z) = 0$. L_c must be large enough to satisfy such condition but not much larger since the fluctuations of $\sum_i Z_i \rho_i(z)$ (computed from simulations) could be considerably amplified due to the term $(a_1 - z)$ of eq. 3.

3. Experimental.

The sulfonated polystyrene latex used in this work was prepared in absence of emulsifier by a two-stage 'shot-growth' emulsion polymerization process and cleaned then by serum

replacement. The particle diameter, determined by photon correlation spectroscopy, turned out to be 196 ± 3 nm. This technique also provides a polydispersity index defined as the quotient between the first and the second moment of the cumulant expansion of the logarithm of the so-called normalized field autocorrelation function. In our case, the measured index was found to be 0.05, which means that this latex is practically monodisperse. Conductimetric and potenciometric titrations were used to determine its surface charge density. These experiments were performed with Crison instruments (pH-meter and conductimeter), at 25ºC in a stirred vessel flushed with nitrogen and using NaOH and HCl as titration agents. A surface charge density of 0.115 ± 0.002 Cm^{-2}, which did not depend on pH, was obtained.

Table 3. Dispersion parameters and hydrated anion radius for electrolytes with Na^+.

Electrolyte	$B_{anion\text{-}anion}/k_BT$ (nm^6)	$B_{Na^+\text{-}Na^+}/k_BT$ (nm^6)	$B_{anion\text{-}Na^+}/k_BT$ (nm^6)	$B_{macroion\text{-}anion}/k_BT$ (nm^3)	$B_{macroion\text{-}Na^+}/k_BT$ (nm^3)	a_{anion} (nm)
NaCl	$8.03\cdot10^{-4}$	$1.31\cdot10^{-5}$	$6.54\cdot10^{-5}$	$8.67\cdot10^{-3}$	$1.09\cdot10^{-3}$	0.325
NaI	$2.34\cdot10^{-3}$	$1.31\cdot10^{-5}$	$9.94\cdot10^{-5}$	$1.07\cdot10^{-2}$	$1.09\cdot10^{-3}$	0.325
NaSCN	$4.69\cdot10^{-3}$	$1.31\cdot10^{-5}$	$2.00\cdot10^{-4}$	$2.43\cdot10^{-2}$	$1.09\cdot10^{-3}$	0.25

A *ZetaPALS* setup (Brookhaven, USA), based on the principles of phase analysis light scattering, was used to obtain electrophoretic mobilities. In this technique a mixing of scattered light from a suspension of colloidal particles moving in an electric field with light directly from the source is analyzed. The scattered light is frequency shifted by the Doppler effect and its superposition with the *unshifted* one leads to a beating at a frequency dependent on the speed of the particles. Nonetheless, some problems arise when the particle velocity is low. For those cases, spectral analysis is not able to generate a complete cycle of the detected signal. However, phase analysis takes place over many cycles of the respective waveforms since the optical phase of the scattered light is characterized by means of the so-called *amplitude-weighted phase difference* (AWPD) function instead of a simple correlation treatment.

Electrophoretic mobility measurements were performed at 25 ^{o}C. The particles concentrations (ρ_p) were 4.9×10^{10} particle·ml^{-1}. The mobility data shown in this work were obtained averaging on series of six measurements (at least) and taking the standard deviation as error bar. Their reproducibility (within this estimated uncertainty) was checked in three different ways: i) measuring for several samples at the same conditions; ii) measuring in different days; iii) and changing the particle concentration (above the critical value needed for a right performance of the mentioned setup).

4. Results and discussion.

Monovalent cations. First, the case of monovalent salts with different cations (and a negatively charged wall) is looked into. Two representative electrolytes, LiCl and CsCl, have been chosen for this task, since Li^+ and Cs^+ have very different polarizabilities. More specifically, they possess the

smallest and the largest (respectively) cation-cation and macroion-cation dispersion parameters reported for alkaline cations.[40] These values are shown in Table 2. Consequently, the distinct behaviours of the rest of alkaline cations are expected to be comprised between these two extreme cases. Concerning ion size, alkaline cations present very different bare ion radii but very similar hydrated ion radii.[48] The same value has been (deliberately) taken as typical hydrated ion radius for all alkaline cations (0.35 nm). Using identical sizes, only polarizability will contribute to specificity (according to this model) and its effect will be clearly elucidated. In any case, the reader should be aware that the hydrated radius depends on how it is measured. Different methods can yield radii even 0.1 nm larger or smaller than those reported in Reference 48.

In Figure 1, the ζ -potential (calculated from MC simulations) for a charged macroion with a moderate surface charge density (σ_0 =-0.115 Cm^{-2}) is plotted as a function of the electrolyte concentration. The value of surface charge has been chosen because it has been extensively studied in previous works and many experimental, theoretical and simulation data are available.[23, 28, 29, 45,50] As can be seen, the values of ζ -potential obtained for LiCl and CsCl are practically identical. Our results clearly suggest that alkaline cations should not exhibit specific features in their electrokinetic behaviour.

At first sight this seems to contrast with the plethora of specific ion effects observed in colloid science as well as the simulation results reported by Tavares *et al*.[40] These authors find that the mean force between macroions can be quite salt-sensitive (in agreement with experiments). However, it should be

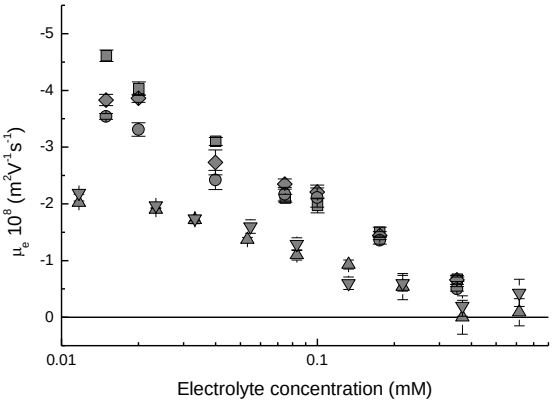

Figure 2. Electrophoretic mobility as a function of the salt concentration for a latex with a surface charge density of -0.115 Cm^{-2} and the following electrolytes: $LiNO_3$ (squares), $NaNO_3$ (diamonds), KNO_3 (circles), $Ca(NO_3)_2$ (up triangles) and $Mg(NO_3)_2$ (down triangles) .

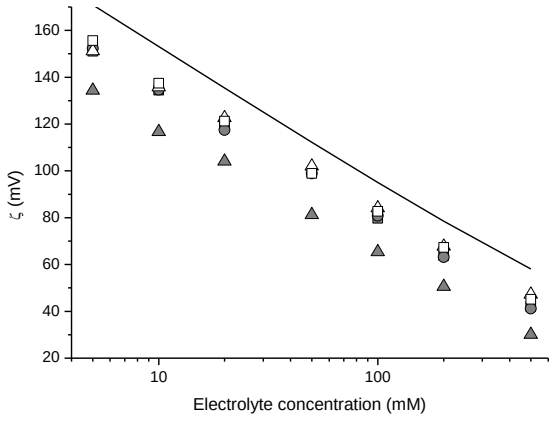

Figure 3. Zeta potential (obtained from simulations) as a function of the salt concentration for a surface charge density of 0.115 Cm^{-2} and three electrolytes: NaCl (solid squares), NaI (solid circles) and NaSCN (solid triangles). The hydrated anion radii and dispersion parameters are shown in Table 3. The results for non-polarizable ions are also plotted for NaCl and NaI (open squares for both since their sizes are identical) and NaSCN (open triangles). Solid line denotes the prediction obtained from eq. 4 assuming that $\sigma_d = -\sigma_0$.

stressed that their simulations were carried out with an ion radius of 0.2 nm. In order to clarify our apparent discrepancies with the results of Tavares *et al.*, let us consider the case of Cs^+, with the largest cation-cation and macroion-cation dispersions parameters (as a result of its great polarizability). For the mentioned ion size, the cation-cation and macroion-cation dispersion energies at the contact distance (0.4 nm) turn out to be $0.2139\,k_BT$ and $1.273\,k_BT$ (k_B is the Boltzmann constant and T is the absolute temperature), respectively. The latter is comparable to the thermal energy. In other words, van der Waals forces (together with the electrostatic interaction) contribute to the attraction of Cs^+ towards the oppositely charged surface. For the ion radius we have chosen (0.35 nm), the respective energies at the contact distance (now 0.7 nm) are $7.4\cdot10^{-3}\,k_BT$ and $0.238\,k_BT$. The former is negligible and the latter rather small. Thus they should not have outstanding effects. This is just what we observe in Figure 1. Once more we conclude that the effect of the ionic dispersion forces depends, to a large extent, on the ion size.

At any rate, it is quite instructive to compare with experimental results. In Figure 2, the electrophoretic mobility of a sulfonate latex with a surface charge density of -0.115 Cm^{-2} is shown as a function of the salt concentration of three alkaline cations. As can be seen, there are no significant differences among the three cations, which is in agreement with our results of ζ-potential. In principle, one could also compare the experimental electrophoretic mobility data with those calculated from the theoretical (and approximate) ζ-potential. In practice, however, this is not a trivial task. The calculation of the electrophoretic mobility from ζ requires a

conversion theory but the validity of the classical and widely-known O'Brien-White scheme might not be guaranteed (except at high electrokinetic radii) since it does not consider ion size correlations (as the primitive model does). A more sophisticated conversion theory would be demanded in order to incorporate such correlations.[49,50] Nevertheless, this goes beyond the scope of this article. On the other hand, one could think of simulating directly the electrophoretic mobility through molecular dynamics. Unfortunately, this solution is not exempt from technical difficulties (such as the consideration of the solvent molecules). Only a few researchers have recently explored this possibility and their studies present nowadays some limitations.[51-53] For instance, their simulations are mainly restricted to very small macroions and certain conditions. Consequently, comparisons between experiments and simulations can only be semi-quantitative or qualitative. In any case, such qualitative comparisons can supply valuable information on their own.

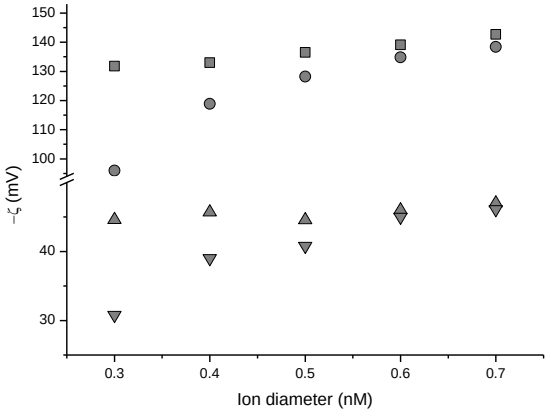

Figure 4. Zeta potential (obtained from simulation) as a function of the cation diameter for a surface charge density of -0.115 Cm^{-2}, a salt concentration of 10 mM and the following electrolytes: LiCl (squares), CsCl (circles), $MgCl_2$ (up triangles) and $BaCl_2$ (down triangles).

Divalent cations. Concerning divalent cations, $MgCl_2$ and $BaCl_2$ were chosen as representative electrolytes since Mg^{2+} and Ba^{2+} have the smallest and the largest (respectively) cation-cation and macroion-cation dispersion parameters of the metallic divalent cations. The same hydrated ion radius was considered for both species as well (0.40 nm). In this way, the effect of polarizability can be unambiguously identified.

Figure 1 also shows the corresponding ζ-potential obtained from simulations as a function of the electrolyte concentration for a surface charge density of -0.115 Cm^{-2}. Again, the results for these two cations (with very different polarizabilities) are nearly identical, which again suggests the absence of salt specificity. The explanation proposed for monovalent cations (the dispersion energies at the contact distance are not intense enough) is suitable for this case as well since the

dispersion parameters of Mg^{2+} and Ba^{2+} are, in round numbers, close to those of Li^{+} and Cs^{+}, respectively.

Electrophoretic mobility measurements also support these simulation data and the conclusions inferred from them. Figure 2 also shows the values of this electrokinetic property for the sulfonate latex with a surface charge density of -0.115 Cm^{-2} as a function of the concentration of two different divalent cations (Mg^{2+} and Ca^{2+}).[50] As can be seen, the measured mobilities for these two cations were almost indistinguishable.

Monovalent anions. The case of monovalent anions (as counterions for a positively charged surface) deserves special attention. As mentioned above, the electrokinetic behaviour of monovalent and divalent metallic cations do not seem to exhibit hallmarks of salt specificity. Concerning this matter, López-León *et al*. have measured the electrophoretic mobility of negative and positively charged latexes in the presence of several anions.[13] As coions of the negatively charged colloid, monovalent anions do not present specific features. On the contrary, the polystyrene spheres show different electrophoretic mobilities when these ions work as counterions of cationic latexes. For that reason, we were particularly interested in simulating this situation.

These ions have been chosen as representative anions: Cl^{-}, I^{-} and SCN^{-}. The anion-anion and surface-anion dispersion parameters were again provided by Tavares *et al*. and Boström *et al*.[40,44] Concerning ionic sizes, the hydrated ion diameters of Cl^{-} and I^{-} were also estimated from Reference 48 (the corresponding diameters were rounded down to 0.65 nm), whereas the one corresponding to SCN^{-} was estimated as follows. First, the length and the width of the bare ion were calculated from the length radii of its atoms covalently bonded. This ion is mostly lineal but it must be modelled as a sphere in the primitive model. Finally, the thickness of the hydration shell (estimated from the nitrate ion) was added. The resulting value is included in Table 3.

In Figure 3 the ζ -potential for $\sigma_0 = 0.115$ Cm^{-2} is plotted as a function of the electrolyte concentration for these three monovalent anions. The reader should keep in mind that the surface charge density is now positive because we are dealing with positively charged surfaces (for which anions are counterions). For the two monoatomic species, the results are again virtually identical. This must not be surprising because both size and dispersion parameters are of the same order than those of the most polarizable alkaline cation (Cs^{+}). For SCN^{-}, however, we find certain specificity: the ζ -potential values obtained are smaller than those obtained from Cl^{-} and I^{-}. This finding somehow resembles the behaviour reported for electrophoretic mobility measurements by López-León *et al*.[13] They also observe smaller electrophoretic mobilities for SCN^{-}. Our results therefore suggest that dispersion forces contribute to the specific electrokinetic behaviour of this anion but one should keep in mind that the ionic size we have employed in simulations for SCN^{-} was smaller than that used for Cl^{-} and I^{-}. Therefore ion size can be responsible for specific features on its own and, in any case, this parameter can reinforce the effect of van de Waals interactions (this will be explicitly discussed in the next section). In order to weigh up the contribution of ion size to specificity in this case, the ζ -potential was again

computed for Cl^-, I^- and SCN^-, but now for non-polarizable ions (*i.e.*, without considering dispersion parameters). The results are also plotted in Figure 3. As can be seen, the simulation data for these anions are quite similar, which means that specificity of SCN^- is mostly due to ionic van der Waals forces (although it would be reinforced by its smaller size).

The role of ion size. The preceding discussion reveals that the specific ion effects due to polarizability are quite sensitive to ion size. We will look into this matter in a bit more detail. Figure 4 shows the ζ-potential for Li^+ and Cs^+ as a function of the ionic diameter for $\sigma_0 = -0.115$ Cm^{-2} and a 10 mM salt concentration. From this figure, one easily concludes that the difference between these two cations increases strongly with decreasing the size. In the same figure, the results for Mg^{2+} and Ba^{2+} are also plotted and similar conclusions can be inferred for them.

In our opinion, however, the sizes required for noticeable specific ion effects in the ζ-potential do not seem to be typical of hydrated metallic ions obtained from several experimental sources.[48] Previous works about electrokinetic properties suggest that the values of hydrated ion radii reported in Reference 48 could justify experimental data fairly well.[28,50] For instance, the experimental mobility reversal observed for sulfonated latexes in the presence of La^{3+} can be explained (from simulations as well as the integral equation formalism) with an ionic diameter of about 0.9 nm but not with 0.425 nm.[28,50] The absence of specificity for monovalent and divalent metallic cations (commented previously) also supports this conjecture.

On the other hand, the EDL model developed by Grahame in 1947 assumes some dehydration for the ions between the outer and the inner Helmholtz planes.[54] Strongly adsorbed ions that have lost their hydration layer are located in the inner Helmholtz plane whereas the outer Helmholtz plane is usually defined as the *locus* of the electrical centres of non-specifically adsorbed ions in their position of closest approach. In any case, and under this assumption, a considerable number of ions in the proximity of the macroion surface could reduce their size and, according to Figure 4, salt-sensitive effects might then emerge. In order to explore this possibility, and just as a preliminary survey, a very simple dehydration mechanism was considered in our simulations for alkaline cations as well as monovalent anions. The Li^+ and Cs^+ ions trying to cross the outer Helmholtz plane were allowed to reduce their radii down to 0.07 and 0.17 nm respectively. Certainly, this is a simple model for dehydration but it offers the advantage of requiring only one additional parameter (the bare ion size). The results for the ζ-potential are shown in Figure 5. For low salt concentrations, no significant differences between Li^+ and Cs^+ were observed. However, for high electrolyte concentrations, ζ exhibits differences of the order of 10-15 mV. Although such differences are not easy to measure experimentally, it should be stressed that the differences between bare ion sizes also contribute to specificity. In order to weigh up the particular effect of ion polarizability, the ζ-potential of non-polarizable Li^+ and Cs^+ ions has also been plotted in Figure 5. In the case of Li^+, the results do not differ significantly from the previous ones since the dispersion parameters are almost negligible. On the contrary, the ionic van der Waals forces reduce ζ in 20 mV approximately for Cs^+.

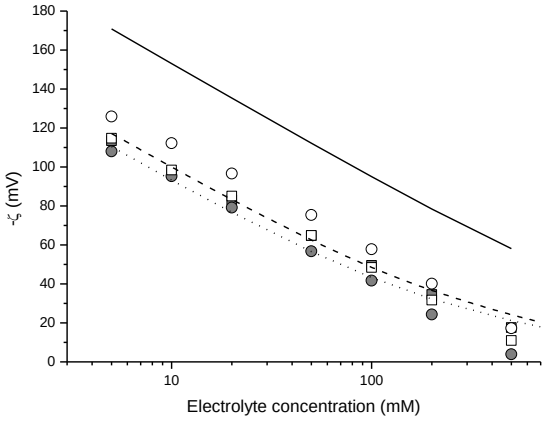

Figure 5. Zeta potential obtained from simulations and considering the dehydration of cations in the proximity of the colloidal surface (see text for further details) as a function of the salt concentration for a surface charge density of -0.115 Cm^{-2} and two electrolytes: LiCl (solid squares) and CsCl (solid circles). The hydrated cation radii and dispersion parameters are shown in Table 2. The results corresponding to non-polarizable cations are also plotted: LiCl (open squares); CsCl (open circles). Dashed and dotted lines denote the predictions obtained from eq. 4 assuming that σ_d = 0.040 and 0.035 Cm^{-2} for LiCl and CsCl, respectively. The prediction for $\sigma_d = -\sigma_0$ is also plotted (solid line).

Finally, we analyze the consequences of a hypothetical dehydration of anions. In this case, ions trying to cross the outer Helmholtz plane were allowed to reduce their radii down to 0.18, 0.215 and 0.175 nm for Cl^-, I^- and SCN^- respectively. The corresponding ζ data are plotted in Figure 6. As can be seen, the results for SCN^- differ noticeably from those of Cl^- and I^-, being shifted towards significantly smaller values. What is more, the electrokinetic property of SCN^- presents a sign reversal. This is an outstanding feature for several reasons. On the one hand, it proves that, according to simulations, the inversion in electrokinetic properties can be explained in terms of specific *adsorption*. It should be pointed out, however, that the origin of such adsorption is perfectly known in this case: the combined action of large polarizability and small ion size. On the other hand, López-León *et al*. have reported a sign reversal of the electrophoretic mobility of a cationic latex in the presence of SCN^-.[13] The qualitative agreement between our simulated ζ and the electrophoretic mobility measured by these authors clearly supports the relevance of ionic dispersion forces under certain circumstances (small but highly polarizable ions).

In Figure 6 we have also plotted the results corresponding to non-polarizable ions. With the representation of these data, the exclusive effect of dispersion forces can be easily assessed. In fact, this figure shows that such interactions reduce the ζ -potential (in the case of non-polarizable SCN^- ions) in 60 mV (approximately). This reduction is certainly remarkable and gives an idea of the importance of ionic van der Waals forces.

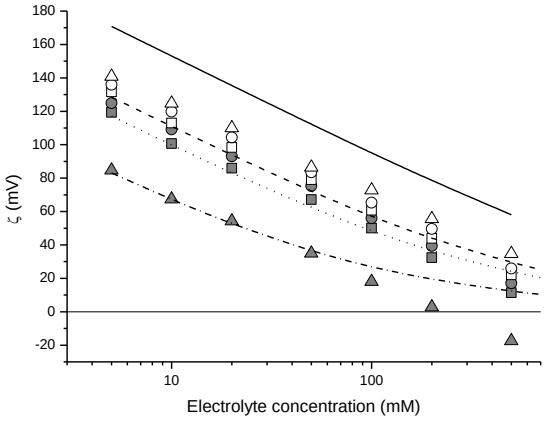

Figure 6. Zeta potential obtained from simulations and considering the dehydration of anions in the proximity of the colloidal surface (see text for further details) as a function of the salt concentration for a surface charge density of 0.115 Cm^{-2} and three electrolytes: NaCl (solid squares), NaI (solid circles) and NaSCN (solid triangles). The hydrated anion radii and dispersion parameters are shown in Table 3. The results corresponding to non-polarizable anions are also plotted: NaCl (open squares), NaI (open circles) and NaSCN (open triangles). Dash, dot and dash-dot lines denote the predictions obtained from eq. 4 assuming that $\sigma_d =$ -0.05, -0.04 and -0.02 Cm^{-2} for NaI, NaCl and NaSCN, respectively. The prediction for $\sigma_d = -\sigma_0$ is also plotted (solid line).

Although the dehydration mechanism described above is rather rudimentary, it somehow considers the ideas about ion hydration developed by Collins.[55,56] According to this author, chaotropic ions (as Cs^+ and SCN^-) bind water molecules weakly relative to the strength of water-water interactions in bulk solutions. As a consequence, these ions are expected to present certain tendency to dehydration and, therefore, ion dispersion forces would become more significant. Concerning these ions, our work proves that specific effects due to dispersion forces are greater when dehydration is assumed for Cs^+ and SCN^- (figures 5 and 6, respectively). In any case, Collins claims that chaotropic ions cannot be properly included in models that consider the solvent as a continuum (especially in the case of hydrophobic surfaces).[55]

On the other hand, strongly hydrated ions are identified as kosmotropes (e.g., Ca^{2+} and Mg^{2+}). Our results also point to this conclusion, since similar data were found in electrophoretic mobility experiments and MC simulations for these two divalent cations when identical hydrated ion sizes were assumed.

A final consideration about the classical EDL theory. Finally, we would like to compare our simulation results with the predictions obtained from classical models. These approaches provide a well-known and widely applied charge/potential relationship, which is usually known as the Grahame equation:[44]

$$\sigma_d = -\mathrm{sgn}(\psi_d)\sqrt{2\varepsilon_0\varepsilon_r k_B T\sum_i \rho_i^0\left[\exp(-Z_i e\psi_d / k_B T)-1\right]} \quad (4)$$

Here, sgn(ψ_d) denotes the sign of ψ_d, ρ_i^0 is the ions density of the ionic species *i* into the solution bulk, and σ_d is the *diffuse* surface charge density. Following the original ideas of Grahame,[44] σ_d is defined as the total charge in a column of liquid of unit cross section extending from the OHP to the bulk of the solution, which can be mathematically expressed as:

$$\sigma_d = \int_{a_1}^{\infty}\sum_i Z_i\rho_i(z)dz \quad (5)$$

In relation to this, one should also bear in mind that the diffuse potential is evaluated (by definition) at the plane of closest approach of the hydrated ions to the charged surface.

First, we will analyze the cases in which the dehydration mechanism is not considered (results shown in Figures 1 and 3). In such cases, the Stern layer (the space between the OHP and the particle surface) does not contain dehydrated ions and, as a result of the electroneutrality condition, $\sigma_d + \sigma_0 = 0$. The ζ-potential obtained for 1:1 electrolytes from eq. 4 (and assuming $\zeta \approx \psi_d$) has also been plotted in Figures 1 and 3. As can be seen, the classical results are close to the simulation data. This is logical since dispersion forces have a negligible effect in this case and it is usually admitted that the classical approach works reasonably well for monovalent electrolytes, except if the surface charge density and/or the salt concentration and/or the ion size are high.[57]

The predictions of this Gouy-Chapman-Stern-Grahame (GCSG) model for 2:1 electrolytes are also shown in Figure 1. In this case, however, a quantitative disagreement between these data and the simulation results can be observed. Since dispersion forces have a negligible effect in this case, ion-ion correlations ignored by the classical theory must be responsible for such disagreement.[50]

If a dehydration mechanism is assumed, the calculation of the diffuse potential from eq. 4 is not a trivial matter any longer since σ_d is again required but $\sigma_d \neq -\sigma_0$. Unfortunately, such property is rarely known *a priori*, which forces us to make some assumptions about the behaviour of σ_d. For sake of simplicity, we will assume that this quantity does not depend on the electrolyte concentration. In this way, one could try to fit (*ad hoc*) the simulation results from eq. 4 using σ_d as the only fitting parameter. For instance, in Figure 5, we have plotted the cases corresponding to σ_d = 0.040 and 0.035 Cm^{-2}. The agreement between these two trials and the simulation data for LiCl and CsCl is much better than that obtained assuming $\sigma_d = -\sigma_0$. Only at high electrolyte concentrations, the GCSG curves deviate from the MC data. Obviously, this reduction in σ_d (as compared to the absolute value of the surface charge density) might be

attributed to specific adsorption. Nevertheless, it should be stressed that we are fitting rather than predicting.

A similar procedure can be applied to NaI, NaCl and NaSCN in presence of positively charged surfaces (Figure 6). After some trials, the values -0.05, -0.04 and -0.02 Cm^{-2} were chosen for σ_d in the cases of NaI, NaCl and NaSCN, respectively. For NaI and NaCl, the agreement is again moderately good. Small differences are reported only at high electrolyte concentrations. For NaSCN, however, the discrepancies at large salt concentrations become important. In particular, we conclude that the reversal found in experiments and simulations cannot be accounted for using a constant diffuse charge density. Then, one could be tempted to vary this parameter from case to case but, in this way, the capability of prediction would be considerably reduced. In any case, the application of charge/potential relationships like eq. 4 must be carefully examined. Previous simulations have proved that the validity of this equation is acceptable in the case of 1:1 electrolytes (see, for instance, reference 57). For multivalent ions, however, ion-ion correlations neglected by the classical EDL models could invalidate the use of these expressions.

5. Conclusions.

In this work, the effect of ionic dispersion forces on the behaviour of the ζ -potential (as a very representative electrokinetic property) has been looked into through Monte Carlo simulations. Our results reveal that the ionic van der Waals interactions could contribute to ionic specificity but ion size plays a fundamental role. According to the data reported here, the hydrated ion size prevents from intense ion-ion and colloid-ion dispersion forces in the case of monoatomic cations and some anions. For ions with smaller diameters and larger ion-ion and colloid-ion van der Waals parameters (such as SCN^-), ionic dispersion forces would be responsible (to great extent) for the specific features of its electrokinetic behaviour. These findings agree with experimental electrophoretic mobility data. In any case, the incomplete hydration of ions at the interface might enhance the specificity due to dispersion forces.

Acknowledgements.

The authors are grateful to “Ministerio de Educación y Ciencia, Plan Nacional de Investigación, Desarrollo e Innovación Tecnológica (I+D+i)”, Project MAT2006-12918-C05-02, “Consejería de Innovación, Ciencia y Empresa de la Junta de Andalucía”, Projects P06-FQM-01869, P07-FQM-02496 and P07-FQM-02517, as well as the European Regional Development Fund (ERDF) for financial support. A.M.-M. also thanks the “Programa Ramón y Cajal, 2005, Ministerio de Educación y Ciencia - Fondo Social Europeo (RYC-2005-000829)”. The helpful discussions of Dr. Ortega-Vinuesa are also sincerely acknowledged.

References.

(1) Gouy, G.; *J. Phys.* **1910**, *9*, 457.

(2) Chapman, D.L.; *Phil. Mag.* **1913**, *25*, 475.
(3) Collins, K. D.; Washabaugh, M. W. *Q. Rev. Biophys*. **1985**, *18*, 323.
(4) Ninham, B. W.; Yaminsky, V. *Langmuir* **1997**, *13*, 2097.
(5) Bostrom, M.; Williams, D. R. M.; Ninham, B. W. *Langmuir* **2001**, *17*, 4475.
(6) Bostrom, M.; Williams, D. R. M.; Ninham, B. W. *Phys. Rev. Lett.* **2001**, *87*, 168103.
(7) Bostrom, M.; Williams, D. R. M.; Ninham, B. W. *Langmuir* **2002**, *18*, 6010.
(8) Bostrom, M.; Williams, D. R. M.; Ninham, B. W. *J. Phys. Chem. B* **2002**, *106*, 7908.
(9) Bostrom, M.; Williams, D. R. M.; Ninham, B. W. *Langmuir* **2002**, *18*, 8609.
(10) Bostrom, M.; Williams, D. R. M.; Ninham, B. W. *Biophys. J.* **2003**, *85*, 686.
(11) Bostrom, M.; Craig, V. S. J.; Albion, R.; Williams, D. R. M.; Ninham, B. W. *J. Phys. Chem. B* **2003**, *107*, 2875.
(12) Kunz, W.; Belloni, L.; Bernard, O.; Ninham, B. W. *J. Phys. Chem. B* **2004**, *108,* 2398.
(13) López-León, T.; Jódar-Reyes, A.B.; Bastos-González, D.; Ortega-Vinuesa, J.L. *J. Chem. Phys. B* **2003**, *107*, 5696.
(14) Torrie, G. M.; Valleau, J. P.; *J. Chem. Phys.* **1980**, *73*, 5807.
(15) van Megen, W.; Snook, I. *J. Chem. Phys.* **1980**, *73*, 4656.
(16) Boda, D.; Ronald Fawcett, W.; Henderson, D.; Sokolowski, S. *J. Chem. Phys.* **2002**, *116*, 7170.
(17) Boda, D.; Henderson, D.; Plaschko P.; Ronald Fawcett, W. *Mol. Simul.* **2004**, *30*, 137.
(18) Valiskó, M.; Henderson, D.; Boda, D. *J. Phys. Chem. B* **2004**, *108*, 16548.
(19) Quesada-Pérez, M.; Martín-Molina, A.; Hidalgo-Álvarez, R. *J. Chem. Phys.* **2004**, *121*, 8618.
(20) Ravindran, S.; Wu, J. *Langmuir* **2004**, *20*, 7333.
(21) Taboada-Serrano, P.; Yiacoumi, S.; Tsouris, C. *J. Chem. Phys.* **2005**, *123*, 054703.
(22) Taboada-Serrano, P.; Yiacoumi, S.; Tsouris, C. *J. Chem. Phys.* **2006**, *125*, 054716.
(23) Madurga, S.; Martín-Molina, A.; Vilaseca, E.; Mas, F.; Quesada-Pérez, M. *J. Chem. Phys.* **2007**, *126*, 234703.
(24) Delville, A.; Gasmi, N.; Pellenq, R. J. M.; Caillol, J. M.; Van Damme, H. *Langmuir* **1998**, *14*, 5077.
(25) Deserno, M.; Jiménez-Ángeles, F.; Holm, C.; Lozada-Cassou, M. *J. Phys. Chem. B* **2001**, *44*, 10983.
(26) Mukherjee, A. K.; Schmitz K. S.; Bhuiyan L. B. *Langmuir* **2004**, *20*, 11802.
(27) Boda, D.; Varga, T.; Henderson, D.; Busath, D. D.; Nonner, W.; Gillespie, D.; Eisenberg, B. *Mol. Simul*. **2004**, *30*, 89.
(28) Quesada-Pérez, M.; Martín-Molina, A.; Hidalgo-Álvarez, R. *Langmuir* **2005**, *21*, 9231.
(29) Martín-Molina, A.; Quesada-Pérez, M.; Hidalgo-Álvarez, R. *J. Phys. Chem. B* **2006**, *110*, 1326.
(30) Valiskó, M. ; Boda, D.; Gillespie, D., *J. Phys. Chem. C*, **2007**, *107*, 15575.
(31) Boda, D.; Valiskó, M.; Eisenberg, B.; Nonner, W.; Henderson, D.; Gillespie, G. *Phys. Rev. Lett.* **2007**, *98*, 168102.
(32) Guldbrand, L.; Jonsson, B.; Wennerstrom, H.; Linse, P. *J. Chem. Phys.* **1984**, *80*, 2221.
(33) Wu, J. Z.; Bratko, D.; Prausnitz, J. M. *Proc. Natl. Acad. Sci. U.S.A.* **1998**, *95*, 15169.

(34) Delville, A.; Gasmi, N.; Pellenq, R. J. M.; Caillol, J. M.; Van Damme, H. *Langmuir* **1998**, *14*, 5077.
(35) Wu, J. Z.; Bratko, D.; Blanch, H. W.; Prausnitz, J. M. *J. Chem. Phys.* **1999**, *111*, 7084.
(36) Linse, P.; Lobaskin, V. *Phys. Rev. Lett.* **1999**, *83*, 4208.
(37) Moreira, A. G.; Netz, R. R. *Eur. Phys. J. E* **2002**, *8*, 33.
(38) Ravindran, S.; Wu, J. *Condens. Matter Phys.* **2005**, *8*, 377.
(39) Trulsson, M.; Jönsson, B. ; Akesson, T. ; Forsman, J. *Langmuir* **2007**, *23*, 11562.
(40) Tavares, F.W.; Brakto, D.; Blanch, H.W. ; Prausnitz, J.M. *J. Phys. Chem. B* **2004**, *108*, 9228.
(41) Boström, M.; Tavares, F.W.; Ninham, B.W.; Prausnitz, J.M. *J. Phys. Chem. B* **2006**, *110*, 24757.
(42) Huang, D.M.; Cottin-Bizonne, C.; Ybert, C.; Bocquet, L. *Phys. Rev. Lett.* **2007**, *98*, 177801.
(43) Huang, D.M.; Cottin-Bizonne, C.; Ybert, C.; Bocquet, L. *Langmuir* **2007,** *17*, 177801**.**
(44) Boström, M.; Tavares, F. W.; Bratko, D.; Ninham, B. W. *J. Phys. Chem. B* **2005**, 109, 24489.
(45) Martín-Molina, A.; Maroto-Centeno, J.A.; Hidalgo-Álvarez, R.; Quesada-Pérez, M. *J. Chem. Phys.* **2006,** *125*, 144906.
(46) Hunter, R. J. *Zeta Potential in Colloid Science. Principles and Applications*; Academic Press: London, 1981.
(47) Lyklema, J. *Solid/liquid dispersions (chapter 3)*; Academic Press: London, 1987.
(48) Israelachvili, J. N. *Intermolecular and Surface Forces*; Academic Press: London, 1992.
(49) Lozada-Cassou, M.; González-Tovar, E.; *J. Colloid Interface Sci*. **2001**, *239*, 285.
(50) Quesada-Pérez, M.; González-Tovar, E.; Martín-Molina, A.; Lozada-Cassou, M.; Hidalgo-Álvarez, R. *Colloid Surf. A* **2005**, *267*, 24.
(51) Tanaka, M. *Phys. Rev. E* **2003**, *68*, 061501.
(52) Lobaskin, V.; Dünweg, B.; Holm, C. *J. Phys.: Condens. Matter* **2004**, *16*, S4063.
(53) Chatterji, A.; Horbach, J. *J. Chem. Phys.* **2007**, *126*, 064907.
(54) Grahame, D. C. *Chem. Rev.* **1947**, *41*, 441.
(55) Collins, K. D. *Biophys. J.* **1997**, *72*, 65.
(56) Collins, K. D. *Biophys. Chem.* **2006**, *119*, 271.
(57) Ibarra-Armenta, J. G.; Martín-Molina, A.; Quesada-Pérez, M. *Phys. Chem. Chem. Phys.* **2009**, *11*, 309.

Paper III

Influence of monovalent ion size in colloidal forces probed by Monte Carlo simulations

José Guadalupe Ibarra-Armenta[1], Alberto Martín-Molina[2] and Manuel Quesada-Pérez[1]•

Phys. Chem. Chem Phys., **2011**, *13*, 13349.

(1) Departamento de Física, Escuela Politécnica Superior de Linares, Universidad de Jaén, 23700, Linares, Jaén, Spain.

(2) Grupo de Física de Fluidos y Biocoloides, Departamento de Física Aplicada, Facultad de Ciencias, Universidad de Granada, 18071 Granada, Spain.

* Corresponding author.

Abstract.
The present work studies the role of ionic size in the interactions between the electrical double layers of colloids immersed into electrolyte solutions of monovalent ions. Such interactions are studied by means of Monte Carlo (MC) simulations and the classical Derjaguin-Landau-Verwey-Overbeek (DLVO) theory. Despite the omission of the steric effects and some other features of real electrolyte solutions, DLVO theory is known to work qualitatively well for 1:1 electrolyte solutions. However, this affirmation is based on previous tests where an ionic diameter around 0.4 nm was taken for all ionic species. In contrast, some experimental studies suggest that larger hydrated ions should be considered and even specified for each type of ion. In this work, the importance of ionic size is analyzed by applying the primitive model of electrolyte to the intermediate region between a pair of equally charged infinite planar surfaces. The double layer interactions were calculated from the ionic densities at the distance of closest approach to the charged surfaces, this method constitutes an alternative to the traditional calculations at the midplane. Our MC simulations predict the existence of negative net pressures for monovalent electrolytes in the case of zero charge density. In addition, MC simulations reveal some disagreements with theoretical predictions for ionic diameters larger than 0.4 nm. These discrepancies can become significant if surface charge density is large enough due to the restructuration of the double layer. The physical mechanisms for these deviations are also discussed.

1. Introduction.

Interactions between charged colloids in aqueous electrolyte solutions have a great practical relevance in natural and industrial phenomena at different levels. It is possible to measure directly the forces between charged surfaces, electrodes or colloids by means of experimental techniques such as the atomic force microscope or the surface force apparatus. A considerable amount of information is available for aqueous electrolyte solutions containing polystyrene spheres, silica, acetate surfactant bilayers, etc.[1-6] and mica surfaces with different geometries from the experiments of Pashley *et al*.[7-10]

Concerning the theoretical description of these forces, the classical DLVO theory was introduced in its definitive form in 1947,[11,12] and since then it has become the most recurrent approach for colloidal stability analyses. Due to its mathematical simplicity, it has been preferred to fit experimental data rather than more recent and sophisticated approaches such as integral equation theories or the density functional theory. All these refined theories have in common that they consider the correlation between ions due their finite size, which is neglected in the classical theory. The reader interested in these topics is referred to some reviews and the references cited therein.[13-18]

Computer simulations have also been a helpful tool in the study of colloidal forces. For instance the works of Guldbrand, Valleau, Martín-Molina and their coworkers proved the existence of attractive electrostatic forces between like-charged plates in the presence of multivalent

counterions.[19-21] Electrostatic attraction between like-charged macroions of other geometries such as cylinders and spheres were also demonstrated using either MC or molecular dynamic simulations.[22-24] More recent simulation works have addressed other related aspects,[25-37] such as the discreteness of the surface charge.[25,32,35] However, an ionic diameter of the order of 0.4 nm was assumed for hydrated ions in the majority of these calculations. Recently, Ravindran and Wu carried out the calculations of double layer interactions between equally charged spherical macroions for different ionic sizes with the help of MC simulations,[33] highlighting the relevance of this parameter. In particular, they found an attractive interaction for a symmetric 2:2 electrolyte system that decreases as the ionic size increases. In the same direction, a very recent publication demonstrates that ionic size could turn attraction into repulsion for divalent counterions if their diameters are larger than 0.4 nm.[21] However, both studies were focused on solutions with multivalent ions where ionic correlations are expected to be more significant. In contrast, the case of monovalent electrolytes has received much less attention in simulations, since it is widely accepted that the DLVO works fairly well (at least qualitatively) for this type of electrolyte solutions. Only a few works have explicitly compared simulated forces/pressures with the DLVO predictions to test this classical theory. In particular, the pioneering work carried out by Guldbrand e*t al.* compared MC pressures with DLVO predictions for two charged plates. The validity of the classical theory for monovalent electrolytes was probed for moderate surface charge densities.[19] Comparisons with more sophisticated approaches also suggest that the forces between two charged plates in the presence of monovalent electrolytes are well described by DLVO theory under certain conditions. For instance, Tang *et al.* presented a direct comparison between density functional theory calculations and classical predictions as well, corroborating the good agreement between them for monovalent ions if the surface charge density and salt concentration are low enough.[38] However, the role of ionic size on colloidal forces was not specifically addressed in these works.

In a previous study, we experimentally demonstrated the occurrence of electrophoretic mobility inversion of colloids immersed in a solution of a monovalent salt made of large molecules. Moreover, the results were successfully fitted by using a simple mean field model in which highly hydrophobic monovalent cations with ionic diameters of 0.94 nm were considered.[39] As a consequence, if the electric properties of colloids immersed in monovalent electrolytes strongly depend on ionic size, the behavior of colloidal forces in monovalent salt is also expected to be influenced by this parameter. Therefore, we think that the validity of the classical theory for monovalent electrolytes should be tested for a wider range of ionic sizes.

In the present work a broad collection of electric double layer forces obtained by means of computer simulations are shown and compared to predictions from the classical DLVO theory. The model system consists of two infinite plates equally and uniformly charged in the presence of monovalent ions, which are modeled as charged hard spheres (primitive model). Computer simulations have been carried out in the grand canonical ensemble. Different ionic diameters are employed in order to clarify the role of ionic size. In particular, results obtained for ionic

diameters different from 0.4 nm are emphasized and compared with DLVO predictions. As will be discussed later, some discrepancies between DLVO and simulation data arise.

The rest of the paper is organized as follows. First, the model system and grand canonical MC simulations are described. Next section is dedicated to the presentation and discussion of simulation results, their comparisons with classical predictions, and the physical meaning of the variation of double layer forces. Finally, some concluding remarks are highlighted.

2. Simulations and force calculations.

Grand canonical MC simulations.

Our MC simulations are based on the primitive model of electrolyte, where the solvent is modelled as a continuum with a uniform dielectric permittivity $\varepsilon_0\varepsilon_r$ and a constant temperature T ($\varepsilon_r = 78.5$ and $T = 298\,K$). The Metropolis algorithm was applied to a grand canonical ensemble for ions modelled as charged hard spheres of diameter d confined into a rectangular simulation cell.[40,41] The simulation cell has the dimensions $L \times W \times W$, where two charged and impenetrable plane walls are located at $x = 0$ and at $x = L$. Each plane carries a uniform surface charge density σ_0. Periodic boundary conditions in the lateral directions (*y* and *z*) are required in the electrolyte solution. The simulation cell contains a fixed counterion excess neutralizing the surface charge deposited on the charged walls to ensure that the whole simulation cell is always neutral. It also contains a variable amount of electroneutral ionic groups from the bulk solution depending on the desired salt concentration.

Any pair of ions has an effective interaction energy given by

$$u(r_{ij}) = \frac{Z_i Z_j e^2}{4\pi\varepsilon_0\varepsilon_r r_{ij}}, \qquad r_{ij} > d$$

$$u(r_{ij}) = \infty, \qquad r_{ij} < d \tag{1}$$

Where Z_i is the ionic valence, e is the elementary charge and r_{ij} is the relative distance between ions *i* and *j*. The first term on eqn (1) is the coulomb interaction. However, a long range energy correction must be considered too. We took as reference that proposed by Boda *et al.* (see the original paper for further details).[42] The second term in eqn (1) accounts for the hard sphere nature of ions. Apart from ion-ion interactions there is also an effective energy of interaction between electrolyte ions and the charged walls and σ_0 is the uniform charge density spread over the charged walls. Our simulations took between 50 and 100 million grand canonical MC steps and the simulated systems were always thermalized around half million steps before collecting data for averaging. The precision of the bulk concentration was controlled within a relative error below 10^{-4}. One of the limitations of the primitive model is that this

representation of reality does not consider the solvent molecules. In relation to this, Pegado *et al.* have recently tested its validity comparing to simulations at molecular level. They concluded that no qualitative differences between the two models were found for the calculation of forces between equally charged plates.[43] In any case, the primitive model can be improved (without involving a molecular description) considering a variable permittivity. For instance, differences in the dielectric properties of the colloidal particles and the solvent in which they are dissolved may lead to image charge effects. The effect of image charges on the force between surfaces has been studied in the primitive model (see reference 16). Therein, authors prove that this effect is expected to be less important in the presence of electrolytes, as the image interaction is screened. Anyhow, we should keep in mind that our main objective is to find out what effects attributed to ion size are left out by DLVO theory, which also assumes a constant permittivity. If other additional aspects were accounted for in our model, ion size effects could not be easily differentiated.

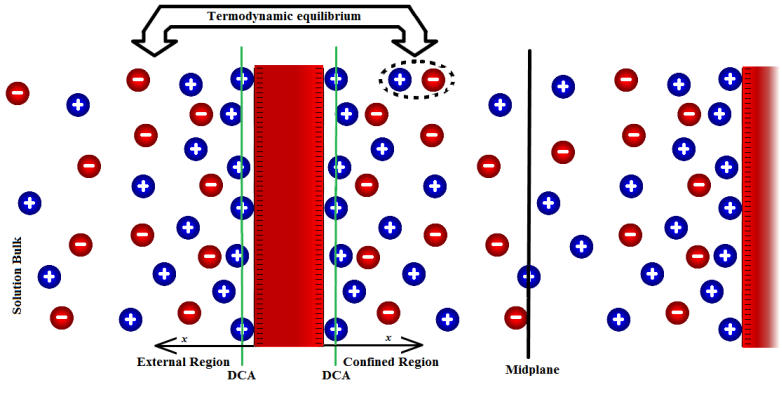

Fig. 1. Simulation model in the grand canonical ensemble.

Force calculations.

In this work a pressure (force per unit area) is reported. This quantity can be identified with the *osmotic* pressure (particularly in regions where the electric field vanishes) as some authors have already stated.[19,20,31,36] The pressure in the confined region (between the charged plates) can be evaluated equivalently at any reference plane parallel to the charged surfaces and requires the evaluation of three different pressure terms:

$$p = p_{kin} + p_{el} + p_{col} \tag{2}$$

The first term, is the kinetic pressure term, which is proportional to the total ionic density of all ionic species in solution, ρ, evaluated at the reference plane: $p_{kin} = k_B T \rho$, where k_B is the Boltzmann constant. The second one is the electric pressure term, which is proportional to the square of the electric field (E) across the reference plane: $p_{el} = -\varepsilon_0 \varepsilon_r E^2 / 2$. The last term

quantifies the contribution to the pressure of collisions between ions at opposite sides of the reference plane. If the reference plane is situated at the distance of closest approach ($x = d/2$) the collisional term vanishes since the ions (whose positions are identified by their centres) are located only beyond such plane. Consequently, the ions with $x > d/2$ cannot collide with ions with $x < d/2$ (because this region does not contain ions). In addition, the electrical term only depends on the surface charge density, since the electric field in the region between the charged wall and the plane of closest approach ($x = d/2$) is given by $p_{el} = \sigma_0 /(2\varepsilon_0\varepsilon_r)$ (Gauss' law) and, therefore, $p_{el} = -\sigma_0^2 /(2\varepsilon_0\varepsilon_r)$.

The pressure in the confined region (*internal pressure*) is a well defined property by eqn (2); however, it cannot be calculated directly since there exist also a pressure exerted by the surrounding bulk solution (*external pressure*) onto the charged plates. In practice, only the difference between the pressure in the confined region and the external pressure can be evaluated directly. In our calculations, the external pressure must be evaluated in the surrounding bulk solution region (where a single charged wall is in equilibrium with the solution bulk), see Fig. 1. This pressure difference is the only one to be reported in this paper and is known as the *net pressure*.[19-21,31,32,36,44] As mentioned previously, the electric terms will only depend on surface charge density. Then, they have the same value on both sides of the charged plate and will cancel each other in the evaluation of the net pressure. Furthermore, the collisional contributions are also zero, and then the net pressure can be calculated entirely from kinetic terms only evaluated at $x = d/2$:

$$p_{net} = p^{internal} - p^{external} = p_{kin}^{internal} - p_{kin}^{external} \tag{3}$$

Which are given in terms of contact densities by[21,23,27,45-47]

$$p_{net} = k_B T\left[\rho_{contact}^{internal} - \rho_{contact}^{external}\right] \tag{4}$$

Where $\rho_{contact}^{internal}$ and $\rho_{contact}^{external}$ are the contact densities at the internal (confined region) and external sides of the charged plate, respectively (see Fig. 1).

As can be easily concluded, the evaluation of *absolute* pressures (those computed from eqn (2)) and *net* pressure (eqn (4)) requires the extrapolation of local ionic densities to the distance of closest approach, $x = d/2$. In the case of *absolute* values, $p = k_B T\rho_{contact} - \sigma_0^2 /(2\varepsilon_0\varepsilon_r)$. These two terms are generally large (particularly in the case of high surface charge density) and nearly equal, as Guldbrand claimed.[19] Consequently, the extrapolation becomes a weak point of the method and leads to limited accuracy of the pressure values obtained. Only in theoretical calculations, these extrapolations are very reliable since contact densities can be computed within high accuracy.[46,48,51-54] The most practical way to avoid the problems derived from extrapolations in simulations is to calculate the pressure at the midplane of the system. Pioneers in these simulations defined in this fashion the midplane method.[13,19,20,22-36,45,49,50]

It should be stressed, however, that we are interested in *net* pressures rather than absolute pressures. Given the contact densities appearing in eqn 4 are very different for moderate and short distances, the reliability of net pressures evaluated at the distance of closest approach could be acceptable, particularly if an extremely high accuracy is not required. Moreover, the simulation cell can be divided into more intervals and the number of simulation steps can be increased to improve accuracy. In any case, the reliability of our method monovalent electrolytes was checked comparing with the results published by Kjellander,[44] which were obtained through the midplane method. Previously, this procedure was also checked for other types of electrolyte.[21] Both comparisons (not shown here) clearly supported the validity of the results obtained here.

3. Results and discussion.

In this section the simulation results are presented and compared to DLVO predictions. Theoretical predictions are calculated from a numerical implementation of the procedure proposed by Tang *et al*.[38] At this point it should be stressed that only the electrostatic force between charged surfaces is reported in this work, which is focused on electrical double layer interactions, *i.e.*, the van der Waals force is not computed by simulation.

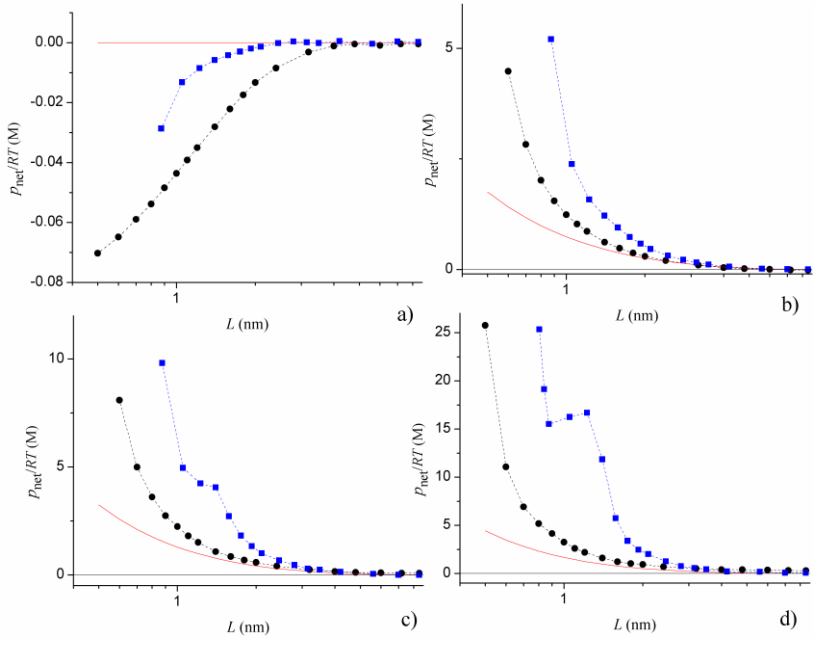

Fig. 2. Net pressure results as function of charged plates separation obtained from simulations (symbols) and theoretical prediction (line) for ionic diameters of 0.4 (circles) and 0.7 nm (squares) at 50 mM salt concentration. Four different charge densities are presented a) 0, b) 5, c) 10 and d) 15 $\mu C/cm^2$. The lines accompanying the symbols from simulations are just a guide for the eye.

We should keep in mind that our net pressure calculations are based on estimations of ionic contact densities (see eqn (4)). According to this, we should analyze the effect of electrostatic and hard-core correlations between ions on such ionic contact densities. Thus, our discussion about the physics behind the double layer interactions could be an alternative to most of the previous publications where the midplane method was employed and such interactions were discussed in terms of three contributions to pressure (see eqn (2)).[13,19,20,22-36,45,49,50]

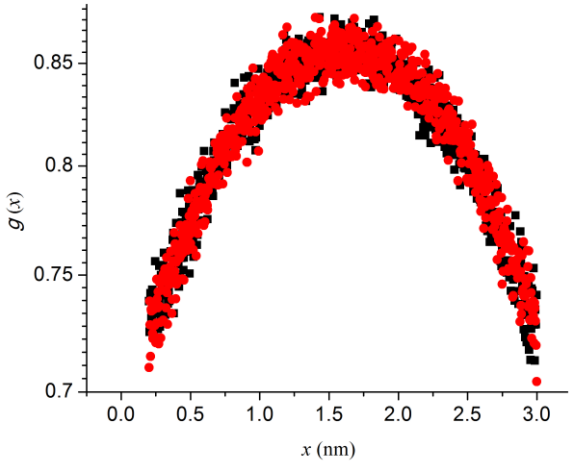

Fig. 3. Ionic distribution function for a 1:1 electrolyte with ionic diameter of 0.4 nm, at a salt concentration of 50 mM and a charge density of 0 μC/cm^2. The squares represent counterion profiles and circles coion profiles.

Pressure variation vs charge density.

First, the variation of the net pressure as a function of the surface charge density will be analyzed. Pressure data are normalized by RT, being R the universal gas constant (following the normalization used by other authors).[19,21,36,44] Consequently, *y*-axis must have units of molarity. Four different cases for monovalent symmetric 1:1 salt at a moderate 50 mM concentration are presented in Fig. 2, with surface charge densities ranging from 0 to 15 μC/cm^2. We have chosen these conditions because they cover a broad-spectrum of experimental systems in colloidal science. In addition, predictions from the classical theory are also plotted. Two representative ionic diameters were chosen: 0.4 and 0.7 nm. The ionic diameter choice of 0.7 nm is based on experimental estimations of hydrated ionic diameters reported by Israelachvili.[55] Values close to these have been employed to justify recent experiments on electrophoretic mobility and atomic force microscope for divalent and trivalent ions.[5,56-59]

The case presented in Fig. 2*a* ($\sigma_0 = 0$) deserves special attention because the electrolyte is completely symmetrical, *i.e.*, there are no excess counterions. As can be seen, the classical theory predicts a zero net pressure at all distances. This prediction relies on the assumption that a null charge density does not produce any electrical field or electrical potential. In contrast, the

simulated net pressure turns out to be negative. The existence of negative interactions between uncharged plates was previously addressed by simulations of colloidal forces in the presence of divalent counterions.[19-21] However, this is a noticeable finding for monovalent electrolyte. Negative net pressures can be justified as follows. Let us imagine a test ion in the confined region near one of the uncharged walls. The system formed by all the ions in this region except the test one will have opposite charge and, consequently, such test ion will be attracted towards the rest of the confined solution. Obviously, this causes a reduction of the ionic concentration near the charged plates (see Fig. 3). As charged plates approach fewer ions remain at contact with the charged plates. In consequence, the contact densities of the confined region are smaller than those of the external region at short distances between the charged plates (see Table 1) and the difference given by eqn (4) become negative. For large ionic species, excluded volume effects push ions near the wall towards the uncharged surface when the distance *L* is reduced. Consequently, the reduction of the inner contact density will be smaller for ions of 0.7 nm, and net pressure will be less negative (see Fig. 2*a*).

Table 1. Values of $\rho_{contact}^{\text{int}}$ and $\rho_{contact}^{ext}$ (divided by Avogadro's number) for the systems of Fig. 2. For $\rho_{contact}^{\text{int}}$ the presented value is calculated for a separation of two ionic diameters in each case.

	$\rho_{contact}^{\text{int}}/N_A$ (M)	$\rho_{contact}^{ext}/N_A$ (M)	$\rho_{contact}^{\text{int}}/N_A$ (M)	$\rho_{contact}^{ext}/N_A$ (M)
	d = 0.4 nm	d = 0.4 nm	d = 0.7 nm	d = 0.7 nm
0 μC/cm^2	0.022	0.075	0.093	0.099
5 μC/cm^2	2.828	0.811	2.042	0.828
10 μC/cm^2	6.501	2.891	7.041	2.987
15 μC/cm^2	11.472	6.290	18.335	6.506

Now we proceed to analyze the three non-zero charge density cases, Fig. 2*b*-*d*. Theoretical predictions and simulation results for ionic diameters of 0.4 nm show similar trends: monotonic and purely repulsive interactions. Tang *et al*. obtained similar results in their comparison with density functional theory assuming ionic diameters of 0.42 nm.[38] However, what happens for larger ionic diameters? Looking at the simulation data for ionic diameters of 0.7 nm we observe some inconsistencies with theory. First, net pressure curves obtained from simulations are shifted toward larger separation distances. Secondly, a non-monotonic behaviour appears for distances below 1.4 nm (two ionic diameters), as charge density increases.

In general, a monotonic repulsive trend is found by theory and simulations as charged plates approach due to the electrostatic repulsion among excess counterions, which rules the system behaviour to a great extent at short distances. As charged plates approach the available volume for ions in the confined region is reduced and coion-counterion pairs are expelled from the solution leading to a situation where excess counterions (placed close to the oppositely charged surfaces) dominate the electrolyte composition. In addition, these excess counterions repel among themselves and this repulsion increases as charged plates approach. This electrostatic

correlation mechanism also holds for point ions in the classical theory; however, theoretical predictions remain under simulation calculations because hard-core correlations do not play any role in the case of the theory. Excluded volume effects have been analyzed previously for a single electric double layer with the help of MC simulations.[60-71] Ionic size correlations contribute to increase the ionic concentrations close to the charged surface,[72,73] thus larger ionic diameters increase contact densities (see Table 1). Then, the observed differences between theory and simulation results for ionic diameters of 0.7 nm could be explained through the consideration of ionic size. The increment of the net pressure produced by electrostatic and hard-core repulsion among excess counterions at very short separations becomes abrupt because the available volume for excess counterions is scarce.

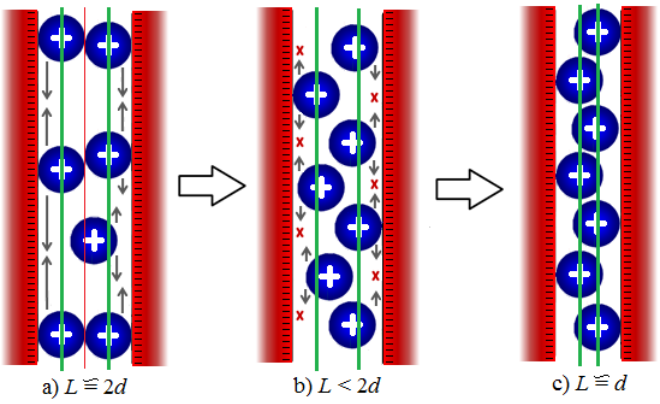

Fig. 4. Rearrangement of ions due to their steric effects crosses remarks regions on the charged plates where ions cannot lie at contact.

As mentioned above, the repulsion observed for large ions and highly charged plates (15 μC/cm^2) is non-monotonic and net pressure decreases for distances below two ionic diameters. Kjellander also reported shoulders breaking the monotonic behaviour for ionic diameters of 0.425 nm similar to those reported in our work in Figures 2 and 5 for ionic diameters of 0.7 nm.[44] It should be stressed, however, that their calculations were performed for a uniform charge density of 26.7 μC/cm^2, which is higher than the values considered in the present study. This suggests that the minimum surface charge density required for this phenomenon decreases with the ionic size. In other words, the ionic volume fraction near the plates for $L = 2d$ must be high enough (Fig. 4*a*). This can be illustrated analyzing Table 2, in which such volume fraction is given. As can be seen, this quantity is larger than 0.2 for the system exhibiting a non-monotonic pressure profile. In any case, Kjellander *et al.* ascribed these non-monotonic trends to the variation of the collisional term (see eqn (2)). We would like to offer an alternative explanation based on the behaviour of the inner contact density: when L is slightly larger than two counterion diameters, coions are expelled from this region, as mentioned before, and two layers of *highly packed*

counterions are forced to rearrange in the way illustrated in Fig. 4*b*. As can be seen, the movement of the ions is considerably restricted in the directions parallel to the plane (providing that the ionic volume fraction is high enough). Thus thermal fluctuations perpendicular to the wall are promoted, which causes a reduction in the inner contact density and the net pressure falls. However, for very short distances (close to one ionic diameter), counterions could contribute to the contact density of both plates simultaneously (see Fig. 4*c*) and net pressure would increase again.

Table 2. Individual and total packing fraction values in the confined region for the systems of Fig. 5 for a separation of two diameters between the charged plates.

	Counterions d = 0.4 nm	Coions d = 0.4 nm	Total d = 0.4 nm	Counterions d = 0.7 nm	Coions d = 0.7 nm	Total d = 0.7 nm
0 μ C/cm^2	0.00011	1.12×10^{-4}	0.00024	0.00251	0.00251	0.00503
5 μ C/cm^2	0.02095	6.72×10^{-6}	0.02096	0.07855	1.48×10^{-5}	0.07857
10 μ C/cm^2	0.04713	2.16×10^{-6}	0.04713	0.15708	3.29×10^{-7}	0.15708
15 μ C/cm^2	0.07723	7.92×10^{-7}	0.07723	0.23562	7.12×10^{-9}	0.23562

Table 3. Values of $\rho_{contact}^{\text{int}}$ and $\rho_{contact}^{ext}$ (divided by Avogadro's number) for the systems of Fig. 5. For $\rho_{contact}^{\text{int}}$ the presented value is calculated for a separation of two ionic diameters in each case.

	$\rho_{contact}^{\text{int}}/N_A$(M) d = 0.4 nm	$\rho_{contact}^{ext}/N_A$(M) d = 0.4 nm	$\rho_{contact}^{\text{int}}/N_A$(M) d = 0.7 nm	$\rho_{contact}^{ext}/N_A$(M) d = 0.7 nm
0 mM	11.539	6.347	18.578	6.183
50 mM	11.472	6.290	18.335	6.506
500 mM	11.527	7.041	18.483	7.743

Pressure variation vs salt concentration.

Fig. 5 shows net pressure for three different salt concentrations, 0, 50 and 500 mM, now the charge density is fixed at 15 μC/cm^2. Ionic diameters chosen for comparison are 0.4 and 0.7 nm again. In Fig. 5*d* the three salt concentration cases for ionic diameters of 0.7 nm are directly compared for sake of clarity. Once more DLVO predictions and simulation results for ionic diameters of 0.4 nm are in agreement to a great extent. Similar net force profiles were obtained; monotonic repulsive curves are reported for an ionic diameter of 0.4 nm whereas and non-monotonic repulsive curves appear in the case of 0.7 nm of diameter. Moreover, the net pressure decreases as salt concentration rises. This behaviour, which qualitatively agrees with classical predictions, can be observed more easily if all data for the case of ionic diameters of 0.7 nm are plotted together (see Fig. 5*d*).

However, from a quantitative point of view, this reduction is not important. Certain saturation effect at high surface charge density could be responsible for this insensitivity to the ionic strength, which has been also reported for asymmetrical electrolytes.[21] For moderate and highly

charged systems, the inner and outer surfaces will be nearly neutralized by the corresponding layer of counterions. If the surface charge density is high enough, this layer will be *saturated*. This means that, due to electrostatic repulsions, many more counterions are not able to approach the surface with adding salt and the contact density will not change considerably. This insensitivity of the inner and outer contact densities to the salt concentration is illustrated in Table 3 for the systems analyzed in Fig. 5 for a distance of two ionic diameters.

Kjellander *et al*. analyzed the variation of net pressure as a function of salt concentration for 1:1 electrolyte solutions with ionic diameters of 0.425 nm.[44] These authors performed MC simulations and compared their results to the anisotropic HNC theory for 0, 1 and 2 M salt concentrations. They obtained purely repulsive net pressures except for a salt concentration of 2 M. In this case a slight attractive interaction at intermediate distances was obtained.

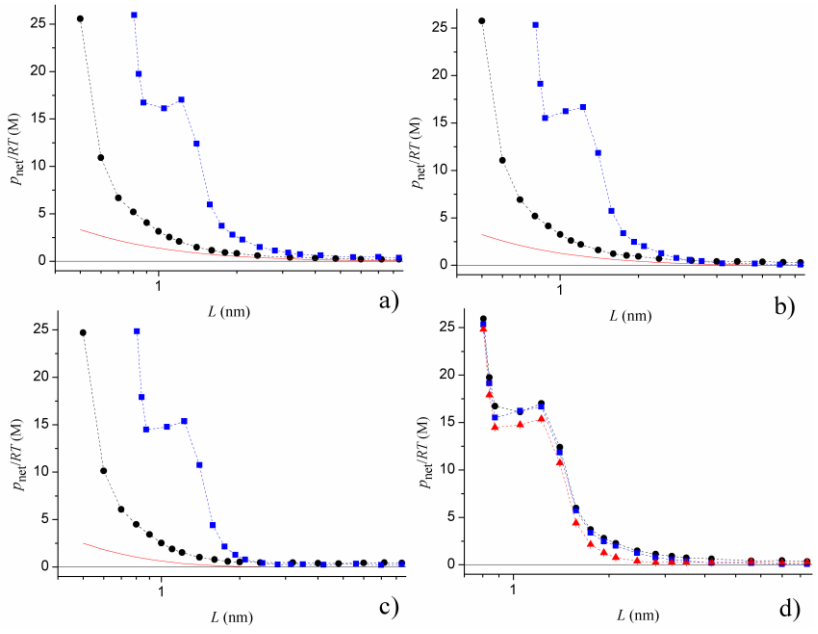

Fig. 5. Net pressure results as function of charged plates separation obtained from simulations (symbols) and theoretical prediction (line) for ionic diameters of 0.4 (circles) and 0.7 nm (squares) at a fixed charge density of 15 μC/cm^2 and a variable salt concentration a) 0, b) 50 and c) 500 mM. Graph d) contains the direct comparison between MC simulation results for ionic diameters of 0.7 nm. In graph d) circles, squares and up triangles represent 0, 50 and 500 mM salt concentrations respectively. The lines accompanying the symbols from simulations are just a guide for the eye.

Effect of ionic size on pressure profiles.

To conclude our comparison between theory and simulations, the direct dependence of net pressure on the ionic size is summarized. Pressure profiles for five different ionic diameters, 0.4, 0.7, 0.8, 0.9 and 1 nm are plotted in Fig. 6. Ionic diameters beyond 0.7 nm would be rather large

values for most monovalent ions,[55] perhaps they might be representative for some monovalent complexes.[39] In any case, the results corresponding to the largest ionic diameters are presented with illustrative purposes. The charge density and salt concentration are fixed at 10 μC/cm^2 and 50 mM, respectively. The corresponding ionic volume fractions near the plates for $L = 2d$ are reported in Table 4. Although the theoretical predictions are independent of ionic size, the corresponding line is also plotted in Fig. 6.

Table 4. Individual and total packing fraction values in the confined region for the systems of Fig. 6 for a separation of two diameters between the charged plates.

	Counterions	Coions	Total
d = 0.4 nm	0.04713	2.167×10^{-6}	0.04713
d = 0.7 nm	0.15708	3.296×10^{-7}	0.15708
d = 0.8 nm	0.20420	4.682×10^{-8}	0.20420
d = 0.9 nm	0.26180	2.194×10^{-9}	0.26180
d = 1 nm	0.32463	0	0.32463

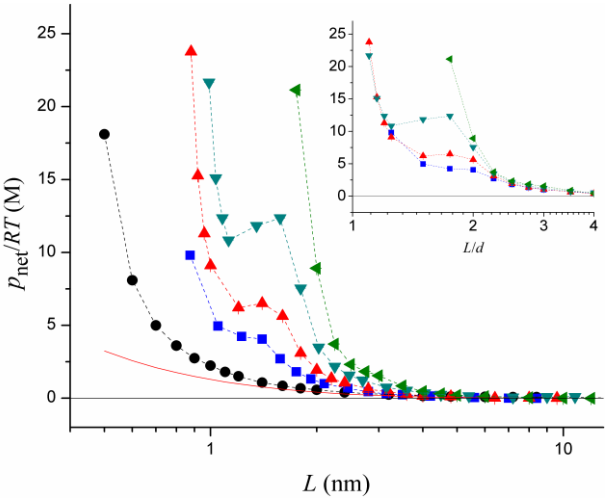

Fig. 6. Net pressure results as function of charged plates separation obtained from simulations (symbols) for ionic diameters of 0.4 (circles), 0.7 (squares), 0.8 (up triangles), 0.9 (down triangles) and 1 nm (left triangles) at a fixed surface charge density of 10 μC/cm^2 and a fixed salt concentration of 50 mM. The theoretical prediction (line) is also plotted. The inset shows the net pressure profiles from ionic diameters where *shoulders* were reported; data are normalized by the corresponding ionic diameter. The lines accompanying the symbols from simulations are just a guide for the eye.

Once more a fairly good agreement is obtained between theory and simulations for ionic diameters of 0.4 nm. The net pressure results for ionic diameters of 0.7 nm and beyond are increasingly farther from classical theory. For ionic diameters of 0.8 and 0.9 nm the non-monotonic behaviour is clearly observed. For 1.0 nm, one might also expect a '*shoulder*' in the net pressure profile for $p_{net}/RT > 25$M, but our results do not seem to support this hypothesis.

In relation to this, it should be kept in mind that some technical problems appear in simulations of so large ions at very high volume fractions. Consequently, the regime of very high net pressures (as well as the existence of the non-monotonic behaviour) cannot be explored in this case. If the results for 1.0 nm are therefore discarded, Table 4 again reveals that the mentioned phenomenon takes place for ionic volume fractions of the order of 0.2 (or larger).

4. Conclusions.

The role of ionic size in colloidal stability has been revisited in this work. We have performed grand canonical MC simulations and calculated the net pressures for a pair of charged infinite plates in the presence of monovalent and symmetric 1:1 electrolyte solutions. The simulations were carried out in the grand canonical ensemble within the primitive model of electrolyte (in which ion size effects are implicitly present). Taking advantage of the current computational resources, net pressure was calculated at the distance of closest approach (after proving its reliability). A broad collection of simulation results were presented in direct comparison with the classical DLVO theory. A procedure to find the net pressure in the frame of the classical DLVO theory was also implemented.

From the comparison between theory and simulations, good agreement was found for ionic diameters of 0.4 nm (ionic diameter widely used in previous simulational works). Net pressure is always repulsive for charged plates in both theoretical predictions and simulation results. Concerning larger ionic diameters (from 0.7 nm), certain disagreements between theory and simulations are reported. For intermediate and large separations these discrepancies are only quantitative, but non-monotonic pressure profiles can be observed for separations smaller than two ionic diameters if the surface charge density and/or ionic size are large enough. If we admit that 0.7 nm is a realistic ionic diameter for many monovalent hydrated ions, the forces predicted by DLVO theory for greater surface charge densities should be carefully considered. Our simulations also reveal significant deviations from the classical monotonic behavior for larger ionic sizes. These discrepancies might be explained by excess counterion rearrangements at small separations.

The case of uncharged plates (or large colloidal particles) also exhibits a qualitative deviation from DLVO predictions: Negative net pressures in the presence of monovalent electrolytes. This outstanding behaviour can be explained in terms correlated attractions of ions in the confined region between the charged plates. This feature cannot be reproduced by the classical description of the double layer.

Acknowledgements

The authors are grateful to “Ministerio de Educación y Ciencia, Plan Nacional de Investigación, Desarrollo e Innovación Tecnológica (I+D+i)”, Project MAT2009-13155-C04-04, “Consejería de Innovación, Ciencia y Empresa de la Junta de Andalucía”, Projects P07-FQM-02496, P07-FQM-

02517 and P09-FQM-4698, as well as the European Regional Development Fund (ERDF) for financial support.

References

1. R. M. Pashley, P. M. McGuiggan, B. W. Ninham, J. Brady and D. F. Evans, *J. Phys. Chem.*,1986, **90**, 1637.
2. P. Kekicheff, S. Marcelja, T. J. Senden and V. E. Shubin, *J. Chem. Phys.*, 1993, **99**, 6098.
3. V. E. Schubin and P. Kekicheff, *J. Colloid Interface Sci.*, 1993, **155**, 108.
4. R. F. Considine, R. A. Hayes and R. G. Horn, *Langmuir*, 1999, **15**, 1657.
5. K. Besteman, M. A. G. Zevenbergen, H. A. Heering and S. G. Lemay, *Phys. Rev. Lett.*, 2004, **93**, 170802.
6. K. Besteman, M. A. G. Zevenbergen and S. G. Lemay, *Phys. Rev. E*, 2005, **72**, 061501.
7. R. M. Pashley and J. N. Israelachvili, *J. colloid Interface Sci.*, 1983, **97**, 446.
8. R. M. Pashley and J. N. Israelachvili, *J. Colloid Interface Sci.*, 1984, **101**, 511.
9. P. M. McGuiggan and R. M. Pashley, *J. Phys. Chem.*, 1988, **92**, 1235.
10. R. Kjellander, S. Marcelja, R. M. Pashley and J. P. Quirk, *J. Chem. Phys.*, 1990, **92**, 4399.
11. B. V. Derjaguin and L. Landau, *Acta Phys. Chim. (URSS)*, 1941, **14**, 633.
12. E. J. W. Verwey and J. T. G. Overbeck, *Theory of the Stability of Lyophobic Colloids;* Elsevier: Amsterdam, 1948.
13. L. Belloni, *J. Phys.: Condens. Matter*, 2000, **12**, R549.
14. J. P. Hansen and H. Löwen, *Annu. Rev. Phys. Chem.*, 2000, **51**, 209.
15. M. Quesada-Pérez, J. Callejas-Fernández and R. Hidalgo-Álvarez, *Adv. Colloid Interface Sci.*, 2002, **95**, 295.
16. M. M. Hatlo and L. Lue, *Soft Matter*, 2008, **4**, 1582.
17. J. Lyklema, *Adv. Colloid Interface Sci.*, 2009, **147-148**, 205.
18. V. Dahirel and M. Jardat, *Curr. Op. Colloid Interface Sci.*, 2010, **15**, 2.
19. L. Guldbrand, B. Jönsson, H. Wennerström and P. Linse, *J. Chem. Phys*., 1984, **80**, 2221.
20. J. P. Valleau, R. Ikov and G. M. Torrie, *J. Chem. Phys.*, 1991, **95**, 520.
21. A. Martín-Molina, J. G. Ibarra-Armenta, E. González-Tovar, R. Hidalgo-Álvarez and M. Quesada-Pérez, *Softmatter*, 2011, **7**, 1441.
22. E. Allahyarov, I. Damico and H. Lowen, *Phys. Rev. Lett.*, 1998, **81**, 1334.
23. J. Z. Wu, D. Bratko, H. W. Blanch and J. M. Prausnitz, *J. Chem. Phys.*, 1999, **111**, 7084.
24. J. Z. Wu, D. Bratko, H. W. Blanch and J. M. Prausnitz, *J. Chem. Phys.*, 2000, **113**, 3360.
25. S. Meyer and A. Delville, *Langmuir*, 2001, **17**, 7433.
26. S. J. Marrink and S. Marcelja, *Langmuir*, 2001, **17**, 7929.
27. A. G. Moreira and R. R. Netz, *Eur. Phys. J. E*, 2002, **8**, 33.

28. D. G. Angelescu and P. Linse, *Langmuir*, 2003, **19**, 9661.
29. F. W. Tavares, D. Bratko, H. W. Blanch and J. M. Prausnitz, *J. Phys. Chem. B*, 2004, **108**, 9228.
30. P. Linse, *Adv. Polym. Sci.*, 2005, **185**, 111.
31. B. Jönsson, A. Nonat, C. Labbez, B. Cabane and H. Wennerström, *Langmuir*, 2005, **21**, 9211.
32. M. O. Khan, S. Petris and D. Y. C. Chan, *J. Chem. Phys.*, 2005, **122**, 104705.
33. S. Ravindran and J. Z. Wu, *J. Condens. Matter Phys.*, 2005, **8**, 377.
34. M. Boström, F. W. Tavares, B. W. Ninham and J. M. Prausnitz, *J. Phys. Chem. B*, 2006, **110**, 24757.
35. P. Taboada-Serrano, S. Yiacoumi and C. Tsouris, *J. Chem. Phys.*, 2006, **125**, 054716.
36. M. Trulsson, B. Jönsson, T. Åkesson and J. Forsman, *Langmuir*, 2007, **23**, 11562.
37. E. R. A. Lima, D. Horinek, R. R. Netz, E. C. Biscaia, F. W. Tavares, W. Kunz and M. Boström, *J. Phys. Chem. B*, 2008, **112**, 1580.
38. Z. Tang, L. E. Scriven and H. T. Davis, *J. Chem. Phys.*, 1992, **97**, 9258.
39. A. Martín-Molina, C. Calero, J. Faraudo, M. Quesada-Peréz, A. Travesset and R. Hidalgo-Álvarez, *Soft Matter*, 2009, **5**, 13550.
40. M. Metropolis, The Beginning of the Monte Carlo Method. *LASL*, 1987, **12**, 125.
41. D. Frenkel and B. Smit, *Understanding Molecular Simulation from Algorithms to Applications;* Academic Press: London, 1992.
42. D. Boda, K. Y. Chan and D. Henderson, *J. Chem. Phys.*, 1998, **109**, 7362.
43. L. Pegado, B. Jönsson and H. Wennerström, *J. Chem. Phys.*, 2008, **129**, 184503.
44. R. Kjellander, T. Åkesson, B. Jönsson and S. Marcelja, *J. Chem. Phys.*, 1992, **97**, 1424.
45. H. Wennerström, B. Jönsson and P. Linse, *J. Chem. Phys.*, 1982, **76**, 4665.
46. D. Henderson, L. Blum and L. Lebowitz, *J. Electroanal. Chem.*, 1979, **102**, 315.
47. D. Henderson, *Prog. Surf. sci.*, 1983, **13**, 197.
48. D. Henderson and L. Blum, *J. Chem. Phys.*, 1978, **69**, 5441.
49. M. A. G. Dahlgren, Å. Waltermo, E. Blomberg, P. M. Claesson, L. Sjöström, T. Åkesson and B. Jönsson, *J. Phys. Chem.*, 1993, **97**, 11769.
50. L. Sjöström and T. Åkesson, *J. Colloid Interface Sci.*, 1996, **181**, 645.
51. R. Kjellander and B. Bunseges. *Phys. Chem*., 1996, **100**, 894.
52. M. F. Holovko, J. P. Badiali, and D. di Caprio, *J. Chem. Phys*., 2005, **123**, 234705.
53. M. F. Holovko and J. P. Badiali, *Condensed Matter Physics*, 2005, **8**, 281.
54. M. F. Holovko, J. P. Badiali, and D. di Caprio, *J. Chem. Phys*. 2007, **127**, 014106.
55. J. N. Israelachvili, *Intermolecular and Surface Forces;* Academic Press: London, 1985.
56. A. Martín-Molina, M. Quesada-Pérez, F. Galisteo-González and R. Hidalgo-Álvarez, *J. Chem. Phys.*, 2003, **118**, 4183.
57. M. Quesada-Pérez, E. González-Tovar, A. Martín-Molina, M. Lozada-Cassou and R. Hidalgo-

Álvarez, *Chem. Phys. Chem.*, 2003, **4**, 234.
58. M. Quesada-Pérez, E. González-Tovar, A. Martín-Molina, M. Lozada-Cassou and R. Hidalgo-Álvarez, *Colloid Surf. A*, 2005, **267**, 24.
59. A. Martín-Molina, J. A. Maroto-Centeno, R. Hidalgo-Álvarez and M. Quesada-Pérez, *Colloid. Surf. A*, 2007, **319**, 103.
60. V. Kralj-Iglic and A. Iglic, *J. Phys. II (France)*, 1996, **6**, 477.
61. K. Bohinc, V. Kralj-Iglic and A. Iglic, *Electrochim. Acta*, 2001, **46**, 3033.
62. R. Messina, E. Gonzalez-Tovar, M. Lozada-Cassou and C. Holm, *Europhys. Lett.*, 2002, **60**, 383.
63. D. Boda, W. R. Fawcett, D. Henderson and S. Sokolowski, *J. Chem. Phys.*, 2002, **116**, 7170.
64. M. Boström, D. R. M. Williams and B. W. Ninham, *Langmuir*, 2002, **18**, 6010.
65. E. González-Tovar, F. Jiménez-Ángeles, R. Messina and M. Lozada-Cassou, *J. Chem. Phys.*, 2004, **120**, 9782.
66. D. Boda, D. Henderson, P. Plaschko and W. R. Fawcett, *Mol. Simul.*, 2004, **30**, 137.
67. L. B. Bhuiyan and C. W. Outhwaite, *Phys. Chem. Chem. Phys.*, 2004, **6**, 3467.
68. M. Valiskó, D. Henderson and D. Boda, *J. Phys. Chem. B*, 2004, **108**, 16548.
69. M. Quesada-Pérez, A. Martín-Molina and R. Hidalgo-Álvarez, *J. Chem. Phys.*, 2004, **121**, 8618.
70. V. Valiskó, D. Boda and D. Gillespie, *J. Phys. Chem. C*, 2007, **111**, 15575.
71. A. Martín-Molina, J. G. Ibarra-Armenta and M. Quesada-Pérez, *J. Phys. Chem. B*, 2009, **113**, 2414.
72. J. G. Ibarra-Armenta, A. Martín-Molina and M. Quesada-Pérez, *Phys. Chem. Chem. Phys.*, 2009, **11**, 309.
73. F. Jiménez-Ángeles and M. Lozada-Cassou, *J. Phys. Chem. B*, 2004, **108**, 7286.

Paper IV

Monte Carlo simulations of the electrical double layer forces in the presence of divalent electrolyte solutions: Effect of the ion size

Alberto Martín-Molina[(1)], José Guadalupe Ibarra-Armenta[(2)], Enrique González-Tovar[(1,3)], Roque Hidalgo-Álvarez[(1)] and Manuel Quesada-Pérez[(2)]*

Soft Matter, **2011**, *7*, 1441.

(1) Grupo de Física de Fluidos y Biocoloides, Departamento de Física Aplicada, Facultad de Ciencias, Universidad de Granada, 18071 Granada, Spain.

(2) Departamento de Física, Escuela Politécnica Superior de Linares, Universidad de Jaén, 23700, Linares, Jaén, Spain.

(3) Permanent address: Instituto de Física, Universidad Autónoma de San Luis Potosí, Álvaro Obregón 64, 78000 San Luis Potosí, S.L.P., México.

* Corresponding author.

ABSTRACT.

In this paper, the effect of ion size on the mean forces between two charged plates in the presence of divalent counterions is analyzed with the help of Monte Carlo simulations in the framework of the primitive model. Inspired by a preliminary work in which a particular and isolated case was presented, we propose a more systematic survey considering both like and oppositely charged plates, different surface charge densities (with magnitudes ranging from 0.01 to 0.2 C/m^2) and two very different ionic strengths (0.5 and 500 mM). The effect of ion size is probed comparing systematically results for the most commonly used ionic diameter (0.425 nm) and greater values reported in the scientific literature for hydrated ions. These greater values were previously and successfully employed in other areas (e.g., electrokinetic behaviour in the presence of divalent and trivalent ions). Our simulations show that force-distance profiles strongly depend on the ion size. Consequently, some of the 'classical' findings obtained from simulations must be carefully reconsidered. In particular, the widely known and reported attraction between like-charged plates (or macroions) becomes repulsion with increasing ion size.

1. INTRODUCTION.

Numerous physical, chemical, and biological processes are governed by electrostatic interactions between dispersed charged colloids such as soluble proteins, micelles, polymer latexes, polyelectrolytes, etc.[1] In all these systems, the effective electrical forces arise from the colloidal surface charges and from the distribution of ions around the charged surface, known as the electric double layer (EDL). This ionic structure plays therefore an important role in the stability of colloidal dispersions. For many decades, classical models based on the Poisson-Boltzmann equation (PBE) have been the traditional approach to describing the EDL. However, this mean field approximation fails under diverse conditions, which include the presence of multivalent ions, elevated monovalent salt concentrations, ions with a large diameter, high surface charges and solvents with a low dielectric constant. Under these situations, classical EDL models break down principally because the PBE neglects certain aspects such as the finite ion size.[2,3] Similar conclusions are expected for colloidal forces given that the electrostatic interaction between colloidal particles is a direct consequence of the interaction between their EDLs,

Historically, the first theoretical approximation to describe the forces between lyophobic colloids is the DLVO theory.[4,5] According to this formalism, the resulting force between two colloids is the sum of an attractive van der Waals term and an effective electrostatic term, which is computed by means of the PBE. Despite the success of the DLVO theory in the qualitative description of some colloidal stability experiments, the model fails to predict other experimental results as well as numerous theoretical and simulation results.[1,6-9] Undoubtedly, one of the most fascinating results in colloidal science, which cannot be described by the DLVO approach, is the attraction between like-charged particles (or repulsion between oppositely charged particles) in the

presence of multivalent counterions. This behaviour has been reported experimentally[10-16] and it is usually explained in terms of ion-ion correlations (neglected by the PBE).[6-8]

Computer simulations in the framework of the primitive model (PM) have been a very useful tool in the study of colloidal forces since the pioneer works by Gulbrand and Valleau.[17,18] In fact, they showed that electrostatic forces between like-charged plates can be attractive in the presence of divalent counterions. This finding clearly demonstrated that the DLVO theory could fail for multivalent counterions. Then, other Monte Carlo or molecular dynamics simulations reported this short-range attraction for other like-charged macroions (such as spheres and cylinders).[19-25]

Computer simulations have also analyzed different issues on colloidal forces, such as the surface charge discretization,[26-27] the inclusion of ionic dispersion forces,[28-29] or the competition between ions with different valence.[30-32] Simulations have also revealed new counterintuitive phenomena related with colloidal forces, such as repulsion between macromolecules with opposite charge.[33,34]

However, the effect of the ionic size on colloidal forces has been scarcely analyzed. In fact, many authors have not paid any attention to this parameter and have used the same ionic diameter, of about 0.4 nm, in their simulations (or theoretical calculations). This value is rather small compared to those found in the scientific literature for hydrated ions.[35] In addition, it has been proven that the use of different ionic radii has a strong influence in the structure of the EDL.[36-39]

Our previous studies about the electrokinetic properties of colloidal particles and charge inversion seem to support this idea as well. For example, the electrokinetic behaviour of some latexes in the presence of calcium, magnesium and lanthanum can be explained with ionic diameters larger than the classical one. In addition, the mobility reversal reported for trivalent cations can be justified with these larger diameters. In any case, we have also concluded from all these prior investigations that ion size plays a key role in the case of systems with divalent and trivalent ions.[40-44]

Although some authors have calculated the interaction between colloids using ion size values larger than the classical one[12,32,34] only Ravindran and Wu have specifically examined the effect of ion size on forces between colloids.[45] In particular, these authors analyzed the effect of the ion size on forces between like-charged spheres immersed in a continuum dielectric in the presence of a 2:2 electrolyte. They used Monte Carlo (MC) simulations within the framework of the restricted PM and reported that the attraction between like-charged spheres decreased with increasing ionic size. This finding is really valuable but it was only obtained for spheres with a particular surface charge density and for a fixed symmetric electrolyte concentration. In our opinion, however, the effect of ion size should be studied for a wider collection of situations (and, specifically, for plates). In addition, they only studied ionic diameters smaller than 6 angstroms, and according to the previously cited literature, one could even consider larger ions.

The goal of the present work is inspired precisely by the cited paper as well as by our own experience studying the effect of the ion size on the colloidal EDL. In this sense, we also use MC simulations within the PM of electrolyte to analyze the effect of the ion size in colloidal forces. In

particular, the electrostatic forces between charged plates in the presence of a 2:1 electrolyte are simulated. However, we propose a broader and more systematic study including like- and oppositely charged plates, different surface charge densities and different salt concentrations. Moreover, the size for hydrated ions will be a bit greater than that suggested by Ravindran and Wu (according to the cited literature and previous works). In this way, our survey offers new insight into the effect of ion size on electrostatic colloidal forces. For instance, we demonstrate that, for like-charged plates with high surface charge densities, an increase of the ion size not only diminishes the attractive interaction between the plates but even causes a repulsive barrier. In any case the reader should keep in mind that we are interested only in forces originated by the EDL. Other interactions (e. g. van der Waals forces, ionic dispersion forces) go beyond the scope of this work and will not be considered.

2. SIMULATIONS.

Grand canonical MC simulations.

The MC simulations are based on a primitive model of electrolyte, in which ions are considered charged hard spheres of diameter d_i (where i stands for the different ionic species) and the solvent is modelled as a continuum with a uniform dielectric permittivity $\varepsilon_0\varepsilon_r$ and a constant temperature T (we set $\varepsilon_r = 78.5$ and $T = 298\ K$). The Metropolis algorithm was applied to a grand canonical ensemble of ions confined into a rectangular simulation cell whose dimensions are $L \times W \times W$. Two charged and impenetrable plane walls are located at $x = 0$ and at $x = L$. The electrolyte composition is constrained to periodic boundary conditions in the lateral directions (y and z). The total electrolyte solution contains a variable quantity of electroneutral ionic groups depending on the desired salt concentration for the bulk solution. It also contains a fixed amount of excess counterions which neutralize the surface charge of the walls ensuring that the whole simulation cell is always neutral.

The interaction energy between mobile ions is given by

$$u(\vec{r}_{ij}) = \frac{Z_i Z_j e^2}{4\pi\varepsilon_0\varepsilon_r}\frac{1}{r_{ij}} \quad r_{ij} > (d_i + d_j)/2$$
$$u(\vec{r}_{ij}) = \infty \qquad\qquad r_{ij} \le (d_i + d_j)/2 \tag{1}$$

where r_{ij} the distance between the ions i and j, e is the elementary charge and Z_i is the valence of species i. The second line in eqn (1) accounts for the hard sphere nature of ions in the PM, whereas the first is the Coulomb interaction energy. In relation with this term and the technical details of the MC simulations, it should be stressed that the energy of the system must be carefully computed if long-range forces are involved. In this work, the method proposed by Boda *et al.* was implemented for long-range corrections.[46] According to this procedure, the effect of the charges surrounding the simulation cell is taken into account by infinite sheets parallel to the

charged walls. The reader interested in further details on the implementation of the technique is referred to the original work by Boda *et al.*[46] The interaction energy of ion i with the charged walls is

$$u(x_i) = -\frac{\sigma_0 Z_i e x_i}{2\varepsilon_0 \varepsilon_r} + \frac{\sigma_L Z_i e x_i}{2\varepsilon_0 \varepsilon_r}, \qquad d_i/2 \le x_i \le L - d_i/2$$
$$u(x_i) = \infty, \qquad x_i < d_i/2,\ x_i > L - d_i/2 \tag{2}$$

x_i is the *x*-coordinate of particle *i* and σ_0 and σ_L are the uniform charge densities spread over both charged planes at $x = 0$ and $x = L$, respectively. In 80% of the simulation steps a single ion displacement is tried. In the remaining 20%, the removal of an electroneutral group of ions or its insertion at random positions of the simulation cell is attempted. Insertions are tried in 10% of the simulation steps and the other 10% are removal attempts. Electroneutral groups of ions to be inserted are taken from a reservoir containing the desired salt concentration for the bulk solution in thermodynamic equilibrium with the electrolyte solution inside the simulation cell.

Our implementation of the Grand Canonical MC (GCMC) technique is based on the works by Adams for neutral hard spheres,[47,48] later extended by Valleau and Cohen in 1980 for charged spheres.[49] In the original implementation by Valleau and Cohen a mean activity coefficient is provided as input and then a salt concentration is obtained. However, the salt concentration to be obtained is *a priori* unknown. We have applied an inverse iterative GCMC technique in order to obtain the corresponding activity coefficient that corresponds to the desired salt concentration. The activity coefficient is periodically recalculated from the output value of the salt concentration and its deviation from the desired one. The relative error in the electrolyte concentration of the bulk solution (deviation from the desired value) was in any case less than 10^{-4}. Recently, other iterative procedures have been proposed by different authors.[50-53] More references and details about these techniques can be found in the original papers by such authors.[47-53]

Pressure calculations.

In order to describe the stability of colloidal systems it is required to calculate first the mean force between a pair of particles at all separations. The model system of planar charged surfaces is suitable for plane electrodes or large enough colloids, for which the effect of surface curvature can be neglected. For this system the force cannot be directly calculated. Instead, pressure (force per unit area) is reported.

The pressure in the region confined between the charged plates can be evaluated equivalently at any reference plane parallel to the charged surfaces. In principle, three different pressure terms have to be computed:

$$p = p_{kin} + p_{el} + p_{col} \tag{3}$$

The first term, p_{kin}, is the kinetic pressure and depends on the total ionic density of all species present in the solution at the reference plane. The second term, p_{el}, is the electric pressure and

depends on the electric field across the reference plane. Finally, p_{col} considers the contribution to the pressure from collisions between ions at opposite sides of the reference plane.[18] On certain planes, some of these terms vanish. For instance, on the plane located at the distance of closest approach (DCA) of the ions to the surface, p_{col} = 0 (because there are not ions on one of the sides of the reference plane) and p_{el} becomes independent of the ion distribution, which makes its computation easier. However, the calculation of p_{kin} requires the extrapolation of the local ion densities to the DCA. As the counterion concentration rises very rapidly near the DCA, the extrapolation must be done carefully to obtain accurate results. Pioneers in these simulations avoided this problem calculating the pressure at the midplane of the system. At this plane, the kinetic term can be calculated by interpolation, but the other terms must be calculated as well. However, this method also presents certain difficulties. As Valleau pointed out, the calculation of the collisional term is not a trivial task because pair correlation functions are presumably anisotropic.[18] Thus we have preferred to calculate pressure at the DCA after checking that reliable extrapolations are feasible with our procedure and the current computational resources.

Theoretically speaking, the pressure given by eqn (3) is a well defined property. In practice, however, the pressure in the confined region between the charged planes cannot be measured, since there is also certain pressure exerted by the external solution. Only the difference between the pressure in the confined region (*internal pressure*) and the *external pressure* can be measured directly. This difference is known as the *net pressure*.[17,18,31,34,54] In this paper, internal and external pressures are calculated, although only net pressure results are reported.

An advantage of evaluating pressure at the DCA is that the electric term is independent of salt concentration. Consequently, p_{el} has the same value on both sides of the plate and internal and external electric terms will cancel each other, reducing to zero the electrical contribution to the net pressure. As the collisional contribution is also zero, the net pressure can be calculated from the kinetic terms only:

$$p_{net} = p^{internal} - p^{external} = p_{kin}^{internal} - p_{kin}^{external} = k_B T\left(\rho_{contact}^{\text{int}} - \rho_{contact}^{ext}\right) \qquad (4)$$

where $\rho_{contact}^{\text{int}}$ and $\rho_{contact}^{ext}$ are the ion concentrations at the DCA in the internal and external EDL, respectively.

This result seems to be also valid if an implicit solvent model is considered. Pegado et al. have recently performed MC simulations for two like-charged infinite plates with solvent in between which is described at the PM level and, alternatively, by Molecular Solvent (MS) simulations.[55] According to this work, changes in the counterion valences, surface charge density of the planes, and dielectric permittivity have the same qualitative effect in the PM and MS models. Furthermore, this study pointed out that the forces are of the same magnitude in the different models. In other words: ion-ion correlations influence the force between two charged surfaces in the same way for a system with an explicit modelling of the solvent and when the solvent is described in terms of a dielectric continuum. These conclusions clearly suggest that the effect of solvent on pressure is not decisive. On the other hand, the influence on the *net* pressure could be

considerably minimized if the contributions to the external and the internal pressure are similar. For that reason, the effect of water on net pressure was neglected in our analysis.

As stated above, the ionic contact densities cannot be calculated exactly at the DCA Thus the simulation data of the adjacent region must be extrapolated. This extrapolation is always done with limited precision and has to be carried out carefully in order to avoid great numerical uncertainties. In general, ionic densities close the DCA rises abruptly complicating the calculations. To overcome this problem, the simulation cell can be divided into more intervals and the number of simulation steps can be increased as well. In the calculations presented in this work, different approximations were used to assure numerical errors lower than 1%. Each simulation took between 50 and 100 million GCMC steps and the simulation systems were always thermalized around 500000 steps before collecting data for averaging. Finally, the reliability of the evaluation at the DCA was tested comparing with data from previous publications.[18,34,54] Such results were reproduced with greater accuracy.

3. RESULTS AND DISCUSSION.

In this section net pressure calculations are presented and discussed. First, the case of equally charged plates is studied. The analysis begins with the dependence of the net pressure on the surface charge density and the ionic strength for ions with the usual diameter (0.425 nm). Then the sizes of the ionic species are changed to probe the effect of these parameters on the calculations. The second part of this section deals with the case of oppositely charged plates. Therein the results are examined following a similar scheme.

Equally charged plates.

We first consider the situation of equally charged plates immersed in an electrolytic bath. These systems are of great relevance since they have been extensively used in the past to represent the interaction between colloids in solution. At first, and due to the bare coulombic forces between the equally charged surfaces, one could expect interactions of repulsive nature. However, it is a well-known fact that an attractive force on the plates appears for certain conditions of the solution due to ionic correlations. In fact, several investigations have sufficiently proved that, at short separations, two surfaces of the same charge attract each other predominantly in the presence of multivalent electrolytes (e.g. divalent salts).[17,18,22] In short, the origin of such attraction can be attributed to the electrostatic and excluded volume correlations among the electrolyte ions. In the case of like-charged plates a fixed amount of excess counterions must always remain in the fluid phase between the surfaces because of the electroneutrality condition. Our study will prove that such counterions rule, sometimes to a great extent, the net pressure variation as the charged plates approach.

First, and in order to evaluate the influence of the surface charge on the net pressure of the system, in Fig. 1a we have plotted the simulated net pressure as a function of the separation between the plates for three different charge densities of the plates, namely, $\sigma_0 = \sigma_L$ = -0.01, -0.1 and -0.2 C/m^2. We believe that these values cover a representative region of surface charge

densities for biological colloids. In turn, the electrolyte corresponds to a 2:1 restricted primitive model solution consisting of ions of 0.425 nm of diameter ions at a fixed ionic strength I = 0.5 mM. In the graphs different qualitative behaviors can be observed when the surface charge varies. For the lower surface charge density $\sigma_0 = \sigma_L$ = -0.01 C/m^2, a monotonic increment of the net pressure (repulsion) is obtained when the distance between the plates decreases. However, this repulsion is weak compared to the other two net pressure curves. For the intermediate case $\sigma_0 = \sigma_L$ = -0.1 C/m^2 a much stronger repulsion is exhibited at short distances and, at intermediate separations, a non-monotonic trend (a subtle attractive interaction) appears. For the higher surface charge density, $\sigma_0 = \sigma_L$ = -0.2 C/m^2, and short distances, a stronger repulsion is even obtained. However, at intermediate separations (for a distance between plates of around 2 ionic diameters), an important attractive interaction can be noted. At large distances, when the EDLs of the charged plates do not interact, the net pressure curve tends to zero.

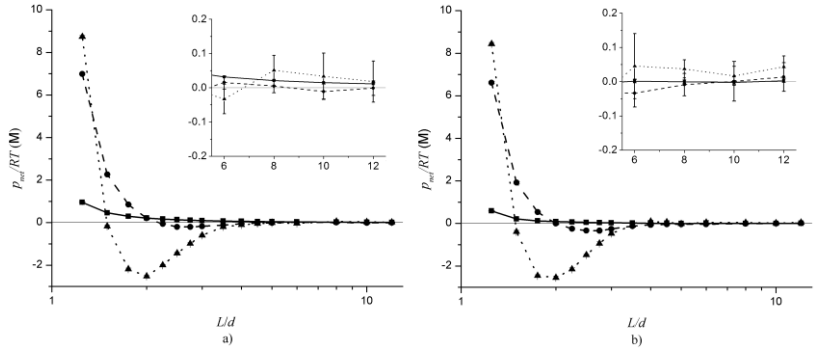

Figure 1. Net pressure for equally charged plates (normalized by RT) as function of the charged plates separation (normalized to the ion diameter). Results for three different surface charge densities are presented $\sigma_0 = \sigma_L$ = -0.01, -0.1 and -0.2 C/m^2 (squares, circles and triangles, respectively). a) I = 0.5 mM and b) I = 500 mM. The electrolyte is a 2:1 restricted primitive model solution with ions of diameter 0.425 nm. The insets show the region of large separation in an expanded scale for sake of clarity.

Table 1. Values of $\rho_{contact}^{\text{int}}$ and $\rho_{contact}^{ext}$ (divided by Avogadro's number) for the systems of Fig. 1 for a distance between the plates of two ionic diameters.

	$\rho_{contact}^{\text{int}}/N_A$ (M)	$\rho_{contact}^{ext}/N_A$ (M)	$\rho_{contact}^{\text{int}}/N_A$ (M)	$\rho_{contact}^{ext}/N_A$ (M)
	I = 0.5 mM	I = 0.5 mM	I = 500 mM	I = 500 mM
$\sigma_0 = \sigma_L$ = -0.01 C/m^2	0.247	0.029	0.529	0.445
$\sigma_0 = \sigma_L$ = -0.1 C/m^2	3.125	2.919	3.316	3.322
$\sigma_0 = \sigma_L$ = -0.2 C/m^2	9.084	11.605	9.356	11.902

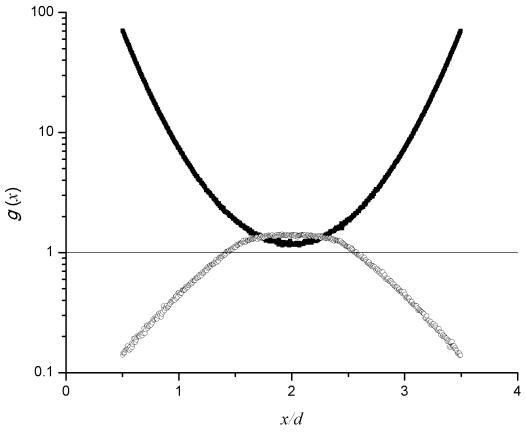

Figure 2. Ionic distributions as a function of the distance (normalized by the ion diameter) for a 2:1 electrolyte of classical size (0.425 nm) ions with $\sigma_0 = \sigma_L$ = -0.2 C/m^2 and I = 500 mM. The separation between the charged plates is of 4 ionic diameters. Solid dots stand for the counterion profile whereas open dots represent the coion profile.

Now we try to elucidate the reasons for the characteristic features shown by the net pressure curves in Fig. 1a. In the first place, we must distinguish between a repulsive trend at short separations, which is common to all the curves and entirely dominant for the lower surface charge density, and an attractive interaction present for $\sigma_0 = \sigma_L$ = -0.1 C/m^2 and, particularly, for the higher surface charge (*i.e.*, -0.2 C/m^2). A repulsive behavior is clearly expected when the separation between the plates is diminished and less space is available for ions. As mentioned above, excess counterions necessarily remain into the solution because of the electroneutrality restriction. Then, very close to the walls, the coulombic and hard-core repulsion among excess counterions force them to stay close to the charged surfaces (at the DCA), which increases $\rho_{contact}^{\text{int}}$ and, concomitantly, the net pressure (see eqn (4)). In other words, the short range repulsion obtained increases as surface charge density is augmented because more excess counterions are needed to neutralize the charged surfaces. The same repulsive trend with surface charge density is predicted by the well-known DLVO theory.

As pointed out previously, the mechanisms behind the attractive interactions exhibited for intermediate and high surface charge densities have been widely discussed by other authors. In this paper, however, this phenomenon will be quantitatively analyzed in terms of the contact densities involved in eqn (4). This is coherent with the procedure chosen for the pressure calculations and, in any case, offers new insights. The internal and external contact densities used in eqn (4) for the systems of Fig. 1 (*a* and *b*) and a distance between the plates of two ionic diameters are given in Table 1. As can be seen, $\rho_{contact}^{ext}$ becomes greater than $\rho_{contact}^{\text{int}}$ with increasing the surface charge density. It is quite instructive to examine the ionic profiles of the

internal double layer when this short-range attraction begins to operate. Just as an example, Fig. 2 shows the distribution functions ($g(x)$) for σ_0 = σ_L = -0.2 C/m^2 and I = 500 mM. As can be concluded, there is a well-defined layer of counterions at the DCA on both charged plates and a layer of coions in the middle of the simulation cell. As charged surfaces approach these coions attract counterions to the center of the solution. On the other hand, the hard-core interaction between counter- and coions at short distances decreases the positions on the charged surfaces where counterions can stay at contact. Both mechanisms reduce $\rho_{contact}^{\text{int}}$, which eventually becomes smaller than $\rho_{contact}^{ext}$. This would justify the appearance of negative net pressures.

The formation of a layer of coions behind the first layer of counterions is usually a hallmark of charge inversion.[3,40,41] Thus we might wonder if this phenomenon is responsible for the layer of coions mentioned before. The existence of charge reversal can be easily proved from simulation data computing the apparent surface charge density 'seen' from a distance x:

$$\sigma_{app}(x) = \sigma_0 + \int_0^x \sum_i eZ_i \rho_i(x')dx' \tag{5}$$

where ρ_i is the number density of species i.[34] The examination of this function (figure not shown) showed that charge inversion is extremely weak (almost inexistent) in this particular case. Trying to go further, we might wonder if the reported electrostatic attraction and charge inversion are intertwined in a general way. The profiles of the apparent surface charge density (not shown either) were analyzed looking for the answer. They revealed that a general and univocal relationship between charge inversion and the electrostatic attraction between like-charged plates cannot be established for divalent counterions. Trulsson *et al*. have also investigated the connection between two counterintuitive phenomena: the electrostatic repulsion between oppositely charged plates and charge inversion.[34] They concluded that an apparent charge reversal is observed together with repulsion only at large separation, whereas at intermediate separations the repulsion can appear without charge reversal.

In Fig. 1b the same system is analyzed, but now the ionic strength is considerably higher (500 mM). The behavior observed for the three surface charge densities is quite similar to that obtained at low ionic strength. Again Table 1 sheds some light on this striking similarity. As can be concluded, the values of $\rho_{contact}^{\text{int}}$ and $\rho_{contact}^{ext}$ for σ_0 = σ_L = -0.1 and -0.2 C/m^2 hardly increase with varying the ionic strength from 0.5 to 500 mM, which can be justified as follows. For moderate and highly charged systems, the contact density is dominated by the surface charge density due to a saturation effect. However, it should be pointed out that excluded volume is not the only cause for such saturation. The contact densities shown in Table 1 are significantly smaller than the concentration corresponding to closest packing (with spheres of 0.425 nm). Thus the electrostatic repulsion must also contribute to the mentioned saturation. In any case, the general picture obtained from these results points to a low dependence of the system behavior on the ionic strength, at least qualitatively. Finally, Fig. 1 also includes insets to show the region of large

separation in an expanded scale. As can be seen, forces are practically zero within the statistical error.

Now we turn to the analysis of results for hydrated ions. In Fig. 3 net pressure for equally charged plates, at the same conditions as in Fig. 1, are presented. However, hydrated ionic sizes are considered in these calculations. Diameters of 0.85 and 0.7 nm were chosen for hydrated divalent cations (counterions) and monovalent anions (coions), respectively. This choice is inspired in experimental measures.[35] In fact, values of about 0.85 nm were used in previous works to explain the electrokinetic behavior of some latexes in the presence of divalent cations (Ca^{2+} and Mg^{2+}).[3,41,42,44] For low ionic strength (Fig. 3a) a monotonically repulsive interaction is obtained for the -0.01 and -0.1 C/m^2 surface charge densities cases. However, a very different qualitative behavior is observed for the higher surface charge density. When approaching from the center of the cell to the charged surface, net pressure increases dramatically while the distance between the plates is larger than two ionic diameters and shows an important drop below this distance. At very short distances, net pressure increases again.

At this point, it is worth comparing Fig. 1 and Fig. 3. Such comparison reveals that the effect of ion size on colloidal forces can be dramatic. As mentioned before, Ravindran and Wu recently concluded that electrostatic attraction in the presence of divalent counterions weakens with increasing ion size.[45] In their study, they analyzed ionic diameters ranging from 0.2 to 0.6 nm. For a bit larger ions, however, our results for highly charged systems clearly show that such attraction can disappear and be replaced by the non-monotonic repulsion commented previously. As far as we know, this behaviour has not been previously reported. To understand why attraction is finally replaced by repulsion with increasing the ion size, it is quite useful to compare the contact densities reported in Tables 1 and 2 for $\sigma_0 = \sigma_L$ = -0.2 C/m^2. In the case of small ions (Table 1) the contact density is greater in the external double layer. For that reason, attraction is found in this case. With increasing the ion size (Table 2), the contact density of the external double layer does not change significantly. However, the situation is quite different in the internal double layer. The corresponding ionic profiles (not shown in this case) show that the coions are expelled from the internal region whereas counterions are pushed to the plates. This is logical since there is less available space for excess counterions due to excluded volume. In any case, the contact density of the internal region increases and can even become greater than $\rho_{contact}^{ext}$ (see Table 2), which eventually causes the repulsion between the plates.

As mentioned above, the repulsion observed for hydrated ions and highly charged plates is non-monotonic and net pressure decreases for distances below two ionic diameters. This behaviour can be understood as follows: for L approaching to two counterion diameters the repulsion experiences the usual rise due to the formation of two layers of counterions adsorbed to the plates. Subsequently, a reduction in the net pressure occurs as a result of the re-accommodation of the adhered counterions, which induces perpendicular ionic fluctuations and a concomitant reduction in the ion contact density. In relation to this fall, one should keep in mind that, for such

short distances, coulombic and hard-core repulsions among excess counterions reduce the accessible space on the plane of minimum approach. In other words, the counterions on one of plates interfere with the counterions on the other. Hence $\rho_{contact}^{\text{int}}$ decreases dramatically below two ionic diameters. However, for very short distances (close to one ionic diameter), counterions could contribute to the contact density of both plates simultaneously and net pressure would increase again.

Finally, the results shown in Fig. 3b are analyzed. At first sight, the qualitative behavior is very similar to that discussed for Fig. 3a. It could be stressed that a subtle attraction has appeared for -0.1 C/m^2. In any case, from Figures 1 and 3, one can conclude that electrostatic forces between like-charged plates in the presence of divalent ions are quite insensitive to the ionic strength.

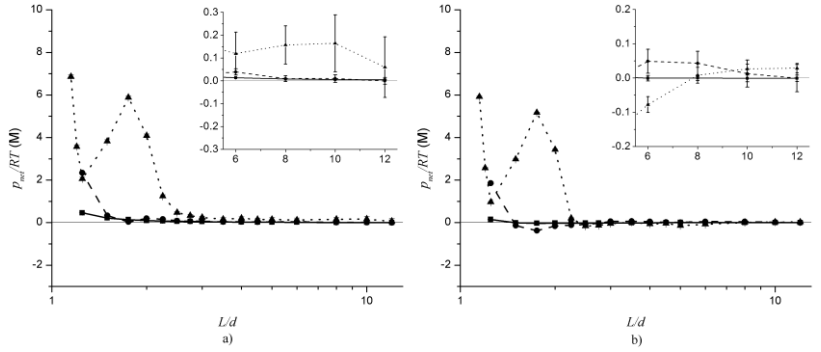

Figure 3. Net pressure for equally charged plates (normalized by RT) as function of the charged plates separation (normalized to the counterions ionic diameter). Results for three different surface charge densities are presented $\sigma_0 = \sigma_L$ = -0.01, -0.1 and -0.2 C/m^2 (squares, circles and triangles, respectively). a) I = 0.5 mM and b) I = 500 mM. The electrolyte is a 2:1 primitive model solution whose divalent and monovalent ions have diameters of 0.85 and 0.7 nm, respectively. The insets show the region of large separation in an expanded scale for sake of clarity.

Table 2. Values of $\rho_{contact}^{\text{int}}$ and $\rho_{contact}^{ext}$ (divided by Avogadro's number) for the systems of Fig. 3 for a distance between the plates of two ionic diameters.

	$\rho_{contact}^{\text{int}}/N_A$ (M) I = 0.5 mM	$\rho_{contact}^{ext}/N_A$ (M) I = 0.5 mM	$\rho_{contact}^{\text{int}}/N_A$ (M) I = 500 mM	$\rho_{contact}^{ext}/N_A$ (M) I = 500 mM
$\sigma_0 = \sigma_L$ = -0.01 C/m^2	0.127	0.028	0.567	0.589
$\sigma_0 = \sigma_L$ = -0.1 C/m^2	3.086	2.892	3.239	3.401
$\sigma_0 = \sigma_L$ = -0.2 C/m^2	15.515	11.426	15.626	12.192

In our opinion, the most important finding of this subsection is the lack of electrostatic attraction between like charged plates in the presence of ions with large diameters. As mentioned in the introduction, this attraction is observed in experiments with some divalent counterions (e.g.,

Ca^{2+}). Thus we might conclude that such large ionic diameters should not be found in practice. However, dehydration could be a feasible explanation for this apparent disagreement between experiments and simulations. In fact, some authors have reported from environment-sensitive laser excitation spectroscopy that the hydrated ion size could be reduced in presence of highly charged surfaces.[56] Moreover, we proved in a previous work that ionic dehydration improves the qualitative agreement between electrokinetic experiments and simulations when ionic dispersion forces and ion size correlations are considered in the calculations.[44] In any case, it should be stressed that our study is focused on the effect of ion size and large ionic diameters were used for testing purposes mainly. For a proper comparison between experiments and simulations, other interactions and more sophisticated models should be considered in the calculations. For instance, the Van der Waals forces between the plates, the ionic dispersion forces and the hydrophobic interactions should be included if the comparison with experiments is the main goal. The effect of the particle curvature should be also considered in such comparisons because our results are strictly valid for plates. Moreover, the effects of dielectric discontinuities and the discreteness of the surface charge could also improve the agreement between real and simulated forces.

Table 3. Values of $\rho_{contact}^{\text{int}}$ and $\rho_{contact}^{ext}$ (divided by Avogadro's number) for the systems of Fig. 4 for the lowest distance simulated in each case.

	$\rho_{contact}^{\text{int}}/N_A$ (M) $I=0.5$ mM	$\rho_{contact}^{ext}/N_A$ (M) $I=0.5$ mM	$\rho_{contact}^{\text{int}}/N_A$ (M) $I=500$ mM	$\rho_{contact}^{ext}/N_A$ (M) $I=500$ mM
$\sigma_0 = \sigma_L$ = -0.01 C/m^2	1.065×10^{-6}	0.028	0.130	0.444
$\sigma_0 = \sigma_L$ = -0.1 C/m^2	1.255×10^{-6}	2.807	0.148	3.318
$\sigma_0 = \sigma_L$ = -0.2 C/m^2	5.245×10^{-6}	11.364	0.210	11.974

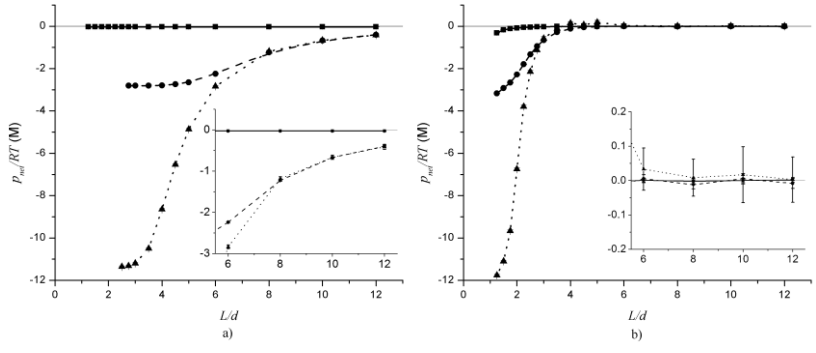

Figure 4. Net pressure for oppositely charged plates (normalized by RT) as function of the charged plates separation (normalized to the ion diameter). Results for three different surface charge densities are presented $\sigma_0 = -\sigma_L$ = -0.01, -0.1 and -0.2 C/m^2 (squares, circles and triangles, respectively). a) I = 0.5 mM and b) I = 500 mM. Electrolyte conditions are the same as in Fig. 1. The insets show the region of large separation in an expanded scale for sake of clarity.

In fact, the effect of the discreteness of the surface charge distribution has been analyzed by means of computer simulations comparing with the uniform distribution.[26,27] In particular, Meyer and Delville proved that the localization of the surface charge has certain influence on the interaction forces between charged lamellae in the presence of divalent counterions.[26] Some years later, Khan *et al.* studied the interaction forces between surfaces characterized by a regular array of discrete charged sites for different electrostatic couplings. They concluded that, at short distances, the forces could be quite different to those originated by surfaces with a uniformly smeared-out charge. In this case, the discrete nature of the surface charge is responsible for the differences in the ionic profile near the surface.[27] These authors also point out that, for high electrostatic coupling, attractive forces are weakened and can even be turned into repulsive forces if discrete surface charges are considered.

Oppositely charged plates.

Once analyzed the forces between like-charged plates, we proceed to study the case of plates with opposite charge. As it has been mentioned in the introduction, this task appears as a novelty of the present work since the study of the effect of the ion size on forces between colloids carried out by Ravindran and Wu only addressed the case of particles with charge of the same sign.[45] Trulsson *et al.* did study the interaction between oppositely planar surfaces in the presence of multivalent electrolytes by means of MC simulations.[33,34] However, their works focused on charge inversion. In particular, these authors chose a specific set of values for surface charge densities, ionic strengths, and ion valences in such a way that charge inversion was induced on just one of the two charged planes. Therefore a net repulsion between the surfaces is reported under such conditions. In contrast, in this section we propose a systematic study of the effect of ion size on the interaction between oppositely charged plates similar to that previously performed for like-charged plates. Before showing the results, it is important to notice that in this case cations and anions act as counterions and coions respectively, on the negatively charged surface (and the other way around for the positively charged surface). Unlike the previous section, an excess of counterions is not required to remain into the solution to hold the electroneutrality condition in this new situation. As we will see in the following figures, this feature will be essential to understand the findings.

Fig. 4a shows the pressure-distance profiles corresponding to plates with the three surface charge densities: $\sigma_0 = -\sigma_L$ = -0.01, -0.1 and -0.2 C/m^2, immersed in a 2:1 restricted primitive model solution consisting of 0.425 nm diameter ions at a fixed ionic strength I = 0.5 mM (similar to Fig. 1a). As can be seen, a classical behaviour of the pressure as a function of the separation distance is reported. That is to say, the attraction between the plates increases as the distance between them decreases. Furthermore, this attraction becomes more important as the surface charge density increases. From a purely coulombic point of view, this finding is a logical consequence of the net attraction between two surfaces with dissimilar sign in their charge. Comparing these results with those shown in Fig. 1a, we see that now the pressure curves are monotonic. In addition, an asymptotic trend to the zero net pressure line is obtained for large

separations between the charged plates. In terms of the contact densities involved by eqn (4), Table 3 shows how $\rho_{contact}^{ext}$ is practically the same to that reported for likely-charged plates (Tables 1 and 2) whereas $\rho_{contact}^{\text{int}}$ is very different to the previous values. Moreover, the ion concentration at the DCA in the internal EDL is a value particularly small. This is a consequence that, within this new scenario, ions between the plates are expelled from the inner solution in order to preserve the equilibrium with the reservoir (that provides a constant ionic strength). Since there is not an excess of counterions now, the corresponding repulsive hard-core interaction at short distances disappears.

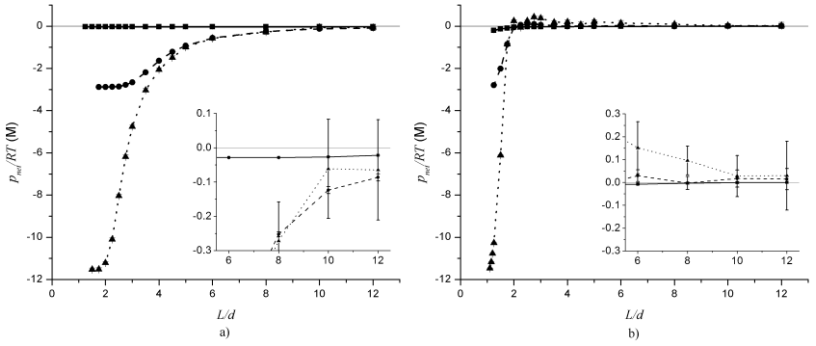

Figure 5. Net pressure for oppositely charged plates (normalized by RT) as function of the charged plates separation (normalized to the counterions diameter). Results for three different surface charge densities are presented $\sigma_0 = -\sigma_L$ = -0.01, -0.1 and -0.2 C/m^2 (squares, circles and triangles, respectively). a) I = 0.5 mM and b) I = 500 mM. Electrolyte conditions are the same as in Fig. 3. The insets show the region of large separation in an expanded scale for sake of clarity.

In general, similar tendencies are found for the case of I = 500 mM (Fig. 4b). Again a typical behaviour is reported; the more surface charge density, the more attraction between the plates at short distances. However, this effect takes place at shorter separations than those observed in the previous case. From a classical point of view this last result is a direct consequence of a reduction of the interaction range for both EDLs since ions screen the electrostatic interactions between the plates and electrostatic forces decay more rapidly when salt is added. Concerning the behaviour at larger distances, it can be observed how a slight repulsion appears for the case of highly charged surfaces. This finding agrees with previous experimental works where the existence of a salt concentration threshold from which a repulsive interaction could appear was measured for oppositely charged particles.[15,16] Therein, the authors explain this repulsion in terms of the ion-ion correlations which become more important as the ion concentration increases.

Unlike the case of equally charged plates, the effect of the ion size is less relevant for oppositely charged plates. This can be inferred by comparing Fig. 4 (electrolyte of an ionic diameter of 0.425 nm) with Fig. 5, in which hydrated ion sizes are considered under the same conditions than those

used in Fig. 4. For such comparison, however, one should keep in mind that the distance between the plates is not normalized by the same size in Figures 4 and 5 (since the ionic diameter is not the same). If the different normalization is taken into account, we can easily conclude that all the features of the pressure profiles are quite similar and, consequently, the effect of ion size is not really important. On the other hand, the repulsive pressures observed for $\sigma_0 = -\sigma_L$ = -0.2 C/m^2 at I = 500 mM in Fig. 5b are more significant that those observed for I = 500 mM in Fig. 4b. Again the ion-ion correlations may be behind this behaviour. Logically, if the ion size increases, the hard sphere correlations between ions tend to be more important. In relation with the effect of ionic strength for large ions, the comparison between Fig. 5a and Fig. 5b again reveals that pressure profiles decay more rapidly (in agreement with the classical theory). Finally, the following question arises: why do not size correlations imply an attraction-repulsion transition like that previously discussed for equally charged plates? The reason is that for the oppositely charged plates, the excess of counterions does not necessarily remain into the solution. Consequently if the distance between plates is reduced, ions are not forced to be located between the surfaces and a repulsive force between them is not observed.

CONCLUSIONS.

In this work, we have carried out a systematic survey on the effect of ion size on electrostatic forces between two charged plates in the presence of divalent counterions. Our study includes both like and oppositely charged plates, different surface charge densities and two very different ionic strengths. The main conclusions can be summarized comparing like and oppositely charged plates. For instance, the effect of ion size is essential in the case of like charges, because it is responsible for the change of attraction into repulsion for highly charged systems. On the contrary, ion size is not really important for opposite charges. Concerning the effect of surface charge density, we report a rich behaviour for like-charged objects, including monotonic repulsion for low surface charge density and attraction or non-monotonic repulsion for high surface charge density (depending on the ion size, precisely). In the case of opposite charges, the behaviour is the expected one according to the classical theory: The electrostatic attraction increases with the surface charge density. In relation to electrolyte concentration, like-charged plates are not very sensitive to the ionic strength in the case of moderate and highly charged plates. On the contrary, we find the expected behavior for opposite charges: electrostatic forces decay more rapidly when salt is added.

In short: Like-charged plates exhibit a more complex and unexpected behavior than that of oppositely charged plates. With regard to this asymmetry, one should keep in mind that there is an excess of counterions for like charged objects neutralizing their net charge. However, this excess is not required in the case of oppositely charged plates. Our simulations reveal that these multivalent counterions rule to a great extent the curious behavior of like-charged plates.

ACKNOWLEDGEMENTS.

The authors thank the financial support from the following institutions: i) 'Ministerio de Ciencia e Innovación, Plan Nacional de Investigación, Desarrollo e Innovación Tecnológica (I+D+i)', Project MAT2009-13155-C04-04. ii) 'Consejería de Innovación, Ciencia y Empresa de la Junta de Andalucía', Projects P07-FQM-02496, P07-FQM-02517, P09-FQM-4698 and sabbatical stay of E. G. T. iii) European Regional Development Fund (ERDF). iv) Grant CONACYT (Mexico) CB-2006-01/58470.

REFERENCES.

[1] V. Dahirel and M. Jardat, *Curr. Opin. Colloid Interface Sci.*, 2010, **15**, 2-7.

[2] Y. Levin, *Rep. Prog. Phys*., 2002, **65**, 1577-1632.

[3] M. Quesada-Pérez, E. González-Tovar, A. Martín-Molina, M. Lozada-Cassou and R. Hidalgo-Álvarez, *Chem. Phys. Chem.*, 2003, **4**, 234-248.

[4] B. V. Derjaguin, and L. Landau, *Acta Phys. Chim. (URSS)*, 1941, **14**, 633-662.

[5] E. J. W. Verwey and J. Th. G. Overbeek, *Theory of the Stability of Lyophobic Colloids*, Elsevier, Amsterdam, 1948.

[6] V. Vlachy, *Annu. Rev. Phys. Chem*., 1999, **50**, 145-65.

[7] L. Belloni, *J. Phys: Condens. Matter*, 2000, **12**, R549-R587.

[8] P. Attard, *Curr. Opin. Colloid Interface Sci.*, 2001, **6**, 366-371.

[9] M. M. Hatlo and L. Leu, *Soft Matter*, 2008, **4**, 1582-1596.

[10] R. M. Pashley, *J. Colloid Interface Sci.*, 1981, **83**, 531-546.

[11] R. Kjellander, S. Marcelja, R. M. Pashley and J. P. Quirk, *J. Chem. Phys.*, 1990, **92**, 4399-4407.

[12] P. Kekicheff, S. Marcelja, T. J. Senden and V. E. Shubin, *J. Chem. Phys.*, 1993, **99**, 6098-6113.

[13] R. F. Considine, R. A. Hayes and R. G. Horn, *Langmuir*, 1999, **15**, 1657-1659.

[14] M. L. Fielden, R. A. Hayes and J. Ralston, *Phys. Chem. Chem. Phys.*, 2000, **2**, 2623-2628.

[15] K. Besteman, M. A. G. Zevenbergen, H. A. Heering and S. G. Lemay, *Phys. Rev. Lett.*, 2004, **93**, 170802-170805.

[16] K. Besteman, M. A. G. Zevenbergen and S. G. Lemay, *Phys. Rev. E*., 2005, **72**, 061501-061509.

[17] L. Guldbrand, B. Jönsson, H. Wennerström and P. Linse, *J. Chem. Phys*., 1984, **80**, 2221-2228.

[18] J. P. Valleau, R. Ikov and G. M. Torrie, *J. Chem. Phys.*, 1991, **95**, 520-532.

[19] N. Gronbech-Jensen, R. J. Mashl, R. F. Bruinsma and W. M. Gelbart, *Phys. Rev. Lett.*, 1997, **78**, 2477-2480.

[20] E. Allahyarov, I. Damico and H. Lowen, *Phys. Rev. Lett.*, 1998, **81**, 1334-1337.

[21] J. Wu, D. Bratko and J. M. Prausnitz, *Proc. Natl. Acad. Sci.,* 1998, **95**, 15169-15172.

[22] J. Z. Wu, D. Bratko, H. W. Blanch and J. M. Prausnitz, *J. Chem. Phys.*, 1999, **111**, 7084-7094.

[23] P. Linse and V. Lobaskin, *Phys. Rev. Lett*., 1999, **83**, 4208-4211.

[24] J. Z. Wu, D. Bratko, H. W. Blanch, and J. M. Prausnitz, *J. Chem. Phys*., 2000, **113**, 3360-3365.

[25] D. G. Angelescu and P. Linse, *Langmuir*, 2003, **19**, 9661-9668.

[26] S. Meyer and A. Delville, *Langmuir*, 2001, **17**, 7433-7438.

[27] M. O. Khan, S. Petris and D. Y. C. Chan, *J. Chem. Phys.*, 2005, **122**, 104705-10711.
[28] F. W. Tavares, D. Bratko, H. W. Blanch and J. M. Prausnitz, *J. Phys. Chem. B*, 2004, **108**, 9228-9235.
[29] M. Boström, F. W. Tavares, B. W. Ninham, M. Prausnitz, *J. Phys. Chem. B*, 2006, **110**, 24757-24760.
[30] A. Delville, N Gasmi, R. J. M. Pellenq, J. M. Caillol and H. Van Damme, *Langmuir*, 1998, **14**, 5077-5082.
[31] B. Jönsson, A. Nonat, C. Labbez, B. Cabane and H. Wennerström, *Langmuir*, 2005, **21**, 9211-9221.
[32] P. Taboada-Serrano, S. Yiacoumi and C. Tsouris, *J. Chem. Phys.* 2006, **125**, 054716.
[33] M. Trulsson, B. Jönsson, T. Åkesson, J. Forsman and C. Labbez, *Phys. Rev. Lett.* 2006, **97,** 068302.
[34] M. Trulsson, B. Jönsson, T. Åkesson and J. Forsman, *Langmuir*, 2007, **23**, 11562-11569.
[35] J. N. Israelachvili, *Intermolecular and Surface Forces*, Academic Press, London, 1992.
[36] P. Taboada-Serrano, S. Yiacoumi and C. Tsouris, *J. Chem. Phys.*, 2005, **123**, 054703-054711.
[37] M. Valisko, D. Boda and D. Gillespie, *J. Phys. Chem.* C, 2007, **111**, 15575-15585.
[38] C. H. Hou, P. Taboada-Serrano, S. Yiacoumi and C. Tsouris, *J. Chem. Phys.*, 2008, **128**, 044705-044712.
[39] A. Diehl and Y. Levin, *J. Chem. Phys.*, 2008, **129**, 124506-124510.
[40] M. Quesada-Perez, A. Martin-Molina, R. Hidalgo-Álvarez, *J. Chem. Phys*., 2004, **121**, 8618–8626.
[41] M. Quesada-Pérez, E. González-Tovar, A. Martín-Molina, M. Lozada-Cassou and R. Hidalgo-Álvarez, *Colloid Surf. A*, 2005, **267**, 24-30.
[42] A. Martín-Molina, J. A. Maroto-Centeno, R. Hidalgo-Álvarez and M. Quesada-Pérez, *Colloid. Surf. A*, 2007, **319**, 103-108.
[43] J. G. Ibarra-Armenta, A. Martín-Molina and M. Quesada-Pérez, *Phys. Chem. Chem. Phys*., 2009, **11**, 309-316.
[44] A. Martín-Molina, J. G. Ibarra-Armenta and M. Quesada-Pérez, *J. Phys. Chem. B*, 2009, **113**, 2414-2421.
[45] S. Ravindran and J. Wu, *Condens. Matter Phys.*, 2005, **8**, 377-388.
[46] D. Boda, K. Y. Chan and D. Henderson, *J. Chem. Phys.*, 1998, **109**, 7362-7371.
[47] D. J. Adams, *Mol. Phys.*, 1974, **28**, 1241-1252.
[48] D. J. Adams, *Mol. Phys.*, 1975, **29**, 307-311.
[49] J. P. Valleau and L. K. Cohen, *J. Chem. Phys.*, 1980, **72**, 5935-5941.
[50] S. Lamperski, *Mol. Sim.*, 2007, **33**, 1193-1198.
[51] S. Lamperski and C. W. Outhwaite, *J. Colloid Interface Sci.*, 2008, **328**, 458-462.
[52] A. Malasics, D. Gillespie and D. Boda, *J. Chem. Phys*., 2008, **128**, 124102-124107.
[53] A. Malasics, and D. Boda, *J. Chem. Phys.*, 2010, **132**, 244103-244112.
[54] R. Kjellander, T. Åkesson, B. Jönsson and S. Marcelja, *J. Chem. Phys.*, 1992, **97**, 1424-1431.

[55] L. Pegado, B. Jönsson and H. Wennerström, *J. Chem. Phys.*, 2008, **129**, 184503.
[56] W. Grygiel and M. Starzak, *J. Lumin.* 1995, **63**, 47.

Paper V

Computer Simulations of Thermo-Shrinking Polyelectrolyte Gels

Manuel Quesada-Pérez [(1)*], **José Guadalupe Ibarra-Armenta**[(1)], **and Alberto Martín-Molina**[(2)]

J. Chem. Phys., **2011**, *135*, 094109.

(1) Departamento de Física, Escuela Politécnica Superior de Linares, Universidad de Jaén, 23700, Linares, Jaén, Spain.

(2) Grupo de Física de Fluidos y Biocoloides, Departamento de Física Aplicada, Facultad de Ciencias, Universidad de Granada, 18071 Granada, Spain.

* Corresponding author.

ABSTRACT

In this work, thermo-responsive polyelectrolyte gels have been simulated using polymer networks of diamond-like topology in the framework of the primitive model. Monte Carlo simulations were performed in the canonical ensemble and a wide collection of situations has been systematically analysed. Unlike previous studies, our model includes an effective solvent-mediated potential for the hydrophobic interaction between non-bonded polymer beads. This model predicts that the strength of the attractive hydrophobic forces increases with temperature, which plays a key role in the explanation of the thermo-shrinking behaviour of many real gels. Although this hydrophobic model is simple (and it could overestimate the interactions at high temperature), our simulation results qualitatively reproduce several features of the swelling behaviour of real gels and microgels reported by experimentalists. This agreement suggests that the effective solvent-mediated polymer-polymer interaction used here is a good candidate for hydrophobic interaction. In addition, our work shows that the functional form of the hydrophobic interaction has a profound influence on the swelling behaviour of polyelectrolyte gels. In particular, systems with weak hydrophobic forces exhibit discontinuous volume changes, whereas gels with strong hydrophobic forces do not show hallmarks of phase transitions, even for highly charged polyelectrolyte chains.

INTRODUCTION

Polyelectrolyte gels are networks of chemically crosslinked polymer chains with ionizable functional groups. Since their first syntheses, these systems have received considerable attention due to their large swelling capacity and the ability to tune their swelling behaviour to different external stimuli, such as temperature, pH, ionic strength, solvent nature, and external stress. Gels and microgels are found in hygiene products and water retainers, but also in novel technological applications such as drug controlled delivery, optoelectronic switches or artificial muscles.[1-6] Obviously, our ability to control the processes in which polyelectrolyte gels are involved resides in a better understanding of their swelling behaviour.

Computer simulations are a powerful tool for achieving such understanding and have been extensively applied to polymers, polyelectrolytes and many of their assemblies.[7] In fact, the first simulations of (neutral) polymer networks date back to 80s and were reviewed by Escobedo and de Pablo.[8] However, (charged) polyelectrolyte gels have been simulated more recently. The first paper appeared in 1996,[9] whereas the rest of them were published in the last decade.[10-22] Although some details change from simulation to simulation, most of these works have been carried out within the primitive model and a diamond-like network. The primitive model (PM) is mostly preferred by many authors due to the large capacity of swelling of polyelectrolyte gels,[7] which would make the number of solvent particles in the simulation box prohibitive. Schneider *et al.* investigated the swelling behavior of polyelectrolyte gels with respect to various parameters (charge density, crosslinker density, chain flexibility, and counterion valence)[10] and reported discontinuous volume phase transitions induced by short-range attractions and reductions in the

dielectric constant of the solvent.[13] Yin *et al.* have investigated the effect of the valence of the counterions on the swelling behavior and concluded that electrostatic interactions play a key role in discontinuous volume phase transitions undergone by these systems.[17] The collapse of the gel has also been reported when counterions are replaced by macroions.[18] Mann *et al.* proposed a scaling relation for the end-to-end distance of the network chains which considers the counterion condensation (through an effective charge fraction) and the finite length of the chains.[16] Most of these studies are restricted to salt-free simulations. However, some authors have also studied the swelling and collapse of polyelectrolyte gels in equilibrium with 1:1 and 2:1 electrolyte solutions.[14,20]. The swelling degree decreases with the electrolyte concentration in the reservoir (behavior observed also in experiments) and is smaller in the presence of divalent counterions. Edgecombe *et al.* have investigated how the polydispersity of the chain length and the topological defects in the network affect the volume and other structural properties.[18] In general they found that polydisperse gels swell less than the perfect ones. The first simulations of polyelectrolyte gels with explicit solvent particles were reported by Lu *et al*.[12] Concerning nanogels, these particles have been explicitly simulated by some authors.[21,22] Claudio *et al.*[21] have calculated the actual fraction of counterions inside the network and conclude that this quantity depends on the nanogel size. This obviously confirms that the gel size (ignored in preceding simulations) can have influence on certain properties. Moreover, Olvera de la Cruz[23] suggests that the asymmetric ionic profiles and the charge excess generated in the gel interface are crucial in the organization and function of ionic hydrogels. Jha *et al.*[22] have also simulated volume phase transitions in explicit nanogels, analyzing the effects of degree of crosslinking, solvent quality, and charge fraction of polymer backbone. They also report a discontinuous volume phase transition in the case of ionic nanogels.

As can be concluded from the preceding paragraph, different aspects of the swelling behaviour of polyelectrolyte gels have been investigated with the help of computer simulations and the primitive model. However, thermo-responsive polyelectrolyte gels have been rarely simulated yet. As far as we know, only Escobedo and de Pablo explicitly simulated swelling curves as a function of this property.[8] But their work was restricted to uncharged networks and focused on sub- and supercritical solvents. In any case, different factors challenge simulations within the PM in the case of thermo-responsive ionized gels. Particularly, the temperature sensitivity of these systems is governed to great extent by polymer-polymer hydrophobic forces and hydrogen bonds.[24-25] Both are molecular interactions and, moreover, hydrophobic forces are solvent-mediated. Thus, an effective polymer-polymer interaction potential is required in coarse-grained and primitive models. In addition, the temperature dependence of these interactions should be known (as will be discussed later).

In this work, thermo-sensitive polyelectrolyte gels have been simulated using also the PM and networks of diamond-like topology (as many researchers did before). Monte Carlo simulations were performed in the canonical ensemble. Unlike previous studies in this framework, our model includes an effective potential for the hydrophobic interaction between non-bonded polymer

beads.[26] This potential was derived from a one-dimensional lattice model and, in spite of its extreme simplicity, presents several advantages: (i) it incorporates the basic mechanism behind hydrophobic forces; (ii) it is analytically solvable; (iii) the potential explicitly accounts for the temperature dependence of hydrophobic forces. More specifically, the model predicts that the strength of the attractive hydrophobic forces increases with temperature. Our work will prove (through simulations) that this feature plays a key role in the explanation of the thermo-shrinking behaviour of many real gels. For instance, *N*-isopropylacrylamide (NIPAM) can be copolymerized with a wide variety of ionic monomers, yielding poly(NIPAM)-based gels and microgels, which shrink upon heating.[5,27-30] But gels based on many other polymers (e.g, those synthesized from vinylcaprolactam (VCP)) also exhibit this behavior.[31-33] The qualitative comparison with experimental data obtained for these systems can serve as a test for the hydrophobic model. In any case, we are particularly interested in analyzing the role of charge, since the classical theories of temperature-sensitive gels and others derived from it are valid only for weakly ionized polyelectrolytes (with only very few charged beads per chain).[24-25]

The paper is organized as follows. First the model is described and some simulation details are given. A particular (and larger) subsection will be devoted to hydrophobic forces and the effective potential accounting for them, since this interaction plays an essential role in our model. Then, the results are presented and discussed. Finally, some conclusions are highlighted.

MODEL AND SIMULATIONS

Primitive model for gel swelling

The polyelectrolyte gel is described within the primitive model. Thus the solvent enters the model only through its dielectric permittivity. Monomer units of polymer chains, cross-linker molecules and ions are explicitly modeled as spheres of diameter σ_M, σ_{CL} and σ_I, respectively. For ions, size includes the corresponding hydration shell. Our work will be restricted to monovalent charged species since the effect of the valence has been previously analyzed.[10,17,20] In this case, previous studies suggest that a diameter of monovalent hydrated ions would be around 0.7 nm.[34,35] We assumed that this value could also be a representative diameter for monomer units and cross-linker molecules. The short-range repulsion between any pair of these particles due to excluded volume effects can be modeled by means of a truncated Lennard-Jones (LJ) potential:[15,16,17,20]

$$u_{LJ}(r) = \begin{cases} 4\varepsilon_{LJ}\left(\frac{\sigma^{12}}{r^{12}} - \frac{\sigma^{6}}{r^{6}} - c\right) & r \le r_c \\ 0 & r > r_c \end{cases} \quad (1)$$

where r is the centre-to-centre distance between a given pair of particles, $\varepsilon_{LJ} = 4.11 \cdot 10^{-21}$ J, σ is the particle diameter (0.7 nm), r_c is the cut-off distance and *c* is a constant chosen so that $u_{LJ}(r_c) = 0$. If $r_c = 2^{1/6}\sigma$, the interaction potential is purely repulsive.

The polymer chains can be considered as a sequence of monomer units (beads) connected by harmonic bonds,[10,13,18,19] whose interaction potential is:

$$u_{bond}(r) = \frac{k_{bond}}{2}(r - r_0)^2 \quad (2)$$

where k_{bond} is the elastic constant ($k_{bond} = 0.4$ N/m) and r_0 is the equilibrium bond length (0.8 nm). The network is realized connecting the chain ends to the tetrafunctional cross-linkers (also through the same harmonic bonds). For simplicity, a defect-free network with diamond-like topology and chains of equal length was assumed.

Such network contains N_{node} nodes and N_{chain} chains (for tetrafunctional cross-linkers $N_{chain} = 2N_{node}$). Each chain is composed of N_{bead} monomers (beads) and certain number of them (f) is charged (with the positive elementary charge, $+e$). In this aspect, our model differs from the previous ones, which assume that the charge of the chain is uniformly distributed. The f charged monomers of each chain are situated equidistantly if $f \le N_{bead}/2$. For instance, for a chain with N_{bead}=12 and $f = 3$, monomers 2, 6 and 10 are charged. If $f > N_{bead}/2$, the uncharged monomers are then equidistantly located. The number of counterions (N_{CI}) neutralizing the gel charge is given by $N_{CI} = f N_{chain}$. All the charged species (monomers and ions) interact electrostatically through the Coulomb potential:

$$u_{elec}(r) = \frac{q_i q_j}{4\pi\varepsilon_0\varepsilon_r r} \quad (3)$$

where q_i is the charge of species i and $\varepsilon_0\varepsilon_r$ is the permittivity of the solvent. Since we are interested in the thermo-responsive gels, it is convenient to consider the temperature dependence of the dielectric permittivity. In this work, we have adopted the following one[36]:

$$\varepsilon_r = \frac{5321}{T} + 233.76 - 0.9297T + 0.1417\cdot10^{-2}T^2 - 0.8292\cdot10^{-6}T^3 \quad (4)$$

Hydrophobic forces

Different functional forms have been used to model hydrophobic interactions in previous simulations of flexible polymers and polyelectrolytes. We would like to cite just a few examples. The square-well potential has been employed in studies of the coil-globule transition of DNA.[37] Other authors have preferred LJ-like potentials to investigate structure and dynamics of polyelectrolyte chains in poor solvents,[38,39,40] whereas Anderson *et al.* analyzed the gelation of block copolymers with this kind of potential.[41] Khalatur and co-workers proposed their own function form for hydrophobic interactions in their study of conformations and aggregation of protein-like copolymers.[42] Concerning polymer networks, the square-well potential was preferred in simulations of charged and uncharged gels.[15,43] It should be mentioned, however, that none of the works cited here employed temperature-dependent hydrophobic forces.

It would be quite instructive to discuss the origin of hydrophobic forces on molecular grounds to justify the effective pair potential used in this work for this solvent-mediated interaction. When non-polar molecules (or macromolecules) are inserted into an aqueous medium, the water molecules must rearrange their hydrogen bonds to form a structure (known as *clathrate* or *iceberg*) that surrounds the non-polar molecule like a cage.[44,45] As the water molecules of this structure are much more restricted in their movement, the clathrate induces order in the system. If the non-polar molecules are dispersed in water, there will be many water molecules forming clathrate structures and entropy will considerably decrease. The best way to avoid this loss of entropy is to keep all the non-polar molecules together in one glob, so that the volume-to-surface area ratio is maximized. For that reason, hydrophobic forces are said to be entropically driven.

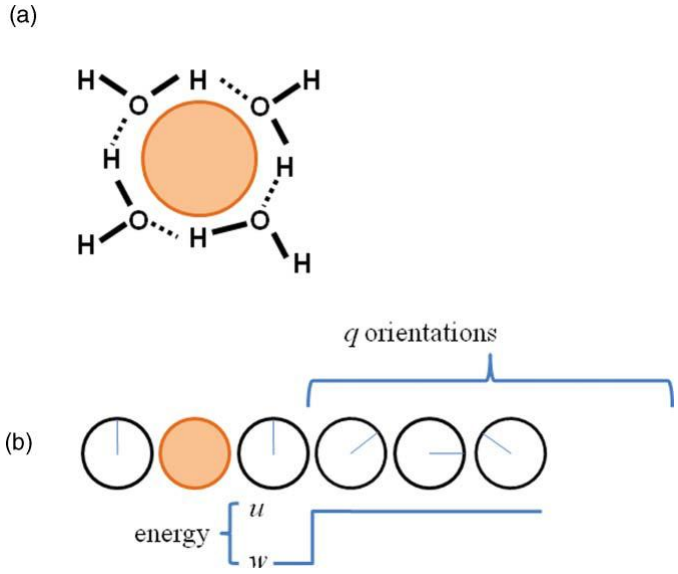

Figure 1. a) When non-polar molecules or macromolecules (shaded circle) are inserted into an aqueous medium, the water molecules must rearrange their hydrogen bonds (dashed lines) to form a structure (known as *clathrate* or *iceberg*) that surrounds the non-polar molecule like a cage. The water molecules of this structure are much more restricted in their movement. They are partly frozen (ice-like structures). **b)** Sketch of the 1-D lattice model of Kolomeisky and Widom: Each solvent molecule of the bulk solution may be in any of *q* orientations and the interaction energy between a pair of neighbouring molecules is *u*. In the immediate vicinity of a hydrophobic solute, however, only one of the *q* orientations is permitted and the interaction energy is *w*. This picture of water in the neighbourhood of non-polar solutes encompasses the essential features of the hydrophobic mechanism: restricted orientations and energy release for solvent molecules near non-polar solutes (due to a freezing-like process).

It should be stressed, however, that the hydrophobic (or hydrophilic) character of a substance is intrinsically temperature-sensitive. This can be easily elucidated as follows. Since clathrates are

ice-like structures, their heat of formation may be thought of as a latent heat of freezing. Consequently, both the enthalpy and entropy of formation of these ordered structures are negative. Thus $\Delta G_f = \Delta H_f - T\Delta S_f > 0$, if temperature is high enough. In other words: if temperature exceeds a critical value, the formation of clathrates is not thermodynamically favoured and a nonpolar solute will aggregate (hydrophobic solute). On the contrary, $\Delta G_f < 0$ and the nonpolar solute is thermodynamically stable dispersed in water if temperature is low enough (hydrophilic solute).

At this point the question is: How are the solvent-mediated (attractive) forces that induce aggregation of hydrophobic solutes? Kolomeisky and Widom calculated the corresponding pair potential in a one-dimensional lattice model.[26] According to this approach, each solvent molecule of the bulk solution may be in any of *q* orientations and the interaction energy between a pair of neighbouring molecules is *u*. In the immediate vicinity of a hydrophobic solute, however, only one of the *q* orientations is permitted and the interaction energy is *w,* with $w < u$ (the notation used by these authors is mostly followed in this work). This picture of water in the neighbourhood of non-polar solutes (sketched in Figure 1) is highly oversimplified. However, it encompasses the essential features of the hydrophobic mechanism (restricted orientations, ordering and energy release for solvent molecules near non-polar solutes).

Two parameters define this pair potential: $w-u$ and q. The former can be identified with the energy released in the formation of a hydrogen bond between two water molecules adjacent to the hydrophobic solute whereas $-k_B \ln(q-1)$ is the decrease of entropy associated to the same process. Consequently, the corresponding free energy (ΔF) is given by:

$$\Delta F = w - u + k_B T \ln(q-1) \tag{5}$$

In order to simplify the expression of the pair potential, Kolomeisky and Widom define four new parameters (c , x , s and Q) related with these thermodynamic quantities. The reader interested in the details is referred to the original work.[26] Using these definitions, the potential is given by the following expression:

$$u_{hyd}(r) = -k_B T \ln\left[1 + \left(\frac{1+Q}{1-Q}\right)\left(\frac{1-S}{1+S}\right)^{r/r_1 - 1}\right] \tag{6}$$

where r_1 is the lattice spacing (identified with the monomer diameter in this work). It should be stressed that the pair potential given by Equation (6) depends on c as follows. On the one hand, the hydrophobic interaction is attractive and its strength increases with temperature. On the other hand, the range of the interaction decreases with T. Finally it should be pointed out that, for large distances, the pair potential decays exponentially, as many experiments suggest.

As mentioned before, this pair potential was derived in a one-dimensional lattice model. However, Barkema and Widom proved through simulations that the main features of the one-

dimensional potential remain valid for two and three dimensions.[46] In addition, Koga and Widom also proved that the one-dimensional model can justify (within good accuracy) solubility data of methane,[47] which clearly supports its applicability to 3D real systems.

However, it should be stressed that charged chemical groups are usually hydrophilic rather than hydrophobic. Thus the hydrophobic forces between beads with charged groups could be considerably weakened. For that reason we have assumed, as a limiting case, that such hydrophobic interaction is not operative if any of the two interacting beads is charged. In other words, hydrophobic forces only work between uncharged non-bonded monomeric beads.

Some simulation details

The simulations were performed using the canonical ensemble, in which volume and temperature are kept constant. The volume fraction corresponding to zero osmotic pressure was estimated by interpolation from several (φ, Π) values. Other authors have employed the isothermal-isobaric (NPT) ensemble, in which the volume fraction for $\Pi = 0$ is straightforwardly obtained.[13,20] However, some of these authors also admit that the NPT φ-value can sometimes depend on the initial volume fraction used as input in the simulation.[13] A preliminary study (carried out by ourselves) confirmed this feature and additionally proved that this effect becomes more pronounced with increasing the chain length, which might make the interpretation of results more difficult. On the other hand, the isotherms obtained in the canonical ensemble are a very useful tool in the study of volume phase transitions, as will be discussed later. In any case, NPT simulations were also used in our work for checking purposes.

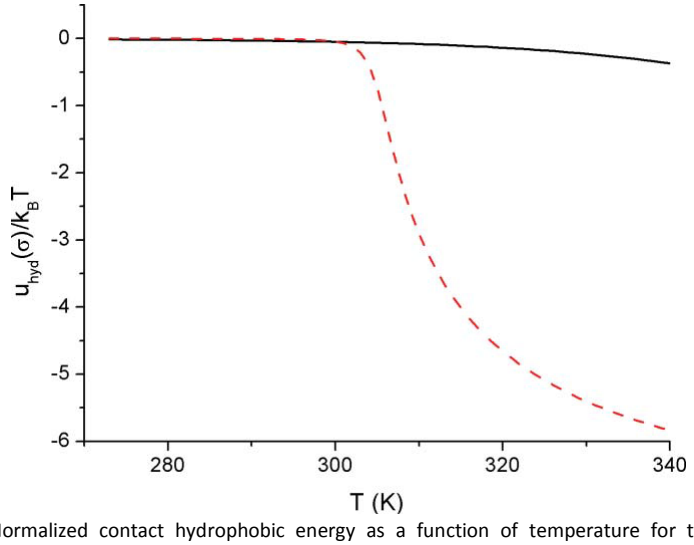

Figure 2. Normalized contact hydrophobic energy as a function of temperature for two pairs of parameters of Widom's model: a) $u - w$ =1.6·10^{-20} J and $k_B \ln(q-1)$ =4.50·10^{-23} J/K, weakly hydrophobic gels (solid line); b) $u - w$ =3.0·10^{-20} J and $k_B \ln(q-1)$ =9.84·10^{-23} J/K, strongly hydrophobic gels (dashed line).

A cubic simulation box contained the particles of different species. Periodic boundary conditions were applied. Initially, the nodes were positioned on a diamond lattice and the monomer beads in the lines connecting them. The simulation cell comprised 8 nodes and 16 chains.[10,16] Counterions were randomly situated. The total number of particles (N_p) in the simulation cell is $N_p = N_{node} + N_{chain}N_{bead} + N_{CI} = N_{node} + N_{chain} f$. $40{\cdot}10^6$ configurations were used for thermalization and the same quantity (at least) for averaging purposes. The energy of the system must be carefully calculated if long-range Coulomb forces are involved. In this work, Ewald sums were implemented following the procedures and recommendation suggested by Linse.[48] Although there are efficient simulation packages, this work was carried out using our own computer code (in C). Taking advantage of the fact that this program can also work in the NPT ensemble, the reliability of the program and the ϕ-values obtained by extrapolation in the canonical ensemble could be checked.

RESULTS AND DISCUSSION

Uncharged polymer networks

Before studying charged gels, it is worth analyzing the effect of certain parameters on the swelling on uncharged networks. In particular, we have considered two pairs of uncharged systems. Each pair is characterized by the same hydrophobic parameters. For one of them, $u - w$=1.6·10^{-20} J and $k_B \ln(q-1)$ =4.50·10^{-23} J/K. These values are of the same order of magnitude than those fitting experimental solubility data of representative hydrophobic solute.[47] One of the gels of this pair has 24 beads per chain whereas the other has a longer chain ($N_{bead} = 48$). We will refer to these systems as WH-SC and WH-LC, respectively (SC and LC stand for *short-chain* and *long-chain*, respectively). These N_{bead}-values were chosen because most the of real gels have chain lengths smaller than 50 beads per chain, in particular those used as experimental references in this work.[27-33] In any case, these hydrophobic parameters give a weakly hydrophobic (WH) interaction. This can be easily deduced from Figure 2, in which $u_{hyd}(\sigma)$ (the contact hydrophobic energy) is plotted as a function of the temperature in the range [275 K,335 K]. This temperature 'window' have been chosen inspired by real swelling behaviour, since volume changes of many gels takes place at 30-40 ºC (e.g., poly(NIPAM), at 32 ºC). As can be seen in Figure 2, $u_{hyd}(r_1)$ is smaller than the thermal energy in this temperature range and varies slowly.

For the second pair of gels, $u - w$=3.0·10^{-20} J and $k_B \ln(q-1)$ =9.84·10^{-23} J/K. Figure 2 also shows the temperature dependence of $u_{hyd}(\sigma)$ corresponding to these values, which are twice larger than the previous ones (in round numbers). As can be seen, the behaviour of the contact energy is very different. The magnitude of the quantity is negligible for temperatures smaller

than 300 K but increases very rapidly from 305 K, which is the quotient $(u-w)/k_B\ln(q-1)$ for this case. This obviously means that (i) the functional form of the hydrophobic interaction strongly depends on the values of $u-w$ and $k_B\ln(q-1)$; (ii) monomeric beads become strongly hydrophobic (SH) with increasing these parameters. In analogy with WH gels, the systems forming this SH pair differ in the number of beads per chain, with $N_{bead}=24$ and 48. These two gels will be identified as SH-SC and SH-LC, respectively.

Figure 3 shows the volume fraction as a function of the temperature for the four reference gels (SH-SC, SH-LC, WH-SC and WH-LC). A logarithmic scale is used in the φ-axis. In this way, the swelling capacity, defined as the quotient between the φ-values corresponding to shrunken and swollen states, can be graphically identified with the 'length' between them in the φ-axis. In all the cases, the volume fraction increases with the temperature. In other words, we are always reporting a thermo-shrinking behaviour. This is not a minor issue, as will be discussed later.

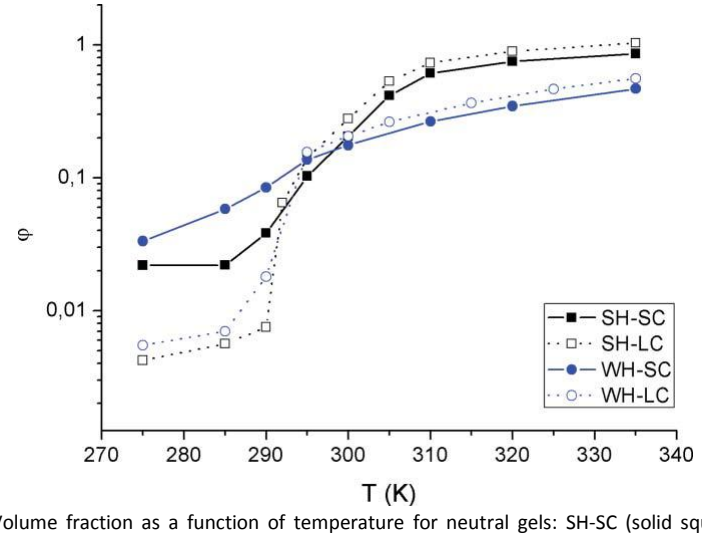

Figure 3. Volume fraction as a function of temperature for neutral gels: SH-SC (solid square), SH-LC (open square), WH-SC (solid circle), WH-LC (open circle).

In any case, the features of the $\varphi-T$ curve depend strongly on the values of the hydrophobic parameters ($u-w$ and $k_B\ln(q-1)$) and N_{bead}. First, we will consider the WH-SC gel. As can be seen in Figure 3, the transition from swollen states (low volume fractions) to shrunken states (high φ-values) is gradual. If the length of chain and/or the hydrophobic parameters are increased (cases WH-LC, SH-SC, SH-LC), the curve describing the volume change becomes more abrupt and clearly resembles the sigmoid function reported in many experimental results.[5,27-33] It should be mentioned, however, that the gentle transition found for WH-SC is more rarely

reported than the sigmoid one, but it has also been experimentally observed, for instance for poly(VCL)-based microgels with high concentrations of crosslinker.[32]

Figure 3 can also illustrate the effect of the number of monomeric beads per chain comparing –SC gels with –LC gels. For instance, at low temperatures, the WH-LC gel swells more than the SC ones. In contrast, the chain length favors the collapse of the network at high temperatures since the volume fractions are a bit larger for the LC network. The comparison of SH-SC and -LC gels confirms the two-fold effect of increasing the number of beads per chain: network swells more at low temperatures but form denser structures at high temperatures.

In experiments, the effect of the number of beads (monomeric units) can be explored in two different ways. On the one hand, we might vary the monomer concentration in the synthesis procedure. On the other hand, the density of cross-linker could also be modified. Shibayama *et al.* investigated both possibilities for the swelling of neutral temperature-responsive poly(NIPAM)-based gels.[28] Their experiments showed that, at low temperatures, the swelling is quite insensitive to the monomer concentration and, consequently, to the number of beads per chain. In such a case, however these authors claimed that entanglements and chain interpenetration increased with the monomer concentration, yielding highly non-ideal networks. Since our networks are presumably ideal, these data should be discarded in comparisons. If the cross-linker density is varied, Shibayama and co-workers reported that the swelling increases with N_{bead} (decreasing cross-linking). The same conclusion is reported for a similar system by László *et al.*[29] In both cases, there is agreement with our simulation results for neutral networks.

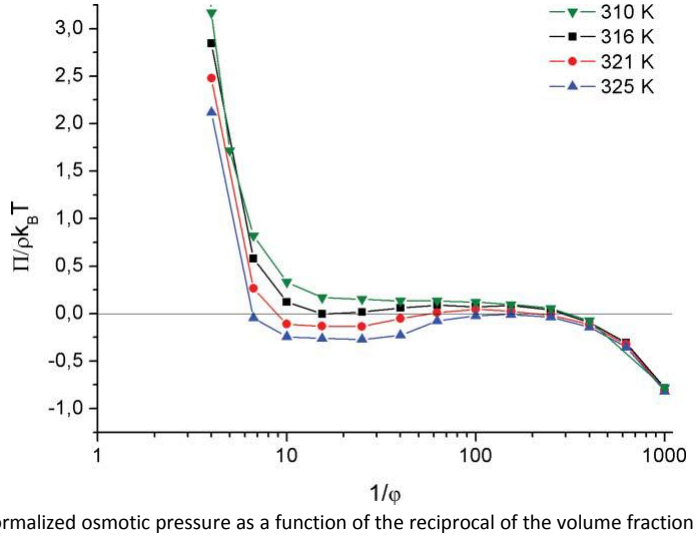

Figure 4. Normalized osmotic pressure as a function of the reciprocal of the volume fraction for the WH-SC gel with f = 8 for T = 310, 316, 321 and 325 K (down triangles, squares, circles and up triangles, respectively).

Concerning high temperatures and shrunken states, Shibayama's results do not confirm in any case that the gels with larger chains reach more collapsed states (in contradiction with our simulation data). In this respect, we would also like to mention that such highly collapsed states (with volume fractions close to 1) do not seem very realistic and clearly suggest that the hydrophobic interaction of Widom's model would be overestimated at high temperatures.

Recently, Imaz *et al.* have also studied the effect of the cross-linker concentration on charged poly(VCL)-based microgels.[32-33] Their results seem to depend on the chemical nature of this reactant. In a first paper, these authors used *N,N'*-methylenebisacrylamide as cross-linker and concluded that the swelling capacity increases with decreasing its concentration (increasing the number of monomeric beads per chain),[32] in agreement with our simulation results for charged networks. In a second paper, they used poly(ethylene glycol) diacrylate (PEGDA).[33] In this case, however, the swelling was not very sensitive to the concentration of this cross-linker. This behaviour was attributed by the authors to the existence of a core mainly formed of PEGDA and a shell containing noncrosslinked VCL units. Again, a nonideal network could explain the disagreement between simulations and experiments.

Charged polyelectrolyte networks

WH-SC gels

In this subsection, the effect of the charge is analyzed. First, WH-SC gels with different degrees of ionization ($f = 0$, 6, 8 and 12) will be investigated but, before presenting such results, it would be quite instructive to examine the isotherms that have been used to determine the volume fraction at equilibrium (when a null osmotic pressure, Π, is achieved).

As a first example, let us consider some isotherms corresponding to WH-SC the system with $f = 8$. In Figure 4, the pressure (normalized by $\rho k_B T$, where ρ is the particle number density and k_B is Botlzmann's constant) is plotted as a function of the reciprocal of the volume fraction, which is proportional to the volume of the system, for several temperatures. The normalization used in this figure allows us to distinguish different isotherms more clearly, particularly in the regime of large volumes. First, let us consider the case $T = 310$ K. As can be seen, pressure decreases monotonically as the volume is increased ($\partial \Pi / \partial V < 0$) and this isotherm intersects the zero pressure only in one point. For lower temperatures, only one intersection (which provides the volume at equilibrium) was also observed. But some new features emerge when temperature is increased up to 316 K. For instance, this isotherm shows a van der Waals loop with instabilities ($\partial \Pi / \partial V > 0$). In addition, this curve exhibits a clear intersection with $\Pi = 0$ for large volumes but also comes into contact with this line for small volumes. This contact point suggests that, for larger temperatures, the isotherms will intersect the zero pressure line three times. This situation is clearly illustrated for $T = 321$ K. The intermediate intersection clearly corresponds to an unstable state (since $\partial \Pi / \partial V > 0$). In general, one of the other two intersections is related to a stable state, whereas the third one is associated to a metastable state.[13] In fact, in NPT simulations, both stable and metastable states can be reached

depending on the initial ϕ-value chosen. For that reason, both will be plotted in the corresponding $\varphi - T$ curve (see next figure). It should be noted, nevertheless, that there is a temperature for which the collapsed and swollen states are stable and a phase transition would take place. This transition temperature can be determined with the help of the Maxwell construction: The two areas enclosed by the isotherm and the zero pressure line must be equal. In our work, the Maxwell construction can be applied only in an approximate way and reveals that the transition temperature is about 319 K. If the gel is again heated, we could eventually find a new situation illustrated in this case by the isotherm $T = 325$ K. As can be seen, there is a clear intersection with $\Pi = 0$ at low volumes whereas such isotherm hardly touches the zero pressure line at high volumes. This suggests that, for larger temperatures, the coexistence of stable and metastable states does not occur any longer. In other words, metastable swollen states tend to disappear for higher temperatures. In short, for $f = 8$, stable and metastable states can coexist from 316 to 325 K.

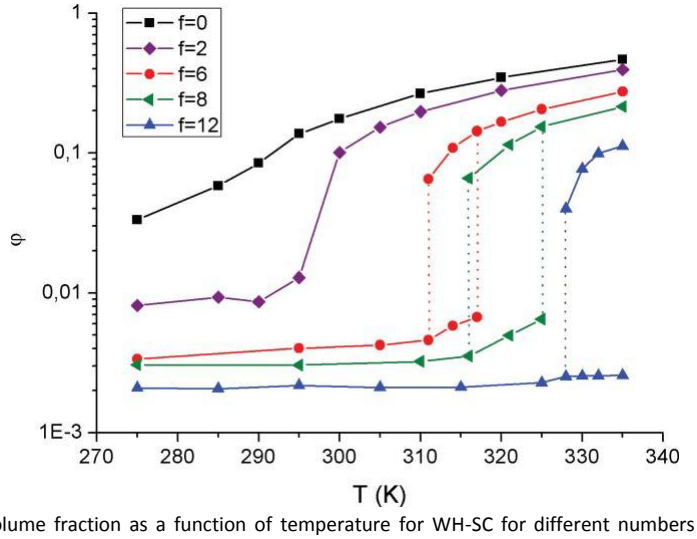

Figure 5. Volume fraction as a function of temperature for WH-SC for different numbers of charged beads per chain (*f*): *f* = 0 (squares), *f* = 2 (diamonds), *f* = 6 (circles), *f* = 8 (left triangles) and *f* = 12 (up triangles). Dotted vertical lines delimit the temperature interval in which coexistence of swollen and shrunken states occur.

It should be stressed, however, that this coexistence might be related to certain thermal hysteresis, which can be elucidated as follows. Let us imagine that, in a heating process, we have just exceeded the transition temperature (319 K in this case). In theory, the network should undergo a sudden collapse, since shrunken states are stable over such temperature. But, due to the existence of swollen metastable states between 319 and 325 K, the gel might be superheated (in the same way as liquids can be supercooled) and the collapse could even occur at 325 K. Analogously, the swelling in the cooling process could take place at temperatures below 319 K

(even at 316 K) since there are metastable shrunken states between 316 and 319 K. A similar analysis carried out for $f = 6$ (figure not included) shows that the coexistence of stable and metastable gels takes places between 311 and 317 K and the transition temperature is about 313 K. For $f = 12$, metastability appears at 328 K and the transition occurs about 331 K.

After the analysis of some illustrative isotherms, the $\varphi - T$ curve for WH-SC gels is plotted in Figure 5 for $f = 0$, 2, 6, 8 and 12. It should be stressed that the charge has different effect on these curves:

(i) At low temperatures: the volume fractions of charged swollen networks are much smaller than those corresponding to the uncharged system and the difference between them grows with the degree of ionization, in agreement with previous simulations.[10,16] The gain of entropy caused by the larger volume available to counterions in the swollen state is said to be the driving force behind the large swelling capacity of ionized gels.[10,16] In other words, the contribution to osmotic pressure due to free counterions is the responsible for such a large swelling. It should be noted, however, that the swelling capacity grows with charge more rapidly for low f-values. This can be easily illustrated comparing $f = 0$ and 2 on the one hand, and $f = 8$ and 12, on the other. The difference is greater in the former case (although the change of f is smaller).

(ii) The compactness of collapsed states decreases with degree of ionization. Obviously, this might be attributed to the osmotic pressure of free counterions as well.

(iii) Figure 5 also shows other important effect: the transition from swollen to collapsed states shifts towards higher temperatures with increasing charge. In fact, for $f = 12$ it is so intense that the transition is partly out of the temperature window. This is a consequence of the competition between the pressure exerted by free counterions (which swells the polyelectrolyte gel) and attractive hydrophobic forces (which tends to shrink it). When the number of ionized beads per chains grows, the ionic contribution to pressure obviously increases, and equilibrium is only restored when hydrophobic forces become stronger with increasing temperature.

(iv) As can be seen, the transitions for $f = 0$ and 2 are continuous. In contrast, the transitions for larger f-values are discontinuous.

(v) For such f-values, the $\varphi - T$ curves exhibit coexistence of swollen and shrunken states in an interval of temperatures as well as some hysteresis. In such cases, both swollen and shrunken states have been plotted and the temperature interval of coexistence is delimited by dashed vertical lines.

The effects of charge commented in items (i), (iii) and (iv) are widely known by theorists, who have developed different approaches that predict and/or justify such behaviors.[27,49-55] These charge effects have been also predicted for nanogels by new and sophisticated theories (based

on coarse-grained models) developed by Jha *et al.*[22] Therein, the volume phase transitions are studied as a function of the Flory-Huggins parameter, which implicitly includes the effect of the temperature and hydrophobic forces. However, it is also instructive to compare with previously published experimental results. In the case of weakly ionized gels, the increase of swelling capacity and the shift of the transition towards larger temperatures was reported for poly(NIPAM)-based gels long time ago.[27] The charge was varied synthesizing several gels with different quantities of sodium acrylate, an ionic group. Hirotsu *et al.* also observed that the transition became more abrupt, and even discontinuous, with increasing *f* (for weakly charged gels), also in agreement with our simulations. As commented before, our simulation results reveal the existence of thermal hysteresis. Thermal hysteresis in the swelling-shrinking behaviour of polyelectrolyte gels has been also reported by experimentalists (but only in a few works).[58-62] Some of them attributed this phenomenon to metaestable states associated to phase transitions.[58,60] Our NVT simulations clearly supports this hypothesis, since thermal hysteresis is always observed together with discontinuous volume changes.

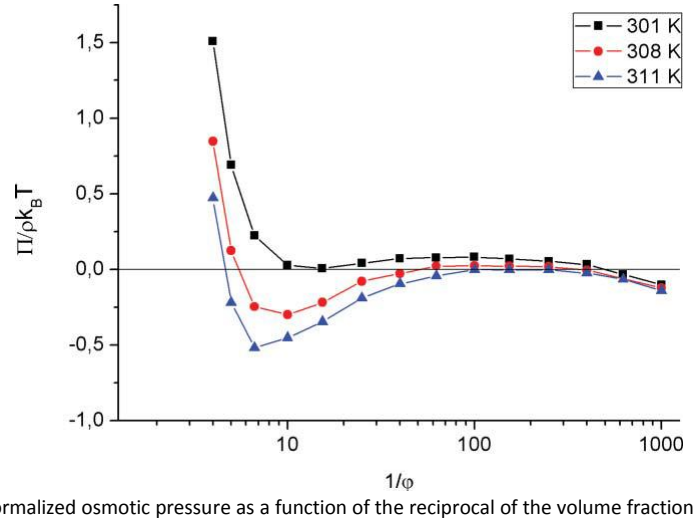

Figure 6. Normalized osmotic pressure as a function of the reciprocal of the volume fraction for the WH-LC gel with *f* = 6 for *T* = 301, 308 and 311 K (squares, circles and triangles, respectively).

WH-LC gels

The results for WH-LC gels with different ionized groups per chain ($f = 0$, 2, 6, and 8) will be also analyzed. Previously, some representative isotherms will be commented (as done with WH-SC systems). Figure 6 shows three isotherms (normalized osmotic pressure vs. $1/\varphi$ for 301, 308 and 311 K). As can be seen, the isotherms corresponding to 308 K intersect the zero pressure line three times. The lowest and the highest intersections are associated to stable/metaestable states. Both will be plotted in the corresponding $\varphi - T$ curve (next figure). For 301 and 311 K, the curves cross the zero pressure line in one point but touch it in another point. Consequently,

for temperatures lower than 301 K or greater than 311, the isotherms intersect the $\Pi = 0$ line only once and the coexistence of swollen and shrunken states occurs between these two limiting temperatures. With the help of the Maxwell construction, we also determined an approximated transition temperature, which turned out to be 305 K. For $f = 8$ and 12, a similar analysis was carried out (not shown).

The volume fraction at equilibrium ($\Pi = 0$) as a function of the temperature is plotted in Figure 7, which resembles to a great extent the figure of WH-SC gels. In particular, thermal hysteresis in a fairly wide temperature interval is again observed for $f = 6$, 8 and 12. The estimated limiting temperatures of coexistence were also indicated in Figure 7. As can be seen, the transitions are now less shifted towards high temperatures (as compared to WH-SC gels, Figure 5). In addition, the case $f = 12$ exhibits thermal hysteresis for T <335 K. In fact, the transition between swollen and collapsed states can be completely observed for $f = 12$ (which was not possible for WH-SC gels). The competition between pressure exerted by free counterions and attractive hydrophobic forces would also explain why the shift of the transition is smaller for LC gels (as compared with SC gels with the same number of charged beads per chain); obviously, the relative weight of the hydrophobic interaction grows with the number of (uncharged) beads per chain.

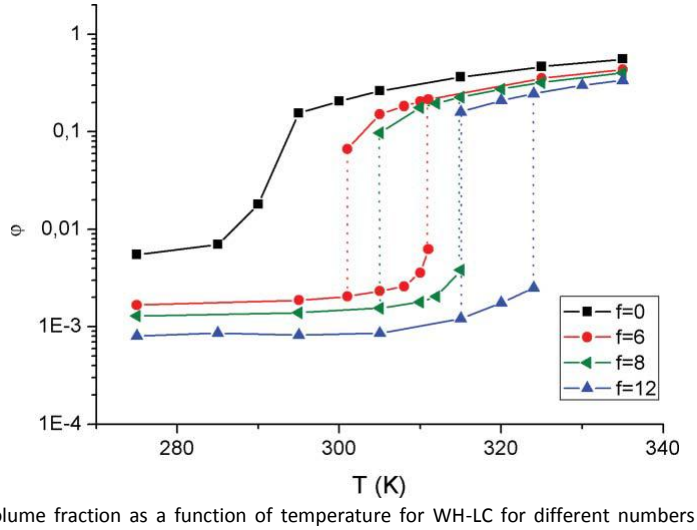

Figure 7. Volume fraction as a function of temperature for WH-LC for different numbers of charged beads per chain (*f*): *f* = 0 (squares), *f* = 6 (circles), *f* = 8 (left triangles) and *f* = 12 (up triangles). Dotted vertical lines delimit the temperature interval in which coexistence of swollen and shrunken states occur.

SH-SC gels

SH-SC networks with different degrees of ionization ($f = 0$, 2, 6, 12 and 20) are now explored. The $\varphi - T$ curves corresponding to these f -values are plotted in Figure 8. As can be seen, all

these curves are again sigmoid functions connecting swollen and shrunken states (low and high φ-values). The curves of this figure also exhibit the features (i), (ii) and (iii) reported for WH-SC gels. However, it should be mentioned that the shift towards higher temperatures with increasing charge is now smaller (as compared to WH-SC networks). This is reasonable since hydrophobic interactions are greater in this case.

In any case, the most noticeable feature of this figure is that our simulations do not reveal discontinuous changes or coexistence of collapsed and swollen phases (although the transition is quite abrupt for $f = 12$, it is not discontinuous). This result strongly contrasts with the predictions of theories based on the formalism of Flory-Rhener for thermo-sensitive gels,[27.49-55] which predict discontinuous volume transitions even for very weakly ionized polyelectrolyte chains.

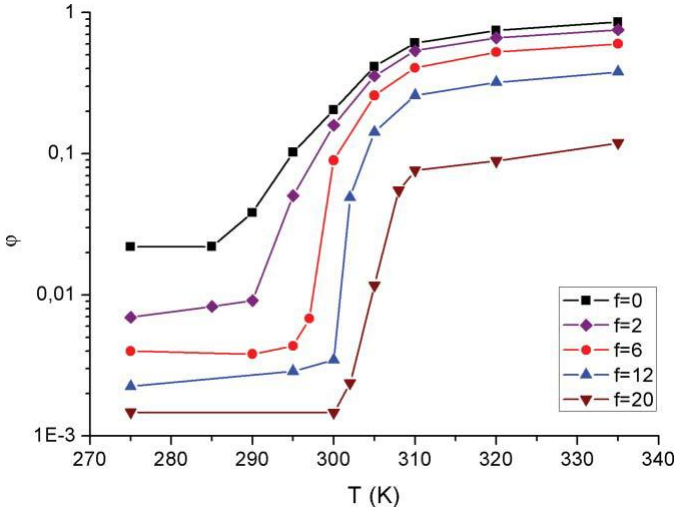

Figure 8. Volume fraction as a function of temperature for SH-SC for different numbers of charged beads per chain (f): f = 0 (squares), f = 2 (diamonds), f = 6 (circles), f = 12 (up triangles) and f = 20 (down triangles).

In relation to this discrepancy between theory and simulations, it will be quite enlightening to compare with some experimental results. In this sense, it should be stressed that some authors have also reported that certain charged gels do not exhibit discontinuous phase transitions. [30,31] For instance, Mamytbekov *et al.*[31] synthesized several poly(VCL)-based gels with different concentrations of an ionic comonomer. In this way, the effect of charge is experimentally investigated. Their results clearly show the shift of the transition towards higher temperatures with increasing the number of ionizable groups per chain but that the transition becomes more gradual (instead of more abrupt or discontinuous).

The effect of charge can also be experimentally explored with the help of a pH-sensitive comonomer, such as the acrylic acid (AA).[30] The ionizable groups of this monomer have a weak

character. Capriles-González *et al.* synthesized poly(NIPAM-AA) microgel particles and reported the diameter as a function of temperature for different pHs: 4.1 (20% of charge) , 4.6 (75% of charge) and 7.8 (100% of charge) and concluded that the transition shifts towards higher temperatures and broadens (becomes more gradual) with increasing the pH/charge.
The absence of discontinuous volume changes reported for these systems[30,31] disagrees with theoretical predictions,[27, 49-55] but agrees to a great extent with the results obtained for SH-SC gels in this work. In fact, Figure 8 also illustrates how the transition becomes more gradual when the number of charged groups is increased from 12 to 20.

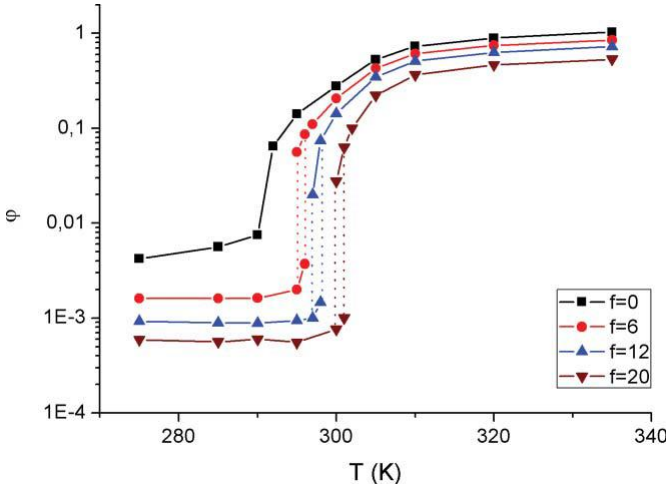

Figure 9. Volume fraction as a function of temperature for SH-LC for different numbers of charged beads per chain (*f*): *f* = 0 (squares), *f* = 6 (circles), *f* = 12 (up triangles) and *f* = 20 (down triangles). Dotted vertical lines delimit the temperature interval in which coexistence of swollen and shrunken states occur.

SH-LC gels

Finally, it is interesting to look into the effect of the number of beads per chain for SH- systems. Figure 9 shows the volume fractions obtained for SH-LC gels with different ionized groups per chain (*f* = 0, 6, 12 and 20). As can be concluded, the presence of charge does not modify some of the conclusions reported for uncharged networks: LC gels swells more than the SC ones and the collapse of the network is favored by the chain length since, given a degree of ionization, the volume fractions reached by LC gels are larger than those of SC networks. The latter effect is particular and clearly observed for *f*=20. However, there is a difference between SH-SC and SH-LC gels that should be stressed: An analysis of isotherms similar to that previously commented for WH-SC networks again reveals the existence of metastable states in some temperature intervals, where discontinuous volume changes also takes place. It should be pointed out, however, that these intervals are much shorter than those corresponding to WH-SC gels. In fact, the amplitude of these intervals would not exceed 1-2 degrees, as can be seen in Figure 6. Consequently, the

thermal hysteresis associated to these metaestable states would be observed in practice only if temperature steps are really short. Otherwise, only an abrupt volume change could be reported.

The thermo-shrinking behavior

Before ending this section, we would like to make an additional consideration. The fact that polymer gels shrink upon heating is widely known by experimentalists. Thermo-shrinking and, in general, temperature-sensitive gels have also attracted the attention of numerous theorists, who have developed different swelling theories for this kind of responsive materials,[27,49-55] mostly inspired in the Flory-Rhener formalism.[56-57] As far as we know, however, only Escobedo and de Pablo reported this behavior from simulations.[8] Their work was focused on sub- and supercritical conditions and restricted to uncharged networks. A solvent-mediated interaction potential between monomer beads was not considered because solvent was explicitly modeled.

As commented before, the model of (solvent-mediated) hydrophobic forces used in these simulations predicts that the strength of this interaction increases with temperature. This feature plays an important role in the explanation of thermo-shrinking gels in the framework adopted here. At first sight, we might expect that polyelectrolyte chains unfold with temperature due to thermal agitation, even in the presence of attractive solvent-mediated forces. In fact, some previous polyelectrolyte simulations point to this conclusion. For instance, Khalatur and coworkers found that charged protein-like copolymers suddenly expand if the temperature exceeds a critical value.[42] The same conclusion can be inferred for polyelectrolyte gels from the results reported by Schneider and Linse.[13] Although these authors did not study the effect of temperature explicitly, they proved that the gel expands if the ratio between the thermal energy and the depth of the square-well potential modeling the hydrophobic interaction is larger than a threshold value. Consequently, the thermo-shrinking behavior would be counterintuitive according to these results. But the situation is rather different if the strength of the hydrophobic forces increases with temperature. In this case, the hydrophobic interaction would be able to prevail over thermal agitation upon heating.

CONCLUSIONS.

In this work, thermo-shrinking polyelectrolyte gels have been simulated within the framework of the primitive model. Hydrophobic forces have been considered through an effective solvent-mediated polymer-polymer interaction (Widom's potential) whose strength increases with temperature. This feature, which constitutes a novelty, plays an essential role in the mechanism underlying the thermo-shrinking behaviour.

Two kinds of hydrophobic systems have been studied. In one of them, this interaction grows rapidly above certain temperature. In the other, hydrophobic forces are weak and increase very gently upon heating. In both cases, polyelectrolyte gels shrink with increasing temperature. However, our work shows that the functional form of the hydrophobic interaction has a profound influence on the swelling behaviour of polyelectrolyte gels. In particular, WH-SC and -LC systems exhibit discontinuous volume changes, in agreement with many theories for thermosensitive gels

and some experimental results. However, SH-SC gels do not show hallmarks of phase transitions, even for highly charged polyelectrolyte chains. Although this finding disagrees with theoretical predictions, it agrees with some experimental results. In the case of large chains, coexistence of swollen and shrunken states was also found for SH-LC gels, but this phenomenon is restricted to such short temperature intervals that would be hardly measurable.

Although the hydrophobic model is oversimplified, our simulation results qualitatively reproduce several features of thermo-shrinking behaviour of real gels and microgels reported by experimentalists. For instance, the swelling increases with the number of charged groups per chain and, in many cases, there is a well defined transition from swollen to shrunken states, which moves toward larger temperatures with increasing the chain charge. The qualitative agreement between simulations and experiments suggests that the effective solvent-mediated polymer-polymer interaction used here is a good candidate for hydrophobic interaction. However, our work also reveals that such potential overestimate the value of this interaction at high temperature.

ACKNOWLEDGEMENTS.

The authors thank the financial support from the following institutions: i) 'Ministerio de Ciencia e Innovación, Plan Nacional de Investigación, Desarrollo e Innovación Tecnológica (I+D+i)', Project MAT2009-13155-C04-04. ii) 'Consejería de Innovación, Ciencia y Empresa de la Junta de Andalucía', Projects P07-FQM-02496, P07-FQM-02517, P09-FQM-4698. iii) European Regional Development Fund (ERDF).

REFERENCES

1. T. Sawai, S. Yamazaki, Y. Ikariyama and M. Aizawa, J. Electroanal. Chem. **322**, 1 (1992).
2. K. Kajiwara and S. B. Rossmurphy, Nature **355**, 208 (1992).
3. M. J. Murray and M. J. Snowden, Adv. Colloid Interface Sci. **54**, 73 (1995).
4. N. A. Peppas, Curr. Opin. Colloid Interface Sci. **2**, 531 (1997).
5. R. Pelton, Adv. Colloid Interface Sci. **85**, 1 (2000).
6. J. Ramos, A. Imaz, J. Callejas-Fernández, L. Barbosa-Barros, J. Estelrich, M. Quesada-Pérez, J. Forcada, Soft Matter **7**, 5067 (2011).
7. A.V. Dobrynin, Curr. Opin. Colloid Interface Sci. **13**, 376 (2008).
8. F. A. Escobedo and de J. J. de Pablo, Phys. Rep. **318**, 85 (1999).
9. D. P. Aalberts, *J. Chem. Phys.* **104**, 4309 (1996).
10. S. Schneider and P. Linse, J. Phys. Chem. B **107**, 8030 (2003).
11. Q. Yan and J. J. de Pablo, Phys. Rev. Lett. 91, 018301 (2003).
12. Z.-Y. Lu and R. Hentschke, Phys. Rev. E **67**, 061807 (2003).
13. S. Schneider and P. Linse, Macromolecules **37**, 3850 (2004).
14. S. Edgecombe, S. Schneider and P. Linse, Macromolecules **37**, 10089 (2004).
15. B. A.Mann, R. Everaers, C. Holm and K. Kremer, Europhys. Lett. **67**, 786 (2004).

16. B. A.Mann, C. Holm and K. Kremer, J. Chem. Phys. **122**, 154903 (2005).
17. D.-W Yin, Q. Yan, and de J. J. de Pablo, J. Chem. Phys. **123**, 174909 (2005).
18. S. Edgecombe and P. Linse, Langmuir **22**, 3836 (2006).
19. S. Edgecombe and P. Linse, Macromolecules **40**, 3868 (2007).
20. D.-W. Yin, M. Olvera de la Cruz and de J. J. de Pablo, J. Chem. Phys. **131**, 194907 (2009).
21. G.C. Claudio, K. Kremer and C. Holm, J. Chem. Phys. **131**, 094903 (2009).
22. P. K. Jha, J.W. Zwanikken, F. A. Detcheverry, J. J. de Pablo and M. Olvera de la Cruz, Soft Matter **7**, 5965 (2011)
23. M. Olvera de la Cruz, Soft Matter **4**, 1735 (2008).
24. M. Shibayama and T. Tanaka in *Phase transitions and related phenomena of polymer gel,* edited by K. Dusek in *Responsive gels: Volume transitions I* (Springer-Verlag, Berlin, 1993).
25. E. Kokofuta, in *Phase Transitions in Polyelectrolyte Gels*, edited by T. Radeva in *Physical Chemistry of Polyelectrolytes* (Marcel Deker, New York, 2001).
26. A.B. Kolomeisky and B. Widom, Faraday Discuss. **112**, 81 (1999).
27. S. Hirotsu, Y. Hirokawa and T. Tanaka, J. Chem. Phys. 87, 1392 (1987).
28. M. Shibayama, Y. Shirotani, H. Hirose and S. Nomura, Macromolecules 30, 7307 (1997).
29. K. László, K. Kosik, and E. Geissler, Macromolecules **37***,* 10067 (2004).
30. D. Capriles-González, B. Sierra-Martín, A. Fernández-Nieves, and A. Fernández-Barbero, J. Phys. Chem. B **112**, 12195 (2008).
31. G. Mamytbekov, K. Bouchal, and M. Ilavsky, Eur. Polym. J. **35**, 1925 (1999).
32. A. Imaz, and J. Forcada, J. Polym. Sci. Part A: Polym. Chem. **46***,* 2510 (2008).
33. A. Imaz, and J. Forcada, J. Polym. Sci. Part A: Polym. Chem. **46***,* 2766 (2008).
34. J. N. Israelachvili in *Intermolecular and Surface Forces* (Academic Press, London, 1992).
35. J. G. Ibarra-Armenta, A. Martín-Molina and M. Quesada-Pérez, Phys. Chem. Chem. Phys. **11**, 309 (2009).
36. *Handbook of Chemistry and Physics*, edited by D. R. Lide (CRC Press, Boca Raton, 1998).
37. M.O. Khan, S.M. Mel'nikov and B. Jönson, Macromolecules **32**, 8836 (1999).
38. U. Micka, C. Holm, and K. Kremer, Langmuir **15***,* 4033 (1999).
39. Chodanowski, P.; Stoll, S. *J. Chem. Phys.*, **1999**, *113*, 6069.
40. N. Lee and D. Thirumalai, Macromolecules **34**, 3446 (2001).
41. J. A. Anderson, and A. Travesset, Macromolecules **39***,* 5143 (2006).
42. P.G. Khalatur, A. R. Khokhlov, D.A. Mologin and P. Reineker, J. Chem. Phys. **113**, 1232 (2003).
43. F.A. Escobedo and J.J. de Pablo, J. Chem. Phys. **104**, 4788 (1996).
44. H.S. Frank and M.W. Evans, J. Chem. Phys. **13**, 507 (1945).
45. W. Kauzmann, Adv. Protein Chem. **14**, 1 (1959).
46. G.T. Barkema, and B. Widom, J. Chem. Phys. **113**, 2349 (2000).
47. K. Koga, P. Bhimalapuram and B. Widom, Mol. Phys. **100**, 3795 (2002).
48. P. Linse, Adv. Polym. Sci. 185, 111 (2005).
49. K. Otake, H. Inomata, K. Konno and S.Saito, J. Chem. Phys. **91**, 1345 (1989).

50. M. Marchetti, S. Prager, and E.L. Cussler, Macromolecules **23**, 1760 (1990).
51. T. Hino and J.M. Prausnitz, Polymer **39**, 3279 (1998).
52. Y. P. Hohng and Y. C. Bae, J. Polym. Sci. B: Polym. Phys. **40**, 2333 (2002).
53. H. Li, X. Wang, G. Yan, K.Y. Lam, S. Cheng, T. Zou, and R. Zhuo, Chem. Phys. **309**, 201 (2005).
54. Y. Huang, X. Jin, H. Liu, and Y Hu, Fluid Phase Equilibria **263**, 96 (2008).
55. S.C. Jung, S.Y. Oh and Y.C. Bae, Polymer **50**, 3370 (2009).
56. P. J. Flory and J. J. Rehner, J. Chem. Phys. **11**, 512 (1943).
57. P. J. Flory and J. J. Rehner, J. Chem. Phys. **11**, 521 (1943).
58. E.S. Matsuo andT. Tanaka, J. Chem. Phys. **89**, 1695 (1988).
59. T. Tomari and D. Masai, Macromolecules **28**, 8334 (1995).
60. A.Suzuki, T. Ishii and Y. Maruyama, J. Appl. Phys. **80**, 131 (1996).
61. B.R. Saunders and B. Vincent, J. Chem. Soc. Faraday Trans. **92**, 3385 (1996).
62. Y. Seida, K. Takeshita and Y. Nakano, J. Appl. Polym. Sci. **90**, 2449 (2003).

Paper VI

Effects of the Internal Structure of Charge of Divalent Ions on the Electrical Double Layer

José Guadalupe Ibarra-Armenta[1], Alberto Martín-Molina[2], Klemen Bohinc [3] and Manuel Quesada-Pérez[1]•

Manuscript to send to *J. Phys. Chem. B.*

(1) Departamento de Física, Escuela Politécnica Superior de Linares, Universidad de Jaén, 23700, Linares, Jaén, Spain.

(2) Grupo de Física de Fluidos y Biocoloides, Departamento de Física Aplicada, Facultad de Ciencias, Universidad de Granada, 18071 Granada, Spain.

(3) Faculty of Health Sciences, University of Ljubljana, SI-1000, Ljubljana, Slovenia.

* Corresponding author.

ABSTRACT.

In this work, the effects of the internal structure of charge for ions is analysed by means of Monte Carlo (MC) simulations within a modified primitive model of electrolyte with spheroidal ions inspired on monoclonal antibodies. The simulation results are contrasted to those from a Density Functional Theory (DFT). Indeed, an analytical DFT that includes ionic correlations was developed on previous studies to probe how giant unilamellar phospholipid vesicles aggregation is mediated by monoclonal antibodies. In order to test this approach, theoretical predictions are compared with those results obtained from computer simulations of a Primitive Model (PM) consisting of spheroidal divalent ions.

Spheroidal divalent ions have finite dimensions with a fixed diameter *d* spatially separating two identical elementary charges. Two structurally equivalent but oppositely charged ionic species are considered, coions and counterions. In the simulation, the number of particles is not fixed and the grand canonical ensemble is employed to obtain the thermodynamic equilibrium conditions. Meanwhile, the variational theory is applied to the analytical DFT model. The inter- and intraionic correlations arising from coulombic interactions and ionic size are assessed by both approaches. However, some intercorrelations related to the excluded volume are out of the theoretical framework. These correlations define the orientational ordering of the spheroidal ions (with quadrupolar charge distributions) leading to very different charge distributions from those of the regular divalent ions from the PM of electrolyte. According to our results, the internal structure of ions become relevant for modelling of large molecules which are known to have complex charge distributions.

INTRODUCTION.

Despite the current knowledge about the interactions between complex macromolecules or colloidal particles, the underlying mechanisms are not completely understood yet. In biology, many of the proteins and lipids in solution dissociate into smaller ionic groups when solved into aqueous media. Thus, coulombic interactions are the main responsible of the Electrical Double Layer (EDL) structures and hence of the stability and electrokinetic properties of charged colloidal systems. For this reason, theoretical models from the very beginning are centred in coulombic interactions as the generator of the EDL conformations. The linearized solution to the Poisson-Boltzmann (PB) equation provides the classical mathematical description of the EDL.[1] This is an analytical framework based on the Gouy-Chapman model which considers continuous functions for the charge distributions.[2,3] Thus, the discreteness of charge of individual ions as well as their excluded volume are neglected in such model.

In consideration of this discreteness, other modern approaches such as computer simulations,[4-7] lattice based models,[8-10] density functional[11,12] and integral equation theories have predicted that ion-ion correlations play an important role on the EDL.[13-15] Accordingly, these approaches give explanations of electrostatic phenomena that cannot be analyzed within the context of the classical theories referred. For instance, the concentration of multivalent counterions in the

vicinity of the charged surface could overcompensate the colloidal charge. This is defined as overcharging, a well known phenomenon reported by experimentalists for long time ago.[16]

In addition to coulombic interactions, the inclusion of ionic size and other non coulombic interactions enhance the connection of models with experimental data. The basic conception of the PM considers ions as individual charged hard entities with spherical shape with all the charge concentrated at their geometric centers. It has been demonstrated that computer simulations within a basic PM of electrolyte are reliable to represent excluded volume and coulombic interactions for mono- and divalent ions.[17,18] Despite the inclusion of ionic size in modern EDL theories, its role has not been addressed in full. It is recurrently assumed an ionic diameter around 0.4 nm for all types of ions, while there is experimental evidence that hydrated ionic diameters could be much larger than 0.4 nm (even for monovalent ions).[1] Apart from the ionic size, the intrinsic molecular structure of ions might also play a very important role in the description of the EDL. Because of polarizability, ions might present ion-ion and ion-colloid dispersion interactions. The inclusion of dispersion forces appeared in the past as an alternative to specific adsorption for the description of ionic specificity.[19-24] In any case, dispersion forces are out of the scope of the present work being our principal aim the influence of the internal structure of ions on the EDL.

Nowadays internal structures of ions have been studied by means of DFT, MC simulations, Langevin dipoles, dendrimers, etc.[25-30] In this manner, it is possible to test intraionic correlations (derived from the internal structure of ion) although some interionic correlations (those arising from the direct interaction between ions) are difficult to sample by the DFT. This limitation may lead to discrepancies between the theoretical predictions and the MC simulations in some particular cases (when interionic correlations are more important). However, it is advantageous to test intraionic correlations at any extent. For instance, the use of rod-like ions instead of the simple charged hard spheres is suitable to explain the linking of DNA to lipid bilayers.[31] It was found that the added orientation degrees of freedom may induce a bridging mechanism between a pair of charged plates with the same sign of charge causing a correlated net attraction. The internal structure is then an important feature to test. In the case of dendrimers, they induce long ranged attractive forces between a pair of equally charged plates.[29] Moreover, this correlated attraction was experimentally confirmed by direct measurements with an atomic force microscope. All these systems are examples in which the internal structure of ions should be taken into account to describe properly the corresponding EDL.

In the present work, we want to test the EDL structure for an electrolyte of spheroidal ions within an added salt inspired on a system of monoclonal antibodies. These monoclonal antibodies were found to induce coalescence on giant unilamellar phospholipid vesicles at short separations.[26,32,33] To this end, modifications to the basic PM are required to include the internal structure of these ions. On the other hand the use of a Grand Canonical MC (GCMC) simulation is also needed to control accurately the concentration of the added salt. By doing so, the role of intra- and interionic correlations will be analyzed. The rest of the paper is organized as follows. First the

GCMC simulations and the DFT model are described. Then, the results are presented and discussed in a single section. Finally, the main conclusions are highlighted.

MODEL AND SIMULATIONS.

Grand canonical MC simulations.

The GCMC simulations carried out in this work are based on a modified PM of electrolyte. The solvent is represented as a continuum of uniform dielectric permittivity $\varepsilon_0\varepsilon_r$ and constant temperature T (for pure water at room temperature $\varepsilon_r = 78.5$ and $T = 298\,K$). The Metropolis algorithm is applied to a grand canonical ensemble of spheroidal divalent ions modelled as charged hard spheres of diameter d with two identical elementary charges at the opposite locations exactly on the surface of the spheroid separated by an ionic diameter. These divalent spheroidal ions are confined into a rectangular simulation cell. The simulation cell is a square parallelepiped with dimensions $L \times W \times W$, where two charged and impenetrable planes are located at $x = 0$ and at $x = L$. The spheroidal ions cannot approach the charged planes below their radius, this defines the Distance of Closest Approach (DCA) equal to $d/2$. Charged planes carry a uniform surface charge density σ_0. Periodic boundary conditions in the lateral directions (y and z) are imposed to the electrolyte solution. The simulation cell contains a fixed counterion excess that neutralizes the charge deposited on the charged planes to ensure that the whole simulation cell is always electro-neutral. It also contains a variable amount of electro-neutral ionic groups composed of coions and counterions from the bulk solution depending on the desired salt concentration. These electro-neutral groups are taken from a reservoir where the salt concentration is held fixed ensuring that the electrolyte in the confined region reaches thermodynamic equilibrium at the desired salt concentration. The original GCMC simulation implementation within a PM of charged hard spheres was proposed by Valleau *et al*.[37] in 1980 based on the previous works of Adams for neutral hard spheres.[38,39] According to this technique, an activity coefficient must be calculated for any desired salt concentration. The activity coefficient is an intensive property independent of the size of the simulation box. For further details about the original implementation of the GCMC simulation we refer the reader to the original papers.[34-36]

Spheroidal ions are free to translate and rotate. The interaction energy between any pair of spheroids arise from the interaction of the two elementary charges on each of them. Any pair of individual elementary charges belonging to spheroidal ions has an effective interaction energy given by

$$u(r_{ij}) = \frac{Z_i Z_j e^2}{4\pi\varepsilon_0\varepsilon_r r_{ij}}, \qquad r_{ij}^{cc} > d$$

$$u(r_{ij}) = \infty, \qquad r_{ij}^{cc} < d \tag{1}$$

Where Z_i is the valence of individual elementary charges (it can be positive or negative but always unitary) e is the value of the elementary charge, r_{ij} is the relative distance between individual charges i and j and r_{ij}^{cc} is the center to center distance between the spheroids to which the individual charges i and j belong. The first line in eqn (1) accounts for the coulombic interaction. However, due to the fact that this interaction is long ranged, an energy correction must be considered too. To this end, energy corrections proposed by Boda *et al.* have been used (see the original paper for further details).[37] The second line in eqn (1) is the hard sphere interaction among spheroidal ions. Nonetheless, as will be discussed later on, the hard sphere nature among ions can be removed without significant effects depending on the simulation conditions. There is also a coulombic interaction between individual elementary charges from spheroidal ions and the the uniform charge density spread over the charged planes.

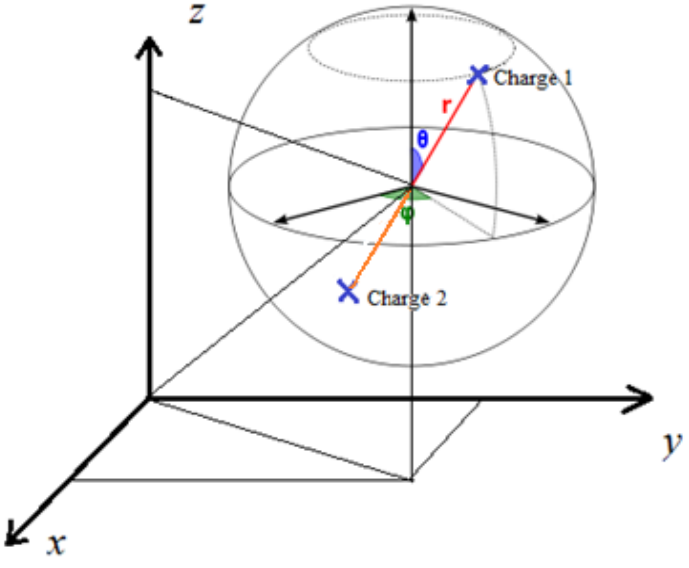

Figure 1. Schematical representation of the spheroidal ions.

A simulation step is defined as the attempt of traslation and rotation of a test spheroidal ion or the attempt of insertion/removal of an electro-neutral group of spheroidal ions (a pair of divalent spheroidal ions, one coion and one counterion). GCMC simulations took 50 million steps and the simulated systems were always thermalized around half million steps before collecting data for averaging. Among the limitations of the PM of electrolyte is the absence of an explicit representation for the solvent molecules. However, Pegado *et al.* have recently tested the validity of the PM by comparing with explicit solvent simulations, supporting the reliability of its results.[38] Due to the internal structure of the charge the PM of spheroidal ions is in fact an

extension of the original PM and had to be tested carefully. The effectiveness of the GCMC technique in controlling correctly the ionic concentration of spheroids was tested by doubling the size of the simulation box and checking that no significant variations in the desired salt concentration were observed.

Theoretical model.

A quadrupole-mediated interaction model is used to model spheroidal ions in which the hard spheres interaction between ions is discarded. Ions can overlap but they preserve their excluded volume condition with the charged planes, *i.e.*, they cannot approach to the charged planes below the DCA. The interacting charged planes are assumed to be large enough compared to their separation in order to neglect any end effects (infinite). The charged surfaces are kept in the $y-z$ plane and because of symmetry the electrostatic field varies exclusively in the x direction (assuming that there are no external electrical fields present). The geometric center of spheroidal ions is also the center of their charge distribution located at some value of x. The two point charges are located at opposite positions on the surface of the spheroidal ion and they have well defined projections on the x -axis. Defining this projection as s, the individual charge positions can be expressed as $x-s$ and $x+s$, respectively (see Fig. 2).

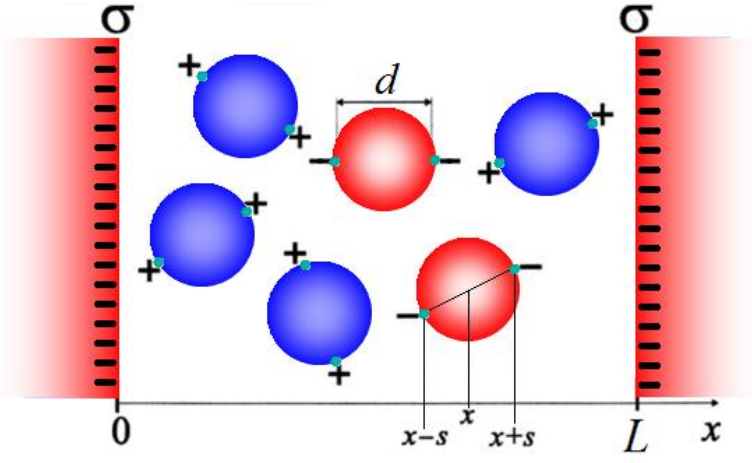

Figure 2. Representation of spheroidal ions according to the theoretical framework.

The free energy of the system per unit area consists of three contributions: one due to coulombic interactions among individual charges, one because of the positional entropy of the spheroidal ions and the last one caused by their orientational entropy. The traslation and orientation of spheroidal ions varies the averaged volume charge density calculations. The whole free energy from the two interacting EDL is minimized to obtain consistent equilibrium profiles for the charge density of co- and counterions, electrical potential and orientational order parameters of the system. We employ a similar method to the one described in references 39 and 40 for rod-like

ions and that for salt free electrolyte solutions with only spheroidal counterions.[26] For small values of electrical potential, the linearized regime corresponding to small values of d is employed to yield an analytical solution.[39] In further elaboration, the free energy is minimized for arbitrary values of d by a rigorous solution of the variational problem that the integrodifferential equation for the electrical potential states. The positional entropy is calculated dividing the region of the electrolyte solution into layers of unit area and infinitesimal thickness dx assuming that each layer is in local thermodynamic equilibrium and all macroscopic quantities are locally constant. A lattice model with a finite number of sites with equal volume is employed to calculate the possible permutations of spheroidal ions on these sites. The entropy is calculated as the negative logarithm of this number of permutations. If the orientational probability of the spheroidal ions is integrated over all possible angles it should be equal to 1 (for the normalization of probability). Assuming that the whole system is electro-neuteutral the variational problem is finally solved to minimize the free energy yielding the analytical solution in thermodynamic equilibrium conditions.

RESULTS AND DISCUSSION

The DFT discards the hard sphere interaction between spheroidal ions, only the DCA is preserved defining an excluded volume condition respect to the charged surface. In order to obtain a better agreement with the DFT calculations, in the GCMC simulations the hard sphere condition is omitted. This omission should not modify the simulation results for diluted systems, but it could lead to notoriously different results for high surface charge densities or large ionic diameters.

In Fig. 3 the first concentration profiles of individual elementary charges are shown. The distance is normalized by the corresponding ionic diameter, in order to clearly represent the structural properties of the EDL based upon the size of the spheroidal ions. The surface charge density and the salt concentration are fixed at -10 μC/m^2 and 0.1 M, respectively. These values are chosen as representative values of biological systems. In Fig. 1 *a)* the results for an ionic diameter of 0.4 nm are sketched. The choice of 0.4 nm is inspired in previous works where this ionic diameter was chosen indiscriminately to represent mono- and multivalent ions. A good qualitative agreement between theoretical predictions and simulations results can be observed. The ionic profiles are dramatically different from those of regular divalent ions with all the charge concentrated in the center of the hard sphere. In Fig. 3 *b)* the system parameters from Fig. 3 *a)* are used again, except the ionic diameter which is now 0.85 nm. The choice of 0.85 nm as a representative value for the diameter of spheroidal ions is based on experimental evidence from the works of Israelachvilli *et al*.[1] Qualitatively, Figures 3 *a)* and *b)* are very similar but they have significant quantitative differences.

The value of the maximum at the midplane in the counterion concentration is almost the double for the ionic diameter of 0.4 nm (around 27 M) respect to the maximum for 0.85 nm (around 15 M). The separation between the charged plates is of two diameters in both cases but we should keep in mind that the separation is normalized by the ionic diameter, *i.e.*, the real separation

between the charged plates is slightly larger than the double for the case of 0.85 nm of diameter. This means that the available volume is also the double in the case of the larger spheroidal ions. However, the number of spheroidal ions (hence the number of individual elementary charges) is practically the same in both cases. This can be inferred from Fig. 3 where it is observed how coions are almost absent from the solution, which means that the electrolyte composition is ruled by excess counterions and the number of excess counterions is the same in both cases. As a consequence, the charge concentration is practically the double in the case of the smaller spheroidal ions, where the available volume between the charged plates is half than that for the larger spheroidal ions.

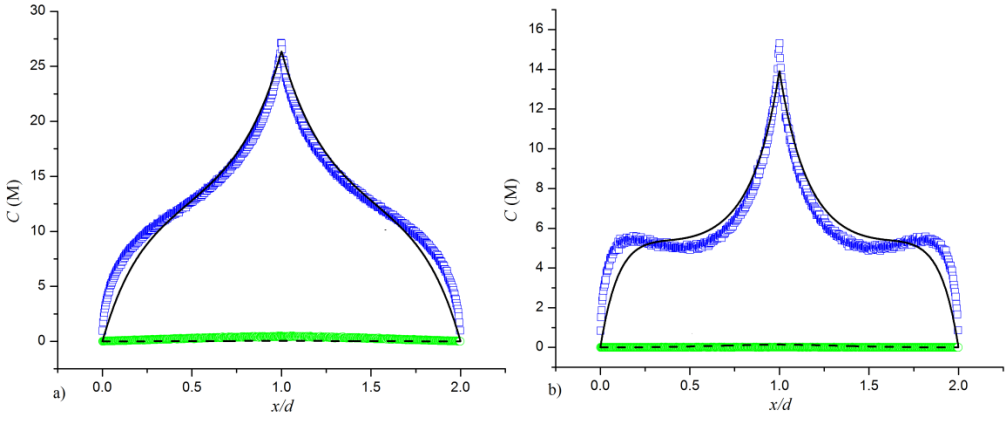

Figure 3. Ionic concentration profiles in Mol units for individual elementary charges from spheroidal ions as function of the distance from one of the charged plates (normalized by the corresponding ionic diameter *d*). The separation between the charged plates is of two ionic diameters. Results for two different ionic diameters are presented a) 0.4 nm and b) 0.85 nm. The surface charge density and the bulk salt concentration are fixed at -10 $\mu C/m^2$ and 0.1 M, respectively. The open symbols correspond to GCMC simulation results (blue squares for counterions and green circles for coions) and lines to the theoretical predictions (solid line for counterions and dashed line for coions).

Despite the good qualitative agreement between theoretical predictions and simulation results, the agreement is still quantitatively slightly better for the case of smaller ions (See Fig. 3). The discreteness of the positions that spheroidal ions can occupy in the lattice model employed in the theoretical framework distorts the calculations. This distortion is less important for the smaller ions due to the fact that in this case the lattice model resembles more to a continuum than the lattice model for larger spheroidal ions. Hence, the deviations from the simulation results are more noticeable for larger spheroidal ions. The local maximum appearing on the individual charge concentration profiles in the midplane and in general the shape of the concentration profiles (See Fig. 3) are caused because spheroidal ions should be preferably oriented perpendicularly to the charged plates in order to minimize the free energy of the system. This feature was tested and confirmed by checking the angular distributions of spheroidal ions in the

simulations. Consequently at two ionic diameters of separation, individual charge of spheroidal ions close to both charged plates contribute to the individual charges concentration calculations at the midplane.

In Fig. 4 the same parameters from Fig. 3 employed and also the same theoretical predictions are shown. However, the GCMC simulations include now the hard spheres condition for the interaction between the spheroidal ions. This modification allows the simulation to test the effect of excluded volume beyond the theoretical framework herein developed. Again, a good agreement between theoretical predictions and simulations is observed. There are no significant differences between the simulation results with and without the hard sphere condition, these are practically indistinguishable for spheroidal ions of 0.4 nm of diameter. However, a significant qualitative difference can be observed for larger spheroidal ions, the midplane maximum in the counterions concentration profile is below the theoretical prediction. This feature points out that hard spheres condition is logically more important for larger ions. The electrochemical potential is now increased for the larger spheroidal ions due to the reduction in the available volume between the charged plates respect to the case without the hard spheres condition. Then, it can be concluded that the proper inclusion of ionic size can have significant effects ever for moderate surface charge densities.

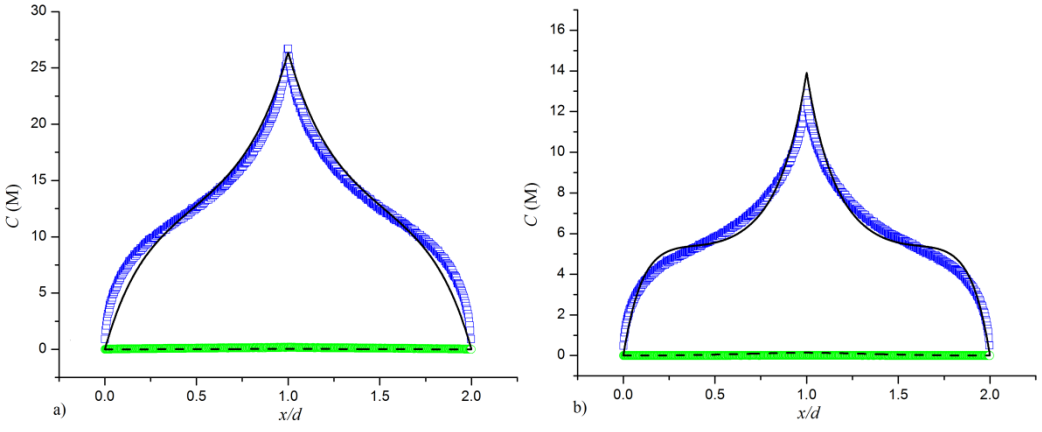

Figure 4. Ionic concentration profiles in Mol units for individual elementary charges from spheroidal ions as function of the distance from one of the charged plates (normalized by the corresponding ionic diameter *d*). The separation between the charged plates is of two ionic diameters. Excluded volume conditions between the spheroidal ions are included in these simulations. Results for two different ionic diameters are presented a) 0.4 nm and b) 0.85 nm. The surface charge density and the bulk salt concentration are fixed at -10 μC/m^2 and 0.1 M, respectively. The lines and symbols represent the same than in Fig. 3.

In Fig. 5 the separation between the charged plates is doubled with the same system parameters than figures 3 and 4. In order to test simulation calculations in the same conditions than the theoretical framework, the hard sphere condition between spheroidal ions is again removed.

Once more, a good qualitative agreement between the theoretical predictions and the simulation results is observed. The simulation results show again lower estimations of the concentrations for larger ions as a consequence of the effect of their larger available volume. However, now the profiles do not exhibit the midplane maximum in the counterion concentration profiles anymore. Instead, two individual maxima close to the charged plates are present for both ionic diameters. The ions are still preferably oriented perpendicularly to the charged surface but the separation between the charged plates is larger than two ionic diameters. For this separation between the charged plates, more salt can enter the simulation cell, as can be confirmed by the simulation coion profiles from Fig. 5. However, this trend is not well reproduced by the theoretical predictions, especially in the case of smaller spheroidal ions.

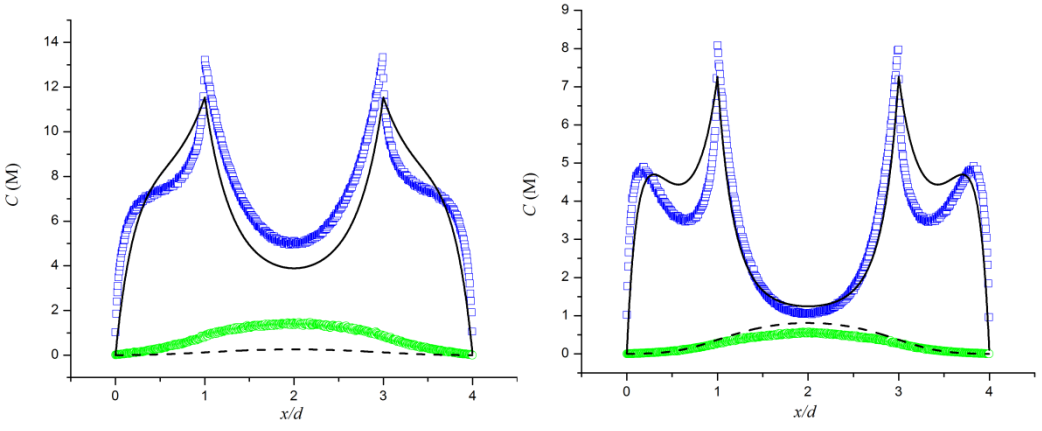

Figure 5. Ionic concentration profiles in Mol units for individual elementary charges from spheroidal ions as function of the distance from one of the charged plates (normalized by the corresponding ionic diameter *d*). The separation between the charged plates is of four ionic diameters. Results for two different ionic diameters are presented a) 0.4 nm and b) 0.85 nm. The surface charge density and the bulk salt concentration are fixed at -10 μC/m^2 and 0.1 M, respectively. The lines and symbols represent the same than in Fig. 3.

More features about the orientational ordering of spheroidal ions can be observed in Fig. 6 where the same parameters from Fig. 3 are used for the case of uncharged plates. This is a special case in which significant disagreements between the classical PB predictions and the results obtained from GCMC simulations within a basic PM of electrolyte, were reported.[6] In this case the electrolyte composition is completely symmetric due to the fact that no excess counterions are present and also the ionic profiles are symmetric, *i.e.*, both counterions and coions show similar trends. The invariance of the electrochemical potential for different ionic diameters clearly evidences the underestimation of the coulombic interactions (see Fig. 6). In the case of GCMC simulations, the thermodynamic equilibrium conditions with an external reservoir define the total particles allowed to lie into the electrolyte solution. For the smaller ions, less

available volume between the charged plates is accessible increasing the strength of coulombic interactions and hence the calculations of the electrochemical potential. Thus, the presence of ions in the electrolyte solution is reduced in comparison with the case of larger spheroidal ions (See Fig. 6) where the available space is double. The theoretical framework predicts profiles with a straight triangular shape because of underestimations of the coulombic interactions and the subsequent major importance of the intracorrelations arising from the internal structure of charge in spheroidal ions. Actually, if no intracorrelations were present in the theoretical framework, no charge concentration could be predicted between the uncharged charged plates (as is in the case of the classical PB framework). The absence of excess counterions for uncharged plates leads to quite different results than those obtained for charged plates. Now, the concentration calculations are larger for the larger spheroidal ions.

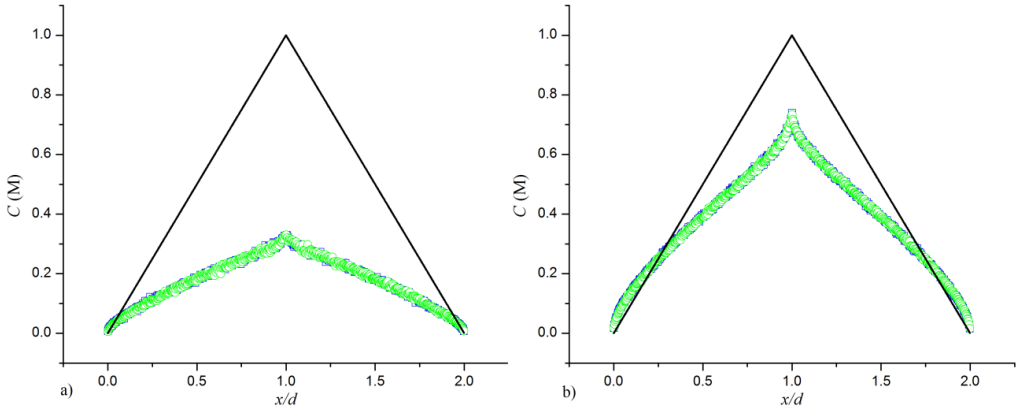

Figure 6. Ionic concentration profiles in Mol units for individual elementary charges from spheroidal ions as function of the distance from one of the charged plates (normalized by the corresponding ionic diameter d). The separation between the charged plates is of two ionic diameters. Results for two different ionic diameters are presented a) 0.4 nm and b) 0.85 nm. The surface charge density and the bulk salt concentration are fixed at 0 μC/m^2 and 0.1 M, respectively. The lines and symbols represent the same than in Fig. 3.

In order to visualize the effects of the charge structuration, in Fig 7 the position of the individual elementary charges respect to the center of the spheroid is varied. It is expressed as a percentage of the ionic radius $d/2$, this rate can be varied from 0 to 100%. The system parameters are again the same than those from figures 3 and 4. In the case of 0%, both charges would be in the center of the sphere and the agreement with a classical PM of electrolyte should be granted. This was verified by carrying out GCMC simulations with a PM of electrolyte. For the 100% case results were already presented in Fig. 3, when ions are on the exactly opposite position on the surface of the spheroid. The intermediate cases (25 % and 75 %) show the transition from one PM of electrolyte to a *modified* PM of electrolyte. No theoretical predictions are shown in Fig. 7. Although it can be inferred that in the case of 0% the theoretical framework predictions should

be in line with those from the classical PB model due to the absence of orientational ordering parameters. We already know the problems of the classical PB framework and its inconsistencies respect the simulation results for a PM of electrolyte.[6]

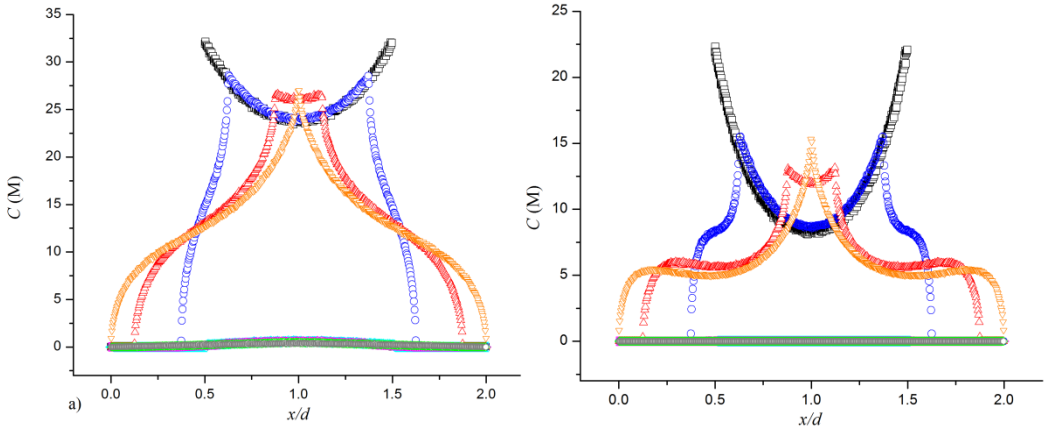

Figure 7. Ionic concentration profiles in MoI units for individual elementary charges from spheroidal ions as function of the distance from one of the charged plates (normalized by the corresponding ionic diameter d). The separation between the charged plates is of two ionic diameters. Results for two different ionic diameters are presented a) 0.4 nm and b) 0.85 nm. The surface charge density and the bulk salt concentration are fixed at -10 μC/m^2 and 0.1 M, respectively. In this case the charges are located at different distances from the center of the spheroid expressed as a percentage of the ionic radius d. The open symbols represent the counter and coions profiles for 0% (black squares and cyan left triangles, respectively), 25% (blue circles and magenta right triangles, respectively), 75% (red up triangles and green diamonds, respectively) and 100% (orange down triangles and gray hexagons).

CONCLUSIONS.

We have developed a GCMC simulation within a modified PM of electrolyte inspired on monoclonal antibodies. In the limit case, the GCMC simulations within the modified PM were found to be in agreement with the basic PM. The obtained results have been compared to those from a DFT that also includes ionic correlations as well. A remarkable agreement between the theoretical predictions and the simulation results is reached. However, slight disagreements are also found. These disagreements are related to the omission of intercorrelations between the spheroidal ions in the theory. However, in both cases the orientational ordering of spheroidal ions and the derived inter- and intracorrelations define ionic profiles beyond those provided by the classical PB theory.

ACKNOWLEDGEMENTS.

The authors thank the financial support from the following institutions: i) 'Ministerio de Ciencia e Innovación, Plan Nacional de Investigación, Desarrollo e Innovación Tecnológica (I+D+i)', Project MAT2009-13155-C04-04. ii) 'Consejería de Innovación, Ciencia y Empresa de la Junta de

Andalucía', Projects P07-FQM-02496, P07-FQM-02517, P09-FQM-4698. iii) European Regional Development Fund (ERDF).

REFERENCES.

1. Israelachvili, J. N. *Intermolecular and Surface Forces;* Academic Press: London, 1985.
2. Gouy, G. *J. Phys. (Paris)* **1910,** *9,* 457.
3. Chapman, D. L. *Philos. Mag.* **1913,** *25,* 475.
4. Quesada-Pérez, M.; González-Tovar, E.; Martín-Molina, A.; Lozada-Cassou, M.; Hidalgo-Álvarez, R. *Chem. Phys. Chem.* **2003,** *4,* 234.
5. Ibarra-Armenta, J. G.; Martín-Molina, A.; Quesada-Pérez, M. *Phys. Chem. Chem. Phys.* **2009,** *11,* 309.
6. Ibarra-Armenta, J. G.; Martín-Molina, A.; Quesada-Perez, M. *Phys. Chem. Chem. Phys.* **2011,** *13,* 13349-13357.
7. Martín-Molina, A.; Ibarra-Armenta, J. G.; González-Tovar, E.; Hidalgo-Álvarez, R.; Quesada-Pérez, M. *Softmatter* **2011,** *7,* 1441-1449.
8. González-Amezcua, O.; Hernádez-Contreras, M. *J. Chem. Phys.* **2004,** *121,* 10742.
9. Hatlo, M.; Bohinc, K.; Lue, L. *J. Chem. Phys.* **2010,** *132,* 114102.
10. Bohinc, K.; Lue, L. *Chin. J. Polym. Sci.* **2011,** *29,* 414.
11. Tang, Z.; Scriven, L. E.; Davis, H. T. *J. Chem. Phys.* **1992,** *97,* 9258.
12. Bhuiyan, L. B.; Outhwaite, C. W. *Phys. Chem. Chem. Phys.* **2004,** *6,* 3467.
13. Carnie, S. L.; Chan, D. Y. C.; Mitchell, D. J.; Ninham, B. W. *J. Chem. Phys.* **1981,** *74,* 1472.
14. Lozada-Casou, M.; Saavedra-Barrera, R.; Henderson, D. *J. Chem. Phys.* **1982,** *77,* 5150.
15. Kjellander, R.; Åkesson, T.; Jönsson, B.; Marcelja, S. *J. Chem. Phys.* **1992,** *97,* 1424.
16. Ottewill, R. H.; Shaw, J. N. *J. Colloid Interface Sci.* **1968,** *26,* 110.
17. Quesada-Pérez, M.; González-Tovar, E.; Martín-Molina, A.; Lozada-Cassou, M.; Hidalgo-Álvarez, R. *Colloid Surf. A* **2005,** *267,* 24.
18. Martín-Molina, A.; Maroto-Centeno, J. A.; Hidalgo-Álvarez, R.; Quesada-Pérez, M. *Colloid. Surf. A* **2007,** *319,* 103.
19. Ninham, B. W.; Yaminsky, V. *Langmuir* **1997,** *13,* 2097.
20. Tavares, F. W.; Bratko, D.; Blanch, H. W.; Prausnitz, J. M. *J. Phys. Chem. B* **2004,** *108,* 9228.
21. Boström, M.; Tavares, F. W.; Bratko, D.; Ninham, B. W. *J. Phys. Chem.* **2005,** *109,* 24489.
22. Boström, M.; Tavares, F. W.; Ninham, B. W.; Prausnitz, J. M. *J. Phys. Chem. B* **2006,** *110,* 24757.
23. Parsons, D. F.; Ninham, B. W. *Langmuir* **2010,** *26,* 1816.

24. Parsons, D. F.; Boström, M.; Maceina, T. J.; Salis, A.; Ninham, B. W. *Langmuir* **2010,** *26,* 3323.
25. Maset, S.; Bohinc, K. *J. Phys. A: Math. Theor.* **2007,** *40,* 11815.
26. Urbanija, J.; Bohinc, K.; Bellen, A.; Maset, S.; Iglič, A.; Kralj-Iglič, V.; Kumar, P. B. S. *J. Chem. Phys.* **2008,** *129,* 105101.
27. Maset, S.; Reščič, J.; May, S.; Pavlič, J. I.; Bohinc, K. *J. Phys. A: Math. Theor.* **2009,** *42,* 105401.
28. Megistu, D. H.; Bohinc, K.; May, S. *EPL* **2009,** *88,* 14003.
29. Popa, I.; Trulsson, M.; Papastavrou, G.; Borkovec, M.; Jönsson, B. *Langmuir* **2009,** *25,* 12435.
30. Grime, J. M. A.; Khan, M. O.; Bohinc, K. *Langmuir* **2010,** *26,* 6343.
31. Megistu, D. H.; Bohinc, K.; May, S. *J. Phys. Chem. B* **2009,** *113,* 12277.
32. Igarashi, M.; Matsuura, E.; Igarashi, Y.; Nagae, H.; Ichikawa, K.; Triplett, D. A.; Koike, T. *blood* **1996,** *87,* 3262.
33. Urbanija, J.; Tomšič, N.; Lokar, M.; Ambrožič, A.; Čučnik, S.; Rozman, B.; Kandušer, M.; Iglič, A.; Kralj-Iglič, V. *Chem. Phys. Lip.* **2007,** *150,* 49.
34. Valleau, J. P.; Cohen, L. K. *J. Chem. Phys.* **1980,** *72,* 5935.
35. Adams, D. J. *Mol. Phys.* **1974,** *28,* 1241.
36. Adams, D. J. *Mol. Phys.* **1975,** *29,* 307.
37. Boda, D.; Chan, K. Y.; Henderson, D. *J. Chem. Phys.* **1998,** *109,* 7362.
38. Pegado, L.; Jönsson, B.; Wennerström, H. *J. Chem. Phys.* **2008,** *129,* 184503.
39. Bohinc, K.; Iglič, A.; May, S. *Europhys. Lett.* **2004,** *68,* 494.
40. May, S.; Iglič, A.; Reščič, J.; Maset, S.; Bohinc, K. *J. Phys. Chem. B* **2008,** *112,* 1689.